1-1-2016

Identification Of Metabolite Biomarkers In Epilepsy Using 1h Mrs

Helen Wu
Wayne State University,

IDENTIFICATION OF METABOLITE BIOMARKERS IN EPILESPY USING ^{1}H MRS

by

HELEN C. WU

DISSERTATION

Submitted to the Graduate School

of Wayne State University,

Detroit, Michigan

in partial fulfillment of the requirements

for the degree of

DOCTOR OF PHILOSOPHY

2016

MAJOR: TRANSLATIONAL NEUROSCIENCE

Approved By:

_____

ADVISOR DATE

_____

ADVISOR

_____

_____

_____

DEDICATION

To my family, including the furkids, for their love and unwavering support.

ACKNOWLEDGEMENTS

I would like to sincerely thank my advisory team, Dr. Loeb and Dr. Stanley for their mentorship and always encouraging me to accept new challenges and overcome new obstacles. I would also like to extend my thanks to the members of my committee: Dr. Berkowitz, Dr. Galloway, Dr. Kuhn, for their generous support and guidance over the last several years. I would also like to thank Caroline for all the amazing things she does that are too numerous to name, Dalal for going out of her way to help me scan patients, Dr. Basha for supporting me in my research and helping me recruit patients, the patients for taking time out of their busy days to come and participate in the study, the DLAR staff for helping me take care of my rats, and the staff of the Small Animal Imaging Core for teaching me the ropes. I am also very thankful to my fellow lab members, TNP students, and fellow MD/PhD students, past and present, as they all have had such a positive influence on so many aspects of my academic life, always challenging me to be more creative and seek out new challenges and new ideas.

This entire journey would not have been possible without the incredible support of my friends and family, especially my parents, who have always encouraged me to be the best person I could be. A special thanks also goes to Arnold for his enthusiastic support during this whole process.

TABLE OF CONTENTS

LIST OF TABLES

LIST OF FIGURES

LIST OF ABBREVIATIONS

ASD	anti-seizure drugs
AUC	area under the curve
BBB	blood brain barrier
Cho	choline
CPMG	Carr-Purcell-Meiboom-Gill
Cr	creatine
CREB	cAMP response element binding protein
CRLB	Cramér-Rao lower bounds
CSF	cerebrospinal fluid
CTL	positive control group – vehicle treated
ECoG	electrocorticography
EEG	electroencephalogram
FDR	false discovery rate
GABA	γ-aminobutyric acid
Gln	glutamine
Glu	glutamate
GPC	glycerophosphorylcholine
GPCR	G-protein coupled receptor
HR	high resolution
IED	interictal epileptiform discharges
Lac	Lactate
m-Ins	*myo*-inositol

MAPK	mitogen-activated protein kinase
MAS	magic angle spinning
MM140	macromolecule at resonance 1.40 ppm
MRS	magnetic resonance spectroscopy
MRSI	magnetic resonance spectroscopic imaging
NAA	N-acetylaspartate
NAAG	N-acetylaspartyl glutamic acid
NCT	negative controls group – typically developing animals
PCA	principal components analysis
PCh	phosphorylcholine
PCr	phosphocreatine
PDE	phosphodiester
PE	phosphorylethanolamine
PME	phosphomonoester
PRESS	Point Resolved Spectroscopy
RF	radio frequency
ROC	Receiver Operating Characteristic
ROI	region of interest
SBEP	Systems Biology of Epilepsy Program
SNR	signal to noise ratio
SVS	single voxel spectroscopy
T	tesla
TAO	triple antibiotic ointment

Tau	taurine
TE	echo time
TR	repetition time
TET	treatment group – tetanus toxin treated

CHAPTER 1: MOTIVATIONS FOR IDENTIFYING BIOMARKERS PREDICTIVE OF EPILEPSY

1.1 Introduction

Epilepsy is a serious neurological disorder that affects 5-10 people out of every 1,000, or approximately 1% of the global population (Hirtz et al., 2007; Sander, 2003) with an estimated 3% lifetime prevalence (Wyllie, 2001). It is also an ancient disorder, with the earliest references dating as far back as 2,000 BCE (Magiorkinis, Sidiropoulou, & Diamantis, 2010). While advancements in technology and scientific understanding in the last century have enabled tremendous improvements in the management of epilepsy (Magiorkinis, Diamantis, Sidiropoulou, & Panteliadis, 2014), relatively little is known about the mechanisms that underlie seizure generation. Because of this lack in understanding, epilepsy remains a disorder that can only be diagnosed upon the presenting symptom of recurring seizures and managed primarily through medication aimed at reducing seizure occurrence but stop short of actually targeting the underlying causes of the disorder (Cendes, 2012; Loeb, 2011; Temkin, 2009).

To better steer research toward a cure for epilepsy, the updated 2014 NINDS Benchmarks for Epilepsy Research continues to promote endeavors that seek to understand causes of epilepsy along with means of preventing epilepsy through the identification of biomarkers as key priorities for the epilepsy research community ("2014 NINDS Benchmarks for Epilepsy Research," 2014). Biomarkers that can be used to detect the development of epilepsy prior to seizure onset, monitor patients for therapeutic efficacy, and inform clinical trials of novel therapeutics are absolutely crucial to the improvement of epilepsy treatment.

For the management of epilepsy, the first line of defense typically involves the trial of numerous anti-seizure drugs (ASDs), in an effort to identify the one or two medications that provide the most therapeutic benefit while balancing side effects and other drug interactions

(Moshé, Perucca, Ryvlin, & Tomson, 2014). Even though many patients can achieve seizure freedom by medications alone, more than 30 percent of epilepsy patients experience inadequate seizure control on anti-seizure drugs (ASDs) (Kwan & Brodie, 2000) and may become candidates for epilepsy surgery if the seizures are of a focal nature (Engel & Ojemann, 1993). Accurate and precise localization of seizure onset regions are essential for treatment success, since failure to accurately and precisely localize these seizure-inducing regions of the brain can lead to the persistence of seizures after surgery. The spatial resolution and sensitivity of scalp EEG is generally inadequate for precise seizure localization, which is generally achieved by using intracranial electrocorticography (ECoG), a highly invasive surgical procedure involving a craniotomy and placement of electrodes directly onto the brain, in conjunction with a battery of various imaging studies (Engel, 1993a; Noachtar & Borggraefe, 2009). Even with such tremendous efforts, success is not guaranteed, as the reported long-term success rate of epilepsy surgery is estimated to vary tremendously between 30-85% (Engel, 1993b; Spencer & Huh, 2008). All of these issues point to the critical need for a non-invasive biomarker that can reliably localize sources of the seizure activity and act as an indicator of disease progression so that early intervention may be attempted and newer disease changing drug therapies may be tested more effectively (Engel et al., 2013).

The fact that surgical resections can be curative implies the existence of key differences between epileptic and non-epileptic tissue in a patient affected by epilepsy. Furthermore, the fact that these differences manifest clinically as large scale synchronized electrical discharges (e.g. seizures) implies the existence of some common final pathway within the disorder. In order to identify and characterize these key differences, previous studies in our laboratory have compared gene expression profiles of tissues from both epileptic and non-epileptic regions of multiple

patients and have identified unique differences in the expressions of MAPK signaling and CREB activation in the superficial layers of the neocortex (Beaumont, Yao, Shah, Kapatos, & Loeb, 2012; Rakhade et al., 2005). The presence of these robust transcriptional differences are suggestive of downstream changes in protein and metabolite expression that can be probed using techniques such as magnetic resonance spectroscopy (MRS), which is ideally suited for such an application. MRS has the ability to measure multiple biochemical species at once and the relative ease by which the technique may be translated from pre-clinical to non-invasive clinical applications makes it unique. By using this technique, identified biochemical differences specific to epileptic regions of the brain can be used to develop non-invasive biomarkers of epileptic activity, addressing an urgent but still unmet need in both epilepsy research and clinical management of the disorder.

1.2 Interictal epileptiform discharges as a surrogate for epileptic activity

Seizures are formally defined as "the clinical manifestation of an abnormal, excessive, hyper-synchronous discharge of a population of cortical neurons". When seizures occur repeatedly without external provocation, it becomes epilepsy (Bromfield, Cavazos, & Sirven, 2006; Fisher et al., 2005). However, in between seizure episodes (i.e. interictal), a form of paroxysmal and abnormally synchronized neuronal discharges called interictal epileptiform discharges (IEDs[1]) can also frequently occur. Intriguingly, IEDs tend to remain relatively localized with minimal spread and are not generally associated with specific observable symptoms but appear as spikes or clusters of spikes on EEG. Nonetheless, they are clinically

[1] Although the terms "IED" and "interictal spikes"/"spikes" may appear interchangeable in some instances through out this text, for the purposes of this dissertation, the term "IED" is generally used to refer to the specific electrophysiological phenomenon, while "spikes" or "interictal spikes" are used to refer to the waveform typically observed on EEG that corresponds to the occurrence of IEDs.

useful for the diagnosis of epilepsy and guiding management approaches (Lüders, Engel, & Munari, 1993; Pillai & Sperling, 2006).

While the exact relationship between IEDs and seizure activity remains to be elucidated, they often occur in close proximity to each other and surgical removal of both seizure onset and IED regions tend to produce superior results over the removal of the seizure onset region alone (Asano et al., 2003; Bautista, Cobbs, Spencer, & Spencer, 1999; Kanazawa, Blume, & Girvin, 1996; Lee, Kim, Jeong, & Chung, 2014). While IEDs are generally perceived as subclinical or asymptomatic (Gibbs, 1936), they have been demonstrated to disrupt cognitive and neurologic functions (Aarts, Binnie, Smit, & Wilkins, 1984; Sanchez Fernandez, Loddenkemper, Galanopoulou, & Moshe, 2015; Schwab, 1939). Suppression of IEDs using lamotragine has demonstrated beneficial behavioral effects in children with well-controlled epilepsy (Pressler, Robinson, Wilson, & Binnie, 2005). Animal studies using a kainate model of epilepsy have also shown that IEDs typically precede the onset of spontaneous recurrent seizures and an increased number of IEDs during the prodromal phase was positively correlated with earlier onset of established epilepsy (White et al., 2010). These observations suggest that IEDs may potentially be used as a predictive biomarker for the development of chronic epilepsy and are worthy of further study.

Previous works in our laboratory have shown that the frequency and amplitude of IEDs are strongly correlated to a set of activity-dependent differences in gene expression (Rakhade et al., 2005), while a similar relationship between gene expression differences and seizure activity was not found (Rakhade et al., 2007). This set of activity-dependent genes strongly implicate the pathway involving cAMP response element binding (CREB) protein dependent transcription via mitogen-activated protein kinase (MAPK) signaling, especially in the superficial layers II/III of

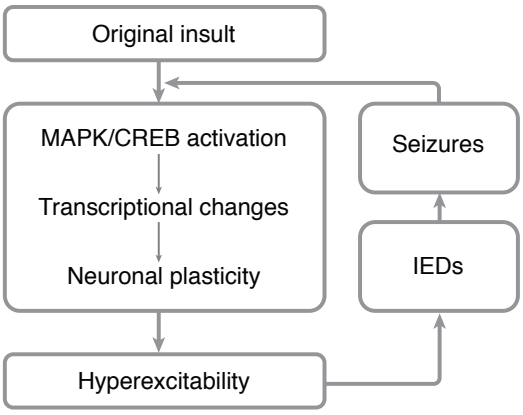

Figure 1.1 A theoretical framework for conceptualizing the interactions between molecular responses to insult, IEDs, seizures, and the self-reinforcing nature of epilepsy.

the neocortex both in humans (Beaumont et al., 2012) and in a rat model of epilepsy (Barkmeier et al., 2012). Collectively, these findings suggest that IEDs may play a key role in generating or maintaining an epileptic focus in a MAPK-CREB dependent manner (Figure 1.1). Furthermore, because IEDs typically occur more frequently than seizures, they can potentially serve as a sensitive marker of epileptogenesis, capable of reflecting epileptogenic changes prior to the establishment of epilepsy (Engel et al., 2013).

1.3 ^{1}H Magnetic resonance spectroscopy as a tool for biomarker detection

The very fact that surgical resection can be curative for epilepsy indicates that affected regions are physiologically different from their normal counterparts. These physiological differences are likely downstream consequences differences in gene expression between epileptic and non-epileptic regions. These differences may further manifest as metabolic differences and be reliably probed by the right tool and used as crucial biomarkers for epileptogenesis or act as surrogate markers for therapeutic efficacy. The ability to simultaneously measure numerous spatially localized compounds associated with brain metabolism and the relative ease by which the technique may be translated between *in vitro*, *ex vivo*, and non-invasive *in vivo* applications, makes MRS a tremendously powerful tool for studying epilepsy and for identifying biomarkers of the disorder. We hypothesized that we can indeed identify potential metabolite biomarkers that are predictive of epilepsy and epileptogenesis using ^{1}H MRS techniques and have formulated our aims and approach accordingly. The section below (Chapter 1, Section 1.4)

provides further details on the aims and scopes of this project. Additional information on the theory of MRS, what it measures, and how it has been applied to epilepsy thus far are provided in Chapter 2.

1.4 Project scope and aims

There are 2 central aims we hope to address in this project: 1) identification of potential biomarkers of *established* epilepsy in human tissue and 2) identification of potential biomarkers for the *development* of epilepsy in an appropriate animal model of epileptogenesis and determine whether these biomarkers of epileptogenesis share commonalities with those of established epilepsy as identified in aim 1.

To address our first aim of identifying biomarkers in established epilepsy, we applied a high resolution version of ^{1}H MRS to surgically resected epileptic and non-epileptic (based on their relative levels of IED activity) tissue samples *ex vivo*. These tissue samples are acquired from patients with intractable epilepsy undergoing surgical resection of their epileptic focus as part of their clinical treatment plan. Using an unbiased statistical classification approach, we demonstrate the ability of ^{1}H MRS *ex vivo* to identify a unique metabolite profile capable of distinguishing between epileptic and non-epileptic tissue samples. We also integrated these metabolite findings with findings obtained from parallel transcriptional microarrays and histology studies to help us better appreciate the possible molecular and cellular features contributing to these metabolite differences. The details of this study are given in Chapter 3.

Studying tissue samples from intractable epilepsy patients allows us to characterize the metabolite profiles of long established epilepsy, but does not necessarily give us information about metabolite changes associated with the development of epilepsy (i.e. epileptogenesis). Studying the latter requires a longitudinal study design, which is most easily implemented in a

suitable animal model of epileptogenesis since we do not have the ability to predict or monitor this process in human patients. Hence, to accomplish our second aim of identifying biomarkers of epileptogenesis, we turned to a rat model of epileptogenesis with persistent and spontaneous IEDs and similar molecular changes in MAPK-CREB expression, achieved by injecting tetanus toxin directly into the animal's somatosensory cortex. After treatment with tetanus toxin, we followed these animals longitudinally over the course of five weeks by performing EEG recordings and ^{1}H MRS scans at periodic intervals to study the interaction between electrophysiology and metabolite levels over time. These animal studies will further help to determine whether or not IEDs could sufficiently account for the metabolite differences observed in our *ex vivo* human study. Detailed descriptions of this study are provided in Chapter 4.

CHAPTER 2: BRIEF INTRODUCTION TO MRS AND ITS APPLICATIONS IN EPILEPSY

2.1 What is MRS and what does it measure?

MRS, also commonly known as nuclear magnetic resonance (NMR) spectroscopy, is one of the oldest magnetic resonance based analytical techniques and the subject of two Nobel Prizes in Physics. The first was awarded to Isidor Isaac Rabi in 1944 for discovering the NMR phenomenon (Nobel Media AB, 2014a) and the second was shared between Felix Bloch and Edward Mills Purcell in 1952 for applying NMR in a way that enabled analysis of ordinary liquids and solids (Nobel Media AB, 2014b). While a full treatise on the theory of MRS and its applications is beyond the scope of this work, a basic summary of relevant concepts is provided and a more thorough treatment of the subject may be found elsewhere (De Certaines, Bovée, & Podo, 1992; De Graaf, 2007; Keeler, 2005).

NMR is a phenomenon where a population of atomic nuclei possessing both intrinsic magnetic moment and angular moment (i.e. non-zero spin), will align themselves along an external magnetic field (B_0) with a net magnetization M_0 and precess at a characteristic resonance frequency, known as the Larmor frequency (Figure 2.1A). This precession frequency (ω, in rad sec^{-1}, or ν, in sec^{-1} or Hz) is predicted by the Larmor equation (Equations 1.1 and 1.2) and is proportional to the strength of the external magnetic field (in Teslas or T) and intrinsic properties of the nucleus given by the gyromagnetic ratio (γ, in rad sec^{-1} T^{-1}). These nuclei can be induced to change orientation when under the influence of an applied magnetic field (B_1) that is usually perpendicular to B_0 (Figure 2.1B) and is generated by an excitatory radio frequency (RF) pulse delivered at the same resonant frequency. As the nuclei relax back to equilibrium, the transverse component of their net magnetization will produce a decaying RF signal with their precession frequency as the carrier frequency (Figure 2.1C-D). This decaying RF signal, called

the free induction decay (FID), is detected by the receiver coil and contains useful information about the nuclei that generated it.

$$\omega = \gamma B_0 \qquad \text{(Equation 1.1)}$$

$$\nu = \frac{\omega}{2\pi} = \frac{\gamma}{2\pi} B_0 \qquad \text{(Equation 1.2)}$$

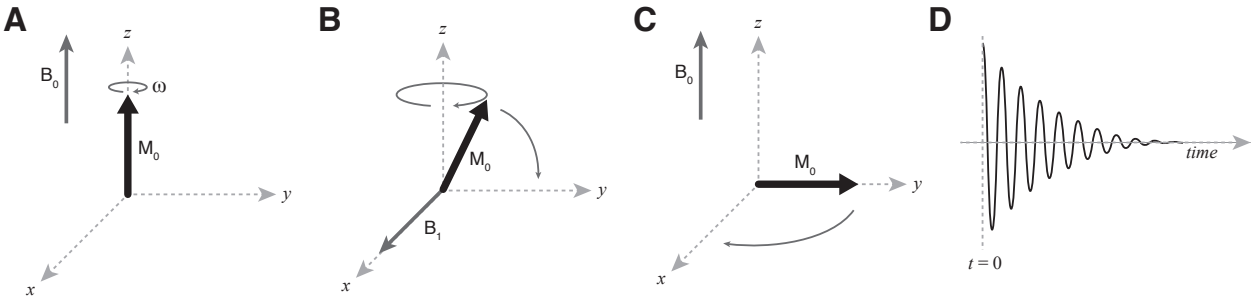

Figure 2.1 Creation of a transverse magnetization. A) Net magnetization (M_0) is created in the presence of an external magnetic field B_0. B) Application of a perpendicular magnetic field (B_1) causes M_0 to precess about B_1. C) Turning off B_1 after M_0 has been flipped 90° will cause M_0 to precess about B_0 once again, but in the transverse plane. D) This transverse magnetization is detected in a receiver coil as it relaxes back to equilibrium, generating the FID signal.

The Fourier transform can be applied to this time domain signal to obtain the frequency components that make up the signal in the form of peaks along a frequency axis, in what is referred to as a spectrum. Ideally, when there is no delay in signal acquisition from the moment the FID is formed, the number of nuclei contributing to the peak is proportional to the integrated area under the peak. A larger area under the peak at a particular frequency indicates more nuclei contributing to the signal at that frequency. The shape of the peak is strongly influenced by the FID decay rate; lower decay rates result in taller but narrower peaks, faster decay rates result in shorter but broader peaks, whilst area under the peak remains the same.

Theoretically any nucleus with non-zero spin, typically isotopes with odd atomic numbers, may be studied using MRS. However, only a relatively short list of nuclei can be studied practically due to restrictions on time, equipment, and abundance. Some of the most

commonly studied nuclei include: ^{1}H, ^{31}P, ^{13}C, ^{23}Na, and ^{19}F. For biological applications, ^{1}H MRS (i.e. applying the RF pulse at the resonance of the ^{1}H isotope) is generally the most common due to its relatively high sensitivity, owing to its high abundance. It also has the ability to simultaneously probe for multiple metabolites that affect various aspects of cell function from membrane components to neurotransmitters. In general, ^{1}H MRS is able to reliably detect metabolites with concentrations of 0.5 to 1 $mmol/kg_{wet\ weight}$ or greater (Govindaraju, Young, & Maudsley, 2000). The work presented here also uses ^{1}H MRS to identify potential biomarkers of epilepsy.

Within a particular compound, MRS is able to resolve and characterize specific chemical moieties involving the nucleus of interest along a chemical shift frequency axis. Each peak along this chemical shift axis reflects the unique resonance frequency (ν) of a particular chemical moiety contain the nucleus of interest. For practical purposes, these frequencies are generally represented as a chemical shift (δ_{ppm}) relative to a reference frequency (ν_{ref}) in parts per million (ppm), which makes it independent of magnetic field strength (Equation 1.3). The additional scaling factor of 10^6 is included to improve legibility, since the shift value is generally very small.

$$\delta_{ppm} = \frac{\nu - \nu_{ref}}{\nu_{ref}} \times 10^6 \qquad \text{(Equation 1.3)}$$

Chemical shifts result from differences in the local magnetic environment experienced by the nuclei of interest. The presence of an electron cloud near a nucleus produces a shielding effect that decreases the strength of the external magnetic field experienced by the nucleus. As a result, the nucleus will precess at a lower resonant frequency than a similar nucleus with less shielding. To illustrate, long triglyceride fatty acid chains with its dense arrangement of hydrogen atoms along a carbon backbone will have a larger electron cloud and consequently

experience stronger shielding than the hydrogen atoms in water, which experiences significantly less shielding in the presence of the electronegative oxygen atom. This difference in shielding produces a 3.5 ppm chemical shift between the water and fat peaks on the chemical shift axis. Most of the metabolites examined in ^{1}H MRS fall between the water and fat peaks. Typical metabolites peaks found in ^{1}H MRS *in vivo* are described in Table 2.1.

Metabolite	Chemical Shift (ppm)	Key Function
Cr+PCr	3.03	Energy metabolism; ATP generation via CK reaction
Gln	2.45	Component of glutamate-glutamine cycle; converted from glutamate in astrocytes
Glu	2.35	Excitatory neurotransmitter; component of glutamate-glutamine cycle
GPC+PCh	3.20	Intermediates of membrane phospholipid breakdown (GPC) and synthesis (PCh) pathways
Lac	1.31	Indicator of hypoxia; insufficiency of oxidative phosphorylation
m-Ins	3.52, 3.62	Part of IP_3 intracellular second messenger system
NAA	2.01	Marker of neuronal integrity

Table 2.1 List of common metabolites seen *in vivo*, their chemical shift positions, and their known key functions. In general, NAA, Cr+PCr, and GPC+PCh are the three most visible metabolite peaks on 1H MRS. Lac is generally below threshold of detection under normal physiologic conditions. Glutamate and glutamine peaks show significant overlap at 1.5 T but may be resolved reliably at 3 T or higher. Creatine plus phosphocreatine (Cr + PCr) , glutamine (Gln), glutamate (Glu), glycerophosphorylcholine plus phosphorylcholine (GPC+PCh), lactate (Lac), *myo*-Inositol (m-Ins), N-acetylaspartate (NAA).

To enable spatial localization in MR studies, magnetic field gradients can be added linearly to the main magnetic field as a function of position, such that different locations will experience a slightly different magnetic field strength. Referring back to the Larmor equation (Equation 1.1), a natural consequence of this spatially dependent variation in magnetic field strength is that the nuclei in each of those locations will also precess at a different resonant frequency, depending on where they are located in space. Frequency selective RF pulses can then be applied to study only those nuclei in the region of interest (ROI).

Single voxel spectroscopy (SVS) and MR spectroscopic imaging (MRSI) are the two most common techniques used for spatial localization in MRS studies. SVS uses three

orthogonal slice selective RF pulses to isolate a rectangular or cubic ROI, located at the intersection of those three orthogonal slices. This region of interest may be moved about and adjusted to an adequately small size to ensure that it is not contaminated with signals from adjacent tissue. However, SVS can only acquire from a single location at a time and generally require multiple averaging scans (typically 64 to 256) to produce a spectrum of reasonably quality. This makes the scanning of a large number of voxels prohibitively time consuming. To collect spectra from a larger area, MRSI, which uses a localization scheme different from SVS, can be more efficient approach, as it can makes use of every scan done over the entire area to improve the signal to noise ratio of every voxel in a large array of voxels. The larger ROI associated with MRSI will, however, place a much greater demand on the shim systems to maintain magnetic field homogeneity over the entire area (Hetherington, Kim, Pan, & Spencer, 2004). Poor magnetic field homogeneity will create large variances in precession frequency within the ROI due to the variations in the magnetic field strength. This results in broader peaks in the frequency domain and impairs the ability of MRS to resolve and quantify the detected compounds due to increased overlap of peaks that would have been adequately separated from each other otherwise.

While *in vivo* MRS studies are most ideal for studying the metabolite profile in living organisms, high resolution MRS studies performed on biological samples *ex vivo* can provide provide a wealth of metabolite information with exquisitely high sensitivity not typically achievable *in vivo.* One particular *ex vivo* ^{1}H MRS approach, known as high resolution magic angle spinning ^{1}H MRS (HR-MAS ^{1}H MRS), is unique its ability to analyze frozen intact tissue without the need for histologically disruptive chemical extractions. It does so by rapidly spinning the sample at the so-called magic angle of 54.7° relative to main static magnetic field in

order to minimize the spectral-broadening effects of dipole-dipole interactions in solid state samples (Andrew, Bradbury, & Eades; Beckonert et al., 2010). For the study of intact tissue samples, this technique is superior to many of the common chemical extraction procedures, where the choice of solvent will impact the types of metabolite available for analysis (e.g. hydrophilic versus hydrophobic) and any available information on tissue compartmentalization and localization would also be completely lost (Beckonert et al., 2010; Cheng et al., 1996; Srivastava et al., 2008).

MRS is an inherently non-invasive technique that relies primarily on strong magnetic fields and RF pulses to generate signals of interest that contain valuable information about the concentrations, characteristics, and environments of the compounds contributing to the signals. The ability to change the size and location of ROIs also allows MRS to be very selective about which sites to study while still being flexible enough to study much larger areas (e.g. the entire brain) as needed. When used as a complement to other experimental procedures, MRS can also characterize *in vitro* and *ex vivo* samples, providing results that may be translated to their *in vivo* counterparts with relative ease. These are all very important features for any potential biomarker tool, but especially so for epilepsy, as we would greatly benefit from being able to perform multiple longitudinal measurements to track biochemical changes in the brain, particularly in regions that are most relevant for seizure generation. We can further complement these findings with additional experimentally derived findings obtained *ex vivo* or *in vitro*. For these reasons, MRS can be an extremely powerful tool for the study of epilepsy biomarkers.

2.2 MRS in epilepsy

While ^{1}H MRS is primarily used as an adjunct diagnostic tool for epilepsy in the clinical setting, it can still give important lateralization or localization information, especially in more

difficult cases with negative or ambiguous MRI and EEG findings. In a research capacity, epilepsy has been studied since the mid-1980s using ^{31}P MRS, a method that preferentially probes metabolites associated with tissue energetics such as high-energy phosphates groups of ATP, phosphocreatine (PCr) and low energy inorganic phosphate (Pi). In general, however, there have been more ^{1}H MRS epilepsy studies than ^{31}P due to its relatively high sensitivity, which leads to greater spatial resolution. Furthermore, from a hardware perspective, ^{31}P MRS studies require dual-tuned coils to probe both ^{1}H and ^{31}P nuclei at their own unique resonant frequencies, which is frequently unavailable on clinical MR systems.

The earliest ^{31}P MRS studies characterized animal models during status epilepticus and noted decreases in both PCr and cerebral pH (Petroff, Prichard, Behar, Alger, & Shulman, 1984) as well an elevation in Pi (Young et al., 1989). Concordance between temporal lobe epilepsy lateralization using PCr/Pi and ATP/Pi ratios and final clinical lateralization has been reported to be 70-73%, which was superior to lateralization by MRI or scalp EEG alone (Chu et al., 1998). Later ^{31}P MRS studies of temporal lobe epilepsy patients provided evidence of bioenergetic impairments with consistent decreases in the PCr/Pi ratio (Kuzniecky, Elgavish, Hetherington, Evanochko, & Pohost, 1992) as well as ATP/Pi (Chu et al., 1998) and PCr/ATP (Hetherington et al., 2004). The decreases in PCr/Pi and PCr/ATP may be mitigated or reversed by initiation of the ketogenic diet in some intractable epilepsy cases (Pan, Bebin, Chu, & Hetherington, 1999).

Over the last several decades, most ^{1}H MRS studies of epilepsy, particularly those involving temporal lobe epilepsies, have consistently reported decreases in N-acetylaspartate (NAA), expressed either independently or as a ratio with creatine plus phosphocreatine (Cr+PCr), glycerophosphorylcholine plus phosphorylcholine (GPC+PCh), or Cr+PCr plus GPC+PCh (Cr+PCr+GPC+PCh) (Bernasconi, Tasch, Cendes, Li, & Arnold, 2002; Breiter et al.,

1994; Cendes, Caramanos, Andermann, Dubeau, & Arnold, 1997b; Connelly, 1997; Matthews, Andermann, & Arnold, 1990). NAA is considered to be a marker of neuronal healthy and participates in a number of biochemical processes, including lipid synthesis and mitochondrial energy production (Moffett, Ross, Arun, Madhavarao, & Namboodiri, 2007). The reduction of NAA does not necessarily correlate to neuronal loss in epilepsy (Kuzniecky et al., 2001; Petroff, Errante, Rothman, Kim, & Spencer, 2002) and may be reversed in many cases after successful resective surgery (Cendes, Andermann, Dubeau, Matthews, & Arnold, 1997a; Hugg et al., 1996; Serles et al., 2001). Despite the fewer number of studies on non-lesional and non-temporal lobe epilepsies, similar decreases in NAA and its ratios to Cr+PCr, GPC+PCh, and Cr+PCr+GPC+PCh, have also been reported (Connelly et al., 1998; Garcia et al., 1995; Stanley, Cendes, Dubeau, Andermann, & Arnold, 1998).

In addition to NAA, differences in glutamate, lactate, and γ-aminobutyric acid (GABA) levels have also been reported. Several lines of evidence point to elevated extracellular glutamate levels compared to controls, particularly in temporal lobe epilepsies with negative MRI findings. Glutamate is thought to play a role in promoting hyperexcitability, leading to seizure development (Cavus et al., 2005; Pan et al., 2008; Simister et al., 2002). Patients actively experiencing seizures or shortly after a seizure episode have also been reported to have elevated lactate levels at or near the site of the seizure focus (Cendes, Stanley, Dubeau, Andermann, & Arnold, 1997c). However, interictally, lactate is generally undetectable (Breiter et al., 1994) in otherwise normal appearing tissue using standard ^{1}H MRS approaches. Works by Petroff and colleagues suggest that poor seizure control may be associated with lower levels of GABA in the brain (Petroff, Rothman, Behar, & Mattson, 1996b) and treatment with certain ASDs such as vigabatrin, gabapentin, and topiramate may increase GABA levels and consequently increase

seizure threshold (Petroff, Hyder, Mattson, & Rothman, 1999; Petroff, Rothman, Behar, Collins, & Mattson, 1996; Petroff, Rothman, Behar, Lamoureux, & Mattson, 1996; Petroff, Rothman, Behar, & Mattson, 1996a).

2.3 Challenges of studying epilepsy using ^{1}H MRS

Despite decades of available literature on ^{1}H MRS studies of epilepsy, vast majority of these studies focused specifically on temporal lobe epilepsies. While the study of temporal lobe epilepsies is no doubt important, this skew also highlights the multitude of challenges associated with using MRS for studying epilepsy and points to where progress is urgently needed. Furthermore, the integration of multiple experimental modalities in addition to ^{1}H MRS is needed to better characterize the biochemical changes underlying the observed metabolite differences in order better understand and validate the ability of ^{1}H MRS to identify key biomarkers in epileptogenesis and to serve as a surrogate marker of therapeutic efficacy.

First, most existing ^{1}H MRS methodologies do not have the coverage necessary to study the entire brain with high spatial resolution. Traditional single voxel techniques require the regions of interest to be defined *a priori*, which is frequently the hippocampus in the case of temporal lobe epilepsies. However, such prior knowledge is generally unavailable for non-temporal lobe cases, particularly in the more difficult cases with negative anatomic MRI findings. While spectroscopic imaging studies have made some headway in characterizing the metabolomic profile of epileptic versus non-epileptic brain regions by providing increased coverage with relatively high spatial resolution generally along a pre-defined two-dimensional plane, this plane of interest needs to be defined *a priori*, and as a result these studies also tend to focus on the temporal lobe structures (Hetherington et al., 2007; Pan et al., 2012). Only recently, with continued development of the echo-planar spectroscopic imaging (EPSI) technique (Posse,

DeCarli, & Le Bihan, 1994) by Maudsley and colleagues, has whole brain coverage become a possibility (Maudsley et al., 2006; Maudsley et al., 2009a; Maudsley, Domenig, & Sheriff, 2009b). The application of this technique to epilepsy has been promising for non-temporal lobe epilepsies and its findings have been consistent with those in existing literature (Maudsley, Domenig, Ramsay, & Bowen, 2010; Mueller et al., 2010).

Second, existing MRS studies of epilepsy generally do not have the spatial resolution needed to selectively study a particular tissue type but will instead capture a mixture of gray matter, white matter, and cerebrospinal fluid (CSF) in what is called a partial volume effect. This distinction is important because gray and white matter have differing concentrations of metabolites (Hetherington et al., 1994; Hetherington et al., 1996; Kreis, Ernst, & Ross, 1993). Therefore, varying ratios of gray matter, white matter, and CSF can dramatically impact the interpretation of the findings in a typical MRS study. Although the metabolite values may be statistically corrected to improve sensitivity (Chu et al., 2000), many studies do not perform such corrections or may opt to circumvent the issue by judicious placement of the ROI over a particular structure of interest (e.g. hippocampus). Given the layer-specific distribution of gene expression differences between epileptic and non-epileptic neocortex observed by our laboratory, this issue of gray and white matter composition would appear to be especially important to consider in an MRS study of neocortical epilepsy.

Finally, very few studies have examined the relationship between ^{1}H MRS metabolites and electrophysiology parameters such as IEDs or seizure frequency (Hammen et al., 2007; Park et al., 2002; Serles, Li, Caramanos, Arnold, & Gotman, 1999), and even fewer studies have attempted to further examine those changes in the context of genetic or histologic changes between epileptic and non-epileptic regions (Peeling & Sutherland, 1993; Petroff, Pleban, &

Spencer, 1995) and none of them were done in recent years. The past several years have seen an increased ubiquity of high field strength systems with more advanced hardware capabilities resulting in much improved sensitivity. With this increase in the power of ^{1}H MRS to detect metabolite differences, interpretation and validation of these differences becomes increasingly important in the process of identifying reliable and relevant biomarkers for epilepsy that may be translated for clinical use. This degree of validation and characterization can only be accomplished through the combination of multiple experimental modalities and approaches.

This project seeks to address some of these issues by combining ^{1}H MRS measurements with other transcriptional, cellular, and electrophysiological parameters collected in parallel with our well localized *ex vivo* tissue from the superficial layers of the epileptic human neocortex. Our end goal is to identify relevant ^{1}H MRS metabolite biomarkers that can also inform us about the underlying molecular changes taking place in these patients. Our longitudinal study using a rat model of epileptogenesis *in vivo* attempts to investigate the complex relationship between electrophysiological changes and metabolite changes in the rat neocortex overtime. The results from this *in vivo* animal study can also serve as a validation of our findings from the *ex vivo* human tissue study.

CHAPTER 3: A UNIQUE METABOLITE PROFILE PREDICTIVE OF EPILEPTIC NEOCORTEX IN HUMANS *EX VIVO*

3.1 Summary

Identifying biomarkers that reliably detect epileptic brain regions is crucial for accurate diagnosis and therapy development. At present, only surgically invasive, direct brain recordings are capable of detecting these regions with precision. We performed an integrated metabolomic-genomic-histological analysis of electrically mapped human cortical tissue samples from epilepsy surgery patients using high resolution magic angle spinning (HR-MAS) ^{1}H MRS and cDNA microarrays. We found a highly consistent and predictive metabolite logistic regression model with reduced lactate and increased creatine plus phosphocreatine (Cr+PCr) and choline (Cho), suggesting a chronically altered metabolic state in epileptic brain regions. Linking gene expression, cellular, and histological differences to these key metabolites using a hierarchical clustering approach revealed altered metabolic vascular coupling. Consistently, this pattern correlated strongly to neovascularization associated with recently discovered, millimeter-sized histological microlesions. These results provide evidence for spatially segregated metabolic derangements indicative of underlying vascular and synaptic aberrations in human epileptic brain regions that could be used to develop non-invasive clinical biomarkers of epilepsy.

3.2 Introduction

As mentioned in Chapter 1, epileptic regions of the brain produce abnormal synchronous discharges across large populations of neurons. These discharges can remain isolated, as in the case of IEDs, or they can propagate and affect large regions of the brain, resulting in seizures. While the exact relationship between interictal spiking and seizures is not understood (Gotman, 1991), their localization is highly concordant and the removal of both regions is associated with improved surgical outcome (Asano et al., 2003; Bautista et al., 1999; Kanazawa et al., 1996; Lee

et al., 2014). Animal studies have shown that interictal spikes may precede and hence be a biomarker of seizure development (White et al., 2010). Here, we are specifically interested in identifying metabolite biomarkers that can classify high versus low spiking tissue samples, with the inference that high spiking activity more readily reflects epileptic tissue while low to no spiking tissue more readily reflects normal tissue.

As part of our systems biology of epilepsy program (SBEP) (Loeb, 2011), we collected electrically-mapped regions of human neocortex from patients undergoing long-term invasive monitoring with ECoG to localize precisely regions that produce seizures and interictal spiking (Loeb, 2011) (Figure 3.1). SBEP was designed to integrate quantitative clinical, neurochemical, electrical, and genomic signatures of different brain regions with and without significant epileptic activities (Beaumont et al., 2012; Dachet et al., 2015; Lipovich et al., 2012; Rakhade et al., 2005). By knowing the *in vivo* electrical behavior of each resected piece of tissue, we have a unique ability to compare highly epileptic brain regions to nearby electrically quiet regions of each patient serving as internal controls. Studies from this program have implicated layer-2/3-specific activation of MAPK and CREB signaling and the presence of deeper "microlesions" that show a dramatic reduction in axodendritic connectivity in brain regions with high levels of epileptic activity (Dachet et al., 2015).

MRS is a technique for characterizing compounds associated with tissue metabolism with high translational potential since it can be applied to both intact tissue samples *ex vivo* as well as to animal models and human patients *in vivo*. As reviewed in Chapter 2, previous ^{1}H MRS studies of epilepsy have demonstrated perturbations in the neurochemistry of epilepsy patients and have assisted in efforts to lateralize or localize the epileptic focus, particularly in temporal lobe epilepsies; however, a highly sensitive and specific set of non-invasive biomarkers have yet

to emerge in part due to uncertainties in localization, poor spatial distinction of epileptic and non-epileptic brain regions, and studies being done using relatively low field strength MR systems (e.g. 1.5T systems).

Here, we addressed these challenges by using human tissues precisely localized from ECoG brain recordings *in vivo* and analyzed the samples by using an ultra-high field spectrometer at 11.7 T using HR-MAS ^{1}H MRS, which allows for metabolite profiling of intact brain tissue with superior spectral resolution (Andrew et al., 1959; Cheng et al., 1996; Cheng et al., 1997). We asked whether focal regions of human neocortex have a unique metabolomic signature that may be adapted for use as non-invasive biomarkers of epileptic activity. More specifically, we performed HR-MAS ^{1}H MRS on neocortical tissue samples from 9 patients undergoing surgical treatment for their intractable epilepsy. Their clinical ECoG data were used to quantify the interictal spiking rates in various regions of their brain in order to identify which tissue sample can be classified as high spiking and which sample can be classified as low spiking. Using the measured metabolites, we were able to construct a metabolite profile that is able to predict whether or not a particular piece of tissue sample was high or low spiking with great accuracy. We also performed additional genome wide expression studies using Agilent microarrays and histology on the same tissue samples to characterize transcriptional, cellular, and histological features associated with their metabolite profile (Figure 3.1).

Given the robust gene expression differences between high and low interictal spiking activity in MAPK/CREB activation and the downstream consequences they would presumably have on protein and small molecule expression, we expect to be able to detect differences in downstream ^{1}H MRS metabolite levels between high and low spiking tissues. A relative decrease in NAA levels within high spiking regions is expected, since that is the observed

metabolite feature of epilepsy most consistently reported in literature.

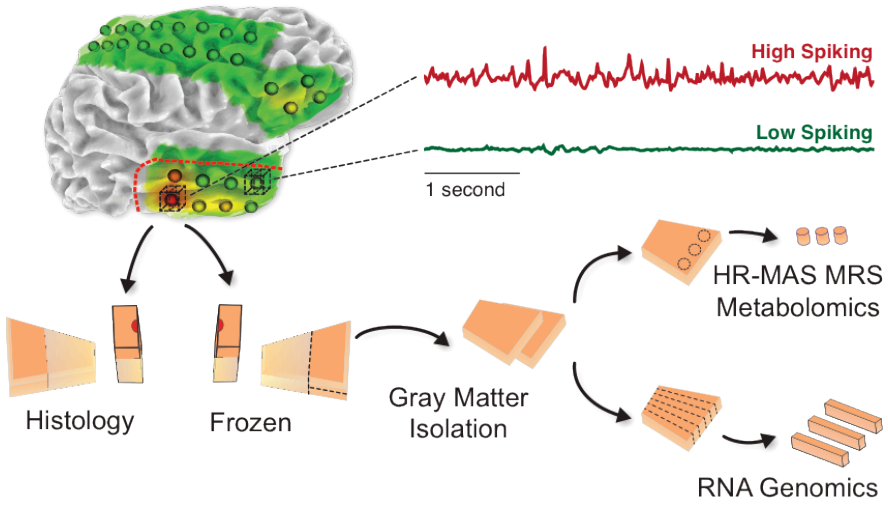

Figure 3.1 Human brain tissues were removed as part of planned surgery for refractory epilepsy. Regions of high and low spiking were identified based on long-term subdural ECoG. Each section of tissue was precisely mapped to the overlying subdural electrode and then split into two halves. One half as used for histology while cortical gray matter is isolated from the other half. The cortical gray matter is then further divided into two portions, half of which is used to generate RNA for microarray analysis while the other half is used for HR-MAS ^{1}H MRS.

3.3 Methods

3.3.1 Isolation of human tissue and electrophysiology

Brain tissue samples from our 9 human subjects with refractory epilepsy were obtained with informed consent as part of a research protocol approved by the Wayne State University Institutional review Board and their participation in the study had no influence on their clinical care or treatment plan. Their age, gender, and other relevant clinical features are given in Table 3.1. All 9 subjects underwent two-stage surgery with long-term subdural ECoG, where Stage 1 consisted of initial electrode placement for long-term recording and observation, followed by Stage 2, where the seizure generating areas identified in Stage 1 were resected. Briefly, interictal spiking activity on ECoG were determined by averaging spike counts from 3 independent 10 min segments of ECoG recording, which were continuously recorded for at least 3 days prior to resection. Electrode placements were mapped precisely to their corresponding locations on the

neocortex using a combination of intraoperative electrode placement photos, as well as pre- and post-placement head CT, MRI, and X-rays. A tissue sample block at each electrode location was removed and divided into two halves. One half fixed in 4% paraformaldehyde for use in histological studies while the other half was stored frozen at minus 80°C until it can be used for further analysis (Figure 3.1).

Patient	ILAE Classification	Age of Onset	Age at Surgery	Sex	Region	MRI Findings	Outcome (Engel 6 months)	Other tissue diagnoses	Spike Frequency		Microarray Characteristics (% genes)		
									Low	High	Increase	Decrease	Total
1	NA	NA	10	F	Temporal	PO	NA	DG, AI, NLP	1	116	7.6	9.2	16.8
2	SG	9	11	F	Frontal	BSH	NA	H	0	5	2.6	5	7.5
3	ES, PC	0.4	3	F	Parietal	PE	I	WG, SupH	66	141	6.2	4.2	10.3
4	ES	0.5	3	F	Temporal	BGW	I	MG	56	212	4.9	5.4	10.2
5	SG	NA	7	F	Frontal	P, W	I	CD, MG	25	215	11.6	11.1	22.7
6	ES	2	6	F	Frontal	TC, CD?	I	MG	26	124	16.5	15	31.5
7	ES	0.5	8	M	Parietal	NA	III	MG	3	172	10.2	9.8	19.9
8	PC, SG	0	16	M	Temporal	PO	I	DG	44	176	6.9	10.6	17.5
9	SG	6	11	F	Frontal	Normal	I	MCD	2	66	4.8	4.1	8.9

Table 3.1 Profile of patients with neocortical epilepsy and the corresponding tissue samples that were used for this study. Spike frequency reflects epileptiform spike rates for both high and low spiking regions in the patient's brain, recorded *in vivo* using ECoG as part of their clinical treatment plan. Microarray characteristics show percent of genes that are at least 1.4 fold increased or decreased (after FDR correction to 1%) in expression in high spiking relative to low spiking samples. Documented tissue pathologies ("Other tissue diagnoses") were made from separate clinical tissue samples and were not present in the tissues used for this study, which were normal appearing on histology. Abbreviations: acute inflammation (AI), blurring of grey-white junction (BGW), bifrontal subcortical heterotopias (BSH), cortical dysplasia (CD), probable cortical dysplasia (CD?); diffuse gliosis (DG), epileptic spasms (ES), heterotopia (H), mild cortical dysplasia (MCD), mild gliosis (MG), data not available (NA), normal laminar pattern (NLP), polymicrogyria (P), partial complex (PC), periventricular mild increase in FLAIR (PE), porencephalic cyst (PO), secondary generalized: evolution from focal to bilateral, convulsive seizure (SG), superficial heterotopia (SupH), thickened cortex (TC), increased white matter signal (W), white matter gliosis (WG).

Because of the great variance between patients in absolute spike frequency between regions considered for high and low spiking, we dichotomized spike frequency into "high" and "low" spiking categories in order to reduce strong leverage effects. For each patient, the subdural electrode demonstrating the highest spiking frequency was classified as "high spiking" and the electrode with the lowest or no spiking is classified was "low spiking." In this manner,

high and low spiking electrodes for each patient were identified and analyzed using both microarray and HR-MAS ^{1}H MRS at 11.7T. For the purposes of this study, low spiking electrodes were considered internal controls for each patient, effectively controlling for within-subject tissue variability (Loeb, 2010). All tissue regions selected for this study were free of apparent pathological changes and surgical hemorrhage based on gross examination and histology. Histological tissue studies were done as described in our previous study (Dachet et al., 2015).

3.3.2 Microarray analysis and detection of differentially expressed genes

For microarray studies, total RNA was isolated from pooled alternating strips of full-thickness (layers I-VI) neocortical gray matter, helpful in averaging out small local differences. A quadruplicate, flip-dye experimental design, as described (Beaumont et al., 2012; Rakhade et al., 2005), was used for each pair of high and low spiking samples within every patient. Briefly, labeled antisense RNAs were spin column purified and hybridized to human, genome-wide 60-mer oligonucleotide arrays (Catalog #G411A, Agilent), in a two-color dye-swap fashion. Differentially expressed genes were identified with a two-step hierarchical linear mixed model, correcting for array, dye, patient, array-die interactions and within-patient effects. Genes that had more than a 1.4-fold change between high and low spiking samples with a false discovery rate of < 0.01 were considered to be differentially expressed. We identified 990 such differentially expressed genes from our samples obtained from 9 subjects.

3.3.3 High resolution Magic Angle Spinning ^{1}H MRS

HR-MAS ^{1}H MRS spectra were acquired from 2 mm punches obtained from the apical neocortical gray matter (layers I-III), for each pair of high and low spiking samples within every patient in triplicate, at minimum, while frozen on solid CO_2. Tissue samples that were larger in

size may have more than 3 replicates. The median number replicates for low spiking tissue was 4 with a range from 3 to 8 and the median number of replicates for high spiking tissue was 6 with a range from 3 to 9. The frozen punches analyzed using HR-MAS ^{1}H MRS on a 500 MHz (11.7T) Bruker Avance DRX-500 spectrometer equipped with a g-HR MAS 500 WB BL4 P-HD probe (Bruker BioSpin Corporation, Billerica, MA) as described by Ghoddoussi and colleagues (Ghoddoussi et al., 2010). The samples were placed directly into a Bruker zirconium rotor containing 5μL phosphate buffer (pH = 7.4), D_2O, trimethylsilyl-proprionate (TSP) as the internal chemical shift reference (0.00 ppm), and formate for phase correction (8.44 ppm). The sample was maintained at 4°C and spun at 4.2 ± 0.002 kHz while positioned at 54.7° relative to the static magnetic field, B_0. Semi-automated and manual first and second order shimming was used to reduce field inhomogeneities. A rotor-synchronized 1-D Carr-Purcell-Meiboom-Gill (CPMG) with $[90°-(\tau-180°-\tau)_n]$ pulse sequence was used to acquire tissue spectra (Cheng et al., 1996). To take advantage of CMPG ability to filter out signals from molecules with short T_2 relaxation values, such as large signals from fat (Mountford, MacKinnon, Delikatny, & Russell, 1992), twelve echo pulses were applied (n = 12) with an inter-pulse delay (τ) of 150 μs for TE = 3.6 ms (echo time) and TR = 6.21 s (repetition time). All spectra were acquired at a spectral bandwidth of 7 kHz (14 ppm) with 128 averages for a total acquisition time of approximately 13 min per sample. A representative high quality sample spectrum is given in Figure 3.2.

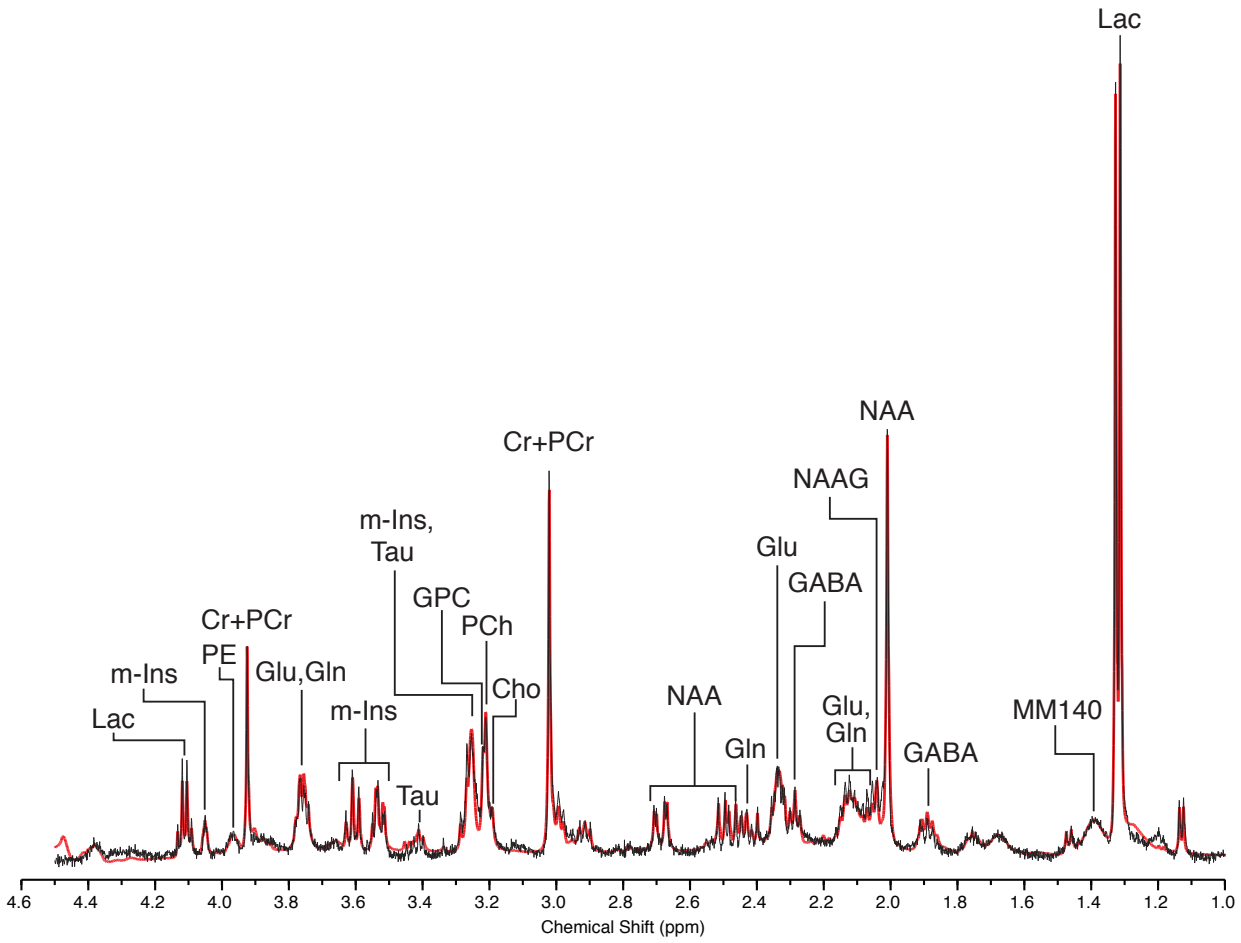

Figure 3.2 Representative high quality HR-MAS ^{1}H MRS spectrum of human brain performed on partial thickness neocortical sample (layers I-III). LCModel fitted spectrum (red line) shows excellent correspondence with averaged raw signal (thin black line). Abbreviations: free choline (Cho), creatine plus phosphocreatine (Cr+PCr), γ-aminobutyric acid (GABA), glutamine (Gln), glutamate (Glu), glycerophosphorylcholine (GPC), *myo*-inositol (m-Ins), lactate (Lac), macromolecules at 1.4 ppm (MM140), N-acetylaspartate (NAA), N-acetylaspartylglutamic acid (NAAG), phosphorylcholine (PCh), phosphorylethanol-amine (PE), taurine (Tau).

3.3.4 ^{1}H MRS quantitation

The raw ^{1}H MRS spectra were analyzed using LCModel (Provencher, 1993) with a custom experimentally derived basis-set containing 27 individual neurochemical metabolite model spectra combined with simulated lipid and macromolecule signals. The experimentally derived basis-set was obtained under identical experimental conditions as the tissue analysis. A complete list of all the metabolites included for fitting is provided in Appendix A. The concentrations of metabolites located between 1.0 to 4.5 ppm, a range containing the major

resonances from all the metabolites of interest, were estimated using LCModel. These concentrations were ultimately expressed as a normalized mole percent of total metabolites, allowing measurements to be relatively insensitive to changes in extracellular volume (Klunk, Xu, Panchalingam, McClure, & Pettegrew, 1994). LCModel's estimated confidence of the fitted metabolite spectra (i.e. how well it matches the original data) is estimated using Cramér-Rao Lower Bounds (CRLB). For this study, only metabolites with average CRLB values less than or equal to 10% were used for analysis.

3.3.5 Tissue discrimination and clustering

In order to get a general sense of whether or not there are detectable differences in metabolites between high and low spiking regions, a t-test was initially performed on all 14 metabolites of interest to determine if significant differences exist between the metabolite in high and low spiking tissues. More refined classification and discrimination of high and low spiking samples using the metabolite profiles of all the samples were performed using generalized estimating equation (GEE) logistic regression model with an exchangeable covariance matrix implemented in R with geepack (Højsgaard, Halekoh, & Yan, 2005; Team, 2014) to help account for within-subject variability, since the samples were measured in multiplicates. Receiver Operating Characteristic (ROC) curves, as a measure of model performance, were calculated using pROC package, together with a bootstrap estimated 95% confidence interval of the model sensitivity (Robin et al., 2011).

Because several metabolites were highly correlated ($r > 0.8$) with each other, principal components analysis (PCA) was initially used to address the underlying issue of multicollinearity. Since the goal of our PCA analysis was to minimize multicollinearity, we chose to include the maximum number of components possible (i.e. 14 components) for our full

model GEE logistic regression, in order to make predictions on whether a particular tissue sample is high or low spiking. The appropriateness of using the varimax orthogonal rotation method of PCA is validated by both an adequate Kaiser-Meyer-Olkin measure of sampling accuracy (MSA = 0.84) as well as significant Bartlett's test of sphericity, $\chi^2(91) = 1109$, $p < .001$, indicating that the data is appropriate for PCA analysis (Dziuban & Shirkey, 1974). The resultant factor scores were used as predictors in our logistic regression model. This resultant logistic regression model used a given sample's measured metabolite profile to determine a predicted probability ($\hat{p}$) that the sample was a high spiking sample.

The full 14 component model performed extremely well in discriminating high versus low spiking tissue with an ROC area under the curve (AUC) of 0.90, 95% CI [0.83, 0.96] (Figure 3.3). For comparison, the AUC for the diagonal line on the ROC is 0.50, and represents the performance of chance classification (i.e. random guessing). A maximum accuracy of 83% along with 85% sensitivity and 81% specificity was achieved using cutoff threshold of 0.57, where all $\hat{p} \geq 0.57$ would be considered "high spiking" while those below the cutoff would be considered "low spiking." Gender was not included as a covariate in the model due to the highly uneven distribution between female (n = 7) and male (n = 2) participants. Effects of both region (based on electrode placement) and subject age were tested and determined to have insignificant effects on the model overall (χ^2 (1) = 0.213), and hence were removed from all analyses to reduce over fitting. The component playing a significant role (Wald p-values < 0.10) in discriminating high from low spiking samples were identified and from them, we then selected the key metabolite from each component demonstrating the highest loading factor from metabolites that showed loading factors of at least 0.80.

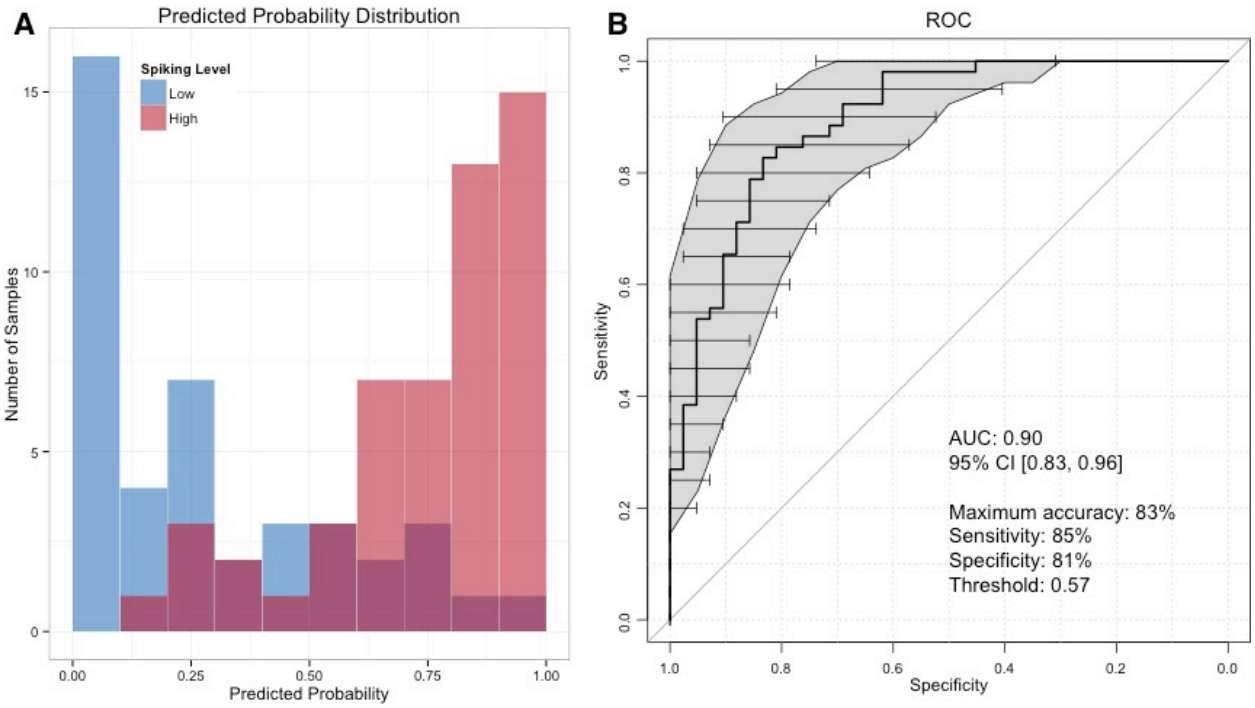

Figure 3.3 Logistic regression performed using the maximum 14 components obtained from principal components analysis demonstrates high sensitivity and specificity in discriminating high spiking tissue samples from low spiking tissue samples. A) Distribution of high and low spiking tissue samples (red and blue shading, respectively) and their predicted probabilities of being high spiking are illustrated in the histogram. B) Overall model performance is characterized by a receiver operating characteristic (ROC) area under the curve (AUC) of 0.90, indicating excellent discrimination between high and low spiking tissues. Gray regions and horizontal error bars indicate the estimated 95% confidence intervals of sensitivity and specificity using non-parametric bootstrapping of 1000 samples

To better understand the mechanisms behind the differences in metabolite expression, these metabolites of interest are used for additional correlational clustering studies in order to observe how changes in key metabolites can correspond to changes in gene expression and cell type distribution. Pearson correlations between the 990 differentially expressed genes (described above) across the 18 high and low spiking samples obtained from our 9 subjects and their corresponding mean metabolite concentrations for each sample were calculated (Dachet et al., 2015). Linkages between two genes were created when Pearson correlations were ≥ 0.70. This cutoff is also consistent with a false discovery rate (FDR) of < 0.07 (Benjamini & Hochberg, 1995). Clusters were further analyzed using a combination of ConsensusPathDB (Kamburov,

Stelzl, Lehrach, & Herwig, 2013) and primary literature searches for functional and pathway enrichment. For enriched pathways proposed by ConsensusPathDB, a cutoff threshold of FDR adjusted $p < 0.05$ was used to selected potentially significant pathways associated with each metabolite-gene clusters. Additional associations between metabolites and putative cell types are explored using Pearson correlation based hierarchical clustering using the average linkage method. Cluster relationships are further characterized using the actual Pearson correlations themselves, where Pearson correlations ≥ 0.70 (FDR adjusted $p < 0.05$) are considered statistically significant.

3.4 Results

Overall, the acquired ^{1}H MRS signals were of very high quality. The mean signal to noise ratio (SNR) was estimated to be 34.3 ± 8.41 (mean ± s.d) by LCModel. A total of 14 metabolites with mean CRLB of less than or equal to 10% were used for analysis. They were: choline (Cho), glycerophosphorylcholine (GPC), γ-aminobutyric acid (GABA), glutamine (Gln), glutamate (Glu), myo-inositol (m-Ins), lactate (Lac), N-acetylaspartate (NAA), N-acetylaspartyl glutamic acid (NAAG), phosphorylcholine (PCh), phosphorylethanolamine (PE), taurine (Tau), simulated macromolecule at resonance position 1.40 ppm (MM140) and creatine plus phosphocreatine (Cr+PCr).

Mean values for the 14 metabolites in high spiking and low spiking tissue samples are summarized in Table 3.2. Statistically significant ($p < 0.05$) differences between high and low spiking tissues based on Student's t-tests were found in 4 of 14 metabolites, namely Cho, PCh, Lac, and PE. All were decreased in high spiking tissue.

Metabolite	Low Spiking Mean (SE)	High Spiking Mean (SE)	Percent Change	t-Test (p, 2-tailed)
* **Cho**	**0.61 (0.04)**	**0.50 (0.02)**	**-19%**	**.01**
Cr+PCr	8.55 (0.24)	8.36 (0.21)	-2%	.56
GABA	3.13 (0.11)	3.10 (0.09)	-1%	.79
Gln	3.75 (0.25)	3.53 (0.15)	-6%	.44
Glu	7.03 (0.19)	6.81 (0.21)	-3%	.44
GPC	0.58 (0.03)	0.58 (0.03)	0%	.98
m-Ins	5.11 (0.22)	4.63 (0.15)	-9%	.07
*** **Lac**	**15.06 (0.38)**	**12.98 (0.48)**	**-14%**	**< 0.001**
MM140	28.80 (1.62)	32.17 (1.42)	12%	.12
NAA	5.40 (0.20)	5.21 (0.18)	-3%	.49
NAAG	0.99 (0.03)	1.00 (0.03)	1%	.78
*** **PCh**	**0.93 (0.04)**	**0.78 (0.03)**	**-16%**	**< 0.01**
* **PE**	**2.36 (0.09)**	**2.11 (0.08)**	**-11%**	**.03**
Tau	2.02 (0.09)	2.03 (0.08)	1%	.90

Table 3.2 Means and standard errors (SE) of key metabolites measured from tissue samples of high and low spiking regions. Statistically significant differences were found between the high and low spiking tissue samples in 4 out of 14 metabolites (in bold) based on two-sample t-tests. All metabolites are normalized to the total fitted signals and expressed as percent total signal. Percent signal changes in high spiking tissue samples relative to low spiking tissue are also indicated for each metabolite. (* $p < 0.05$, ** $p < 0.01$, *** $p < 0.001$, uncorrected)

Further analysis of all 14 metabolites using a combination of PCA and GEE (Liang & Zeger, 1986) based logistic regression yielded a short list of 8 potentially important metabolites. Of these, 6 were identified to make significant contributions (Wald $p < 0.05$) in differentiating high versus low spiking samples (Figure 3.4). They were: Cho, Cr+PCr, GPC, m-Ins, Lac, and NAAG (Figure 3.4B and Table 3.3). Our logistic regression model performed well, with a ROC AUC of 0.88, 95% CI [0.81, 0.95]. Our optimal accuracy in classifying high- versus low-spiking samples using these metabolites was 82% with a sensitivity of 85% and specificity 79% (Figure 3.4C). In summary, this metabolomic signature presents a highly sensitive and specific new way to differentiate epileptic brain regions from their non-epileptic counterparts and provides a potential approach to non-invasively "visualize" epileptic brain regions clinically using ^{1}H MRS.

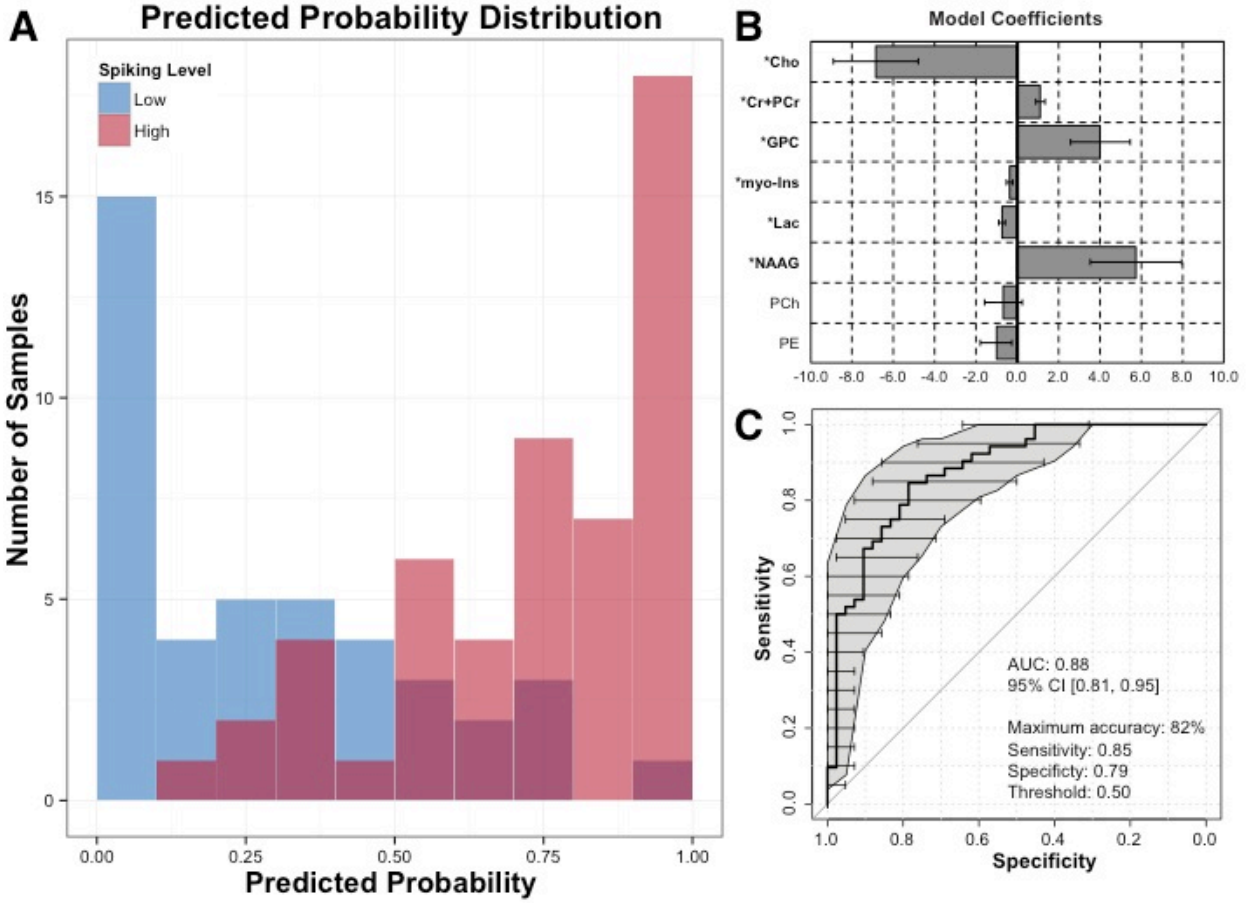

Figure 3.4 Logistic regression using 8 metabolites demonstrated high sensitivity and specificity in discriminating high spiking tissue samples from low spiking tissue samples. A) Distribution of high and low spiking tissue samples (red and blue shading, respectively) and their predicted probabilities of being high spiking are illustrated in the histogram. B) Model coefficients used for predicting high and low spiking tissue. Metabolites with significant ($p < 0.05$) contributions to the model are bolded. C) Overall model performance is characterized by a receiver operating characteristic (ROC) area under the curve (AUC) of 0.88, indicating excellent discrimination between high and low spiking tissues. Gray regions and horizontal error bars indicate the estimated 95% confidence intervals of sensitivity and specificity using non-parametric bootstrapping of 1000 samples.

	Metabolite	Estimate (SE)	SE	95% CI for Odds Ratio			Adjusted OR	Wald p-value
				OR	Lower	Upper		
**	(Intercept)	0.41 (0.14)	0.13	1.50	1.15	1.97	1.04	< 0.01
***	**Cho**	**-6.83 (2.06)**	**1.83**	**1.08E-03**	**1.92E-05**	**6.06E-02**	**0.51**	**< 0.001**
***	**Cr+PCr**	**1.13 (0.22)**	**0.34**	**3.09**	**2.02**	**4.72**	**1.12**	**< 0.001**
**	**GPC**	**4.01 (1.45)**	**1.39**	**55.3**	**3.20**	**9.56E+02**	**1.49**	**< 0.01**
*	**myo-Ins**	**-0.37 (0.17)**	**0.16**	**0.69**	**0.50**	**0.97**	**0.96**	**.03**
***	**Lac**	**-0.74 (0.17)**	**0.17**	**0.48**	**0.34**	**0.67**	**0.93**	**< 0.001**
**	**NAAG**	**5.75 (2.22)**	**0.09**	**315**	**4.08**	**2.43E+04**	**1.78**	**< 0.01**
	PCh	-0.67 (0.91)	2.09	0.51CV	0.09	3.06	0.94	.46
	PE	-1.02 (0.76)	0.81	0.36	0.08	1.59	0.90	.18

Table 3.3 Logistic regression parameter estimates and odds ratios of metabolites included in the final predictive model. Significant metabolite predictors are indicated in bold and are in good agreement with results from the two-sample t-tests. Exponentiation of parameter estimates gives their corresponding odds ratios (OR). An OR greater than 1 indicates that for a given unit increase in the specified metabolite within a sample, there is also an increase in the probability of the tissue sample being high spiking. In contrast, OR less than 1 indicates decrease in the likelihood that a tissue sample is high spiking for a unit increase in the specified metabolite. Adjusted OR are odds ratios calculated for every 0.1 increment of a metabolite instead of the standard 1.0 increment used to calculated standard OR. It is important to note that the odds ratios are multiplied by for every unit increment in the predictor (i.e. metabolite levels) due to the exponential nature of logistic regression. For example, in the case of choline, a 0.20 unit increase in choline reduced the odds of the tissue being high spiking by a factor 0.26 (i.e. $0.51 \times 0.51 = 0.26$) (* $p < .05$, ** $p < .01$, *** $p < .001$)

In order to better understand the significance of these findings, we performed an integrative analysis of metabolomic, transcriptional, and histological measures from each of the 18 brain samples, as outlined in Figure 3.1. Two major clusters of gene-metabolite interactions emerged, centering on changes in energy state, with a down regulation of lactate and upregulation of Cr+PCr (Figure 3.5). Down-regulated lactate clustered with a group of genes associated with G-protein coupled receptor (GPCR) signaling and angiogenesis pathways (FDR adjusted $p < 0.01$), specifically *VEGFA*, *FLT1*, *RGS1*, *RGS2*, *RHOU*, *GNA13*, and *TFRC*, all of which were up-regulated in high-spiking brain regions. Also notable from the cluster was the upregulation of multiple genes associated with ubiquitination, highly suggestive of the preferential involvement of the ubiquitin-proteasome pathway (UPP) in high spiking areas.

Using a larger set of brain samples, some of which were included here, we developed a novel clustering approach to predict cell-type specific changes in regions of high versus low epileptic spiking, creating what we called a "cellular interactome" (Dachet et al., 2015). In that study, we showed consistent differences in high spiking tissues that included increases in blood vessel density, inflammatory microglia, and millimeter-sized microlesions in deeper cortical layers. These microlesions contain a unique population of neurons with reduced NeuN staining (Type 1 Neurons) and increased microglia (Type 1 Microglia). Combining the cellular interactome with the present metabolomic dataset, we found significant correlations between reduced lactate and Neuron 1 ($r = 0.76$; $p < 0.05$) and increased Cr+PCr and Microglia 1 ($r = 0.72$; $p < 0.05$) (Figure 3.6A-B). Both cell populations correlated with the degree of epileptic activity and the number of microlesions (Dachet et al., 2015). Histological examination of the specific tissue samples used here consistently showed the increased presence of microlesions and increased vascular density in high versus low spiking regions (Figure 3.6C). Taken together the combined genomic-metabolomic and cellular interactome suggests the existence of a unique signature linked to altered tissue energy demand and consumption in high spiking brain tissue that could serve as a clinically translatable, non-invasive biomarker for the functional and structural abnormalities that underlie human neocortical epilepsy.

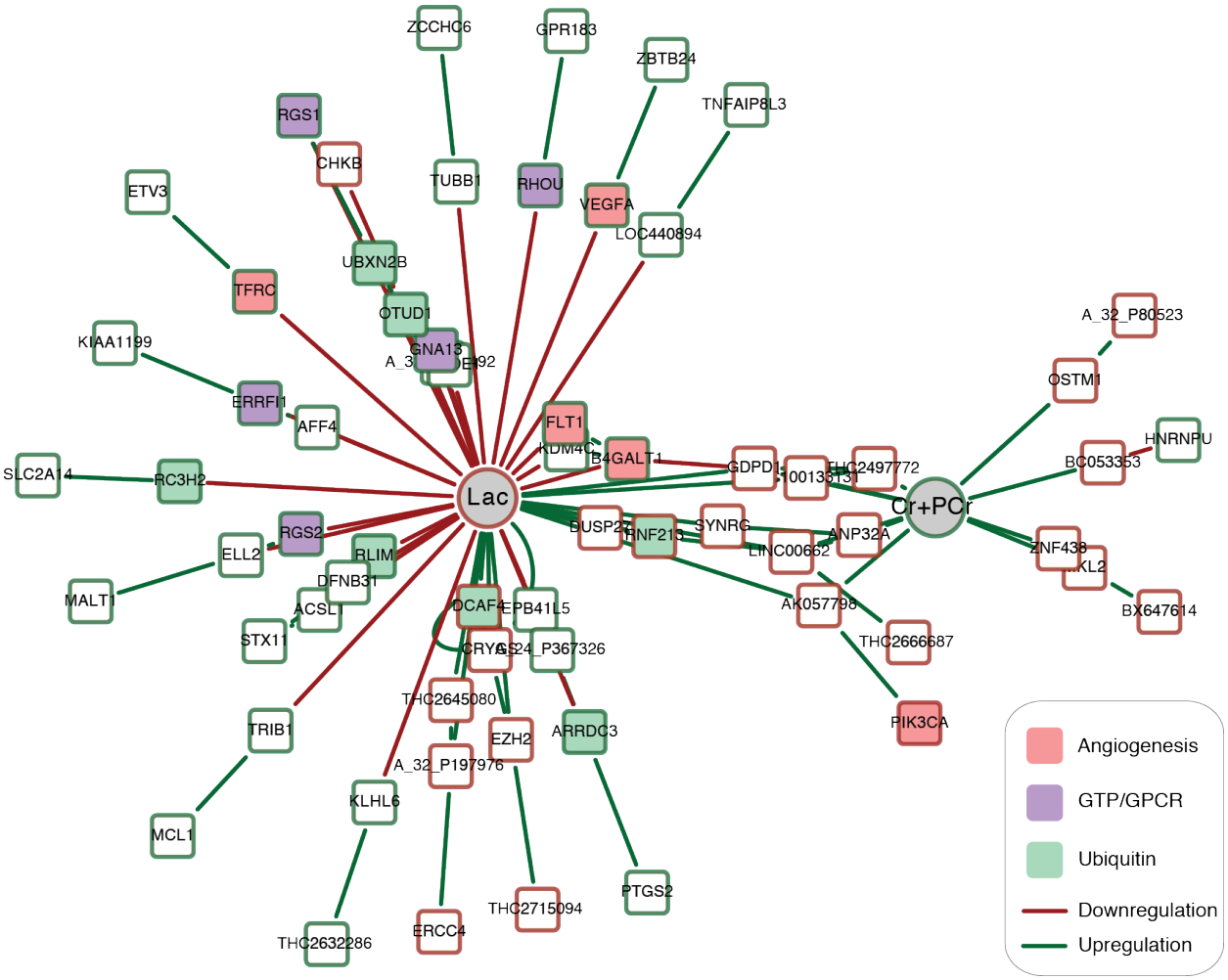

Figure 3.5 Correlational clustering between predictor metabolites and differentially expressed genes in high spiking tissues demonstrate a large cluster of up-regulated genes around lactate, a negative predictor of high spiking. Upregulated genes are indicated in green and downregulated genes are indicated in red. Pathway enrichment analyses indicate many of these differentially expressed genes to be involved in G-protein signaling, angiogenesis as well as ubiquitination. Relevant genes in the lactate cluster include: VEGFA, FLT1, RGS1, RGS2, RHOU, GNA13, PK3CA, and TFRC.

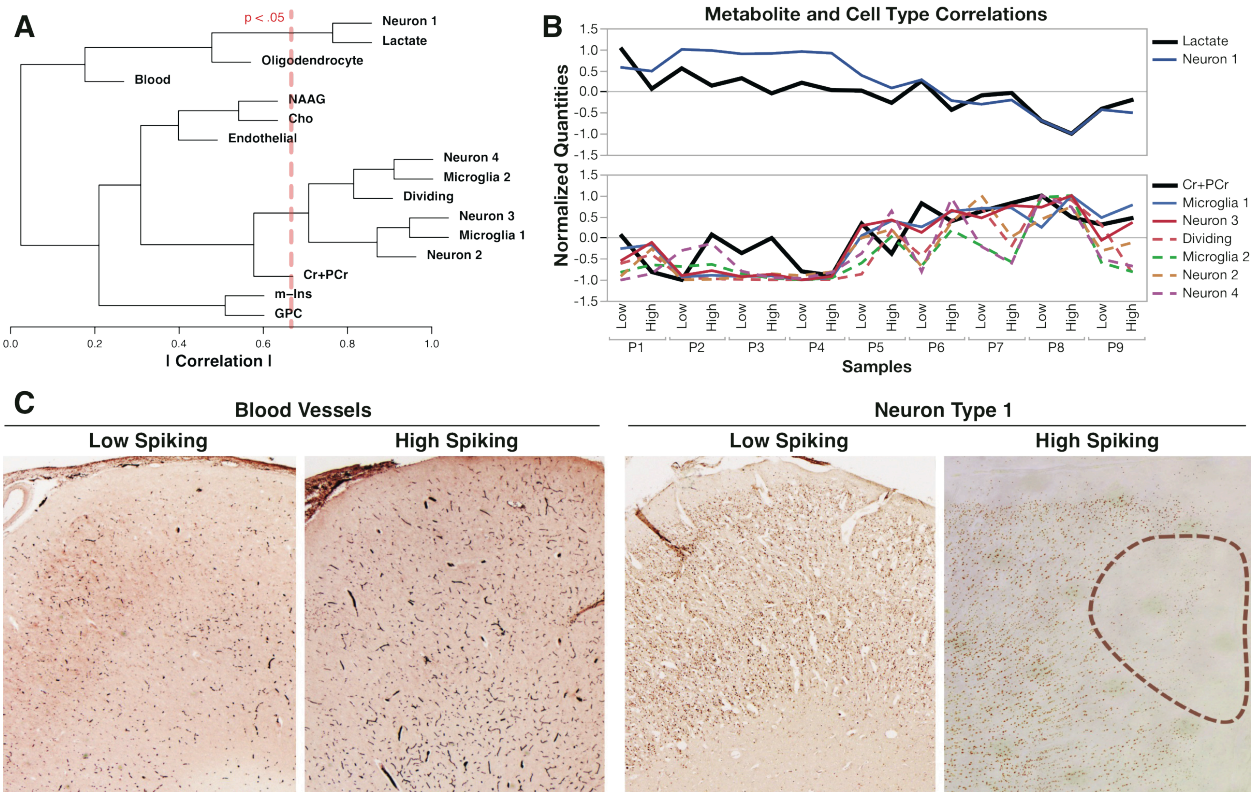

Figure 3.6 A) Hierarchical clustering between metabolites and cell types show significant associations between lactate and Neuron Type 1 (Neuron 1) and also between Cr+PCr and Microglia Type 1 (Microglia 1). The red line indicates significance threshold of correlation, where paired relationships to the right of the line are significant. B) Normalized expression over all 18 samples between Lactate and Neuron Type 1 and between Cr+PCr and the cluster consisting of Microglia Type 1 and several other cell correlational clusters show stronger clustering between lactate, Cr+PCr and several cell types with the correlations between Microglia Type 1 and Neuron Type 3 being significant (solid lines). Other correlations in the same cluster, while not statistically significant, are also shown (dashed lines). C) Representative histology from Patient 1 demonstrating increased blood vessels and the presence of microlesions (outlined) showing reduced NeuN staining in high spiking tissue compared to its low spiking counterpart.

3.5 Discussion

Epilepsy has been a challenging disease to diagnose and develop novel treatments for due to limitations in non-invasive methods to identify epileptic brain regions. Scalp EEG recordings can reliably detect epileptic discharges occupying at least 10 cm^2 of brain tissue (Tao, Ray, Hawes-Ebersole, & Ebersole, 2005). ^{1}H MRS, with its ability to simultaneously measure multiple metabolites, offers a potentially powerful means to detect epileptic brain regions. While

previous ^{1}H MRS epilepsy studies have focused on epilepsy associated differences in individual metabolites or the ratios of a few metabolites, changes in the entire metabolite profile, as demonstrated by our findings here, could be informative for the development of high resolution brain maps of epileptic activities. The unique metabolomic-genomic differences discovered here for high-spiking epileptic human brain suggest that high spiking regions of the neocortex have a unique metabolic and energetic signature that could enable non-invasive ^{1}H MRS approaches to differentiate these brain regions from their normal counterparts.

The systems biology approach applied here linking human brain electrical activity to metabolomics, genomics, and cellular/histological changes offers a powerful, unbiased approach to discover and simultaneously validate biomarkers of human epileptic brain. Hierarchical clustering between metabolites and cellular changes, as defined by their transcriptional profile, showed a close parallel between the down-regulation of both lactate and Type 1 Neurons. This was validated through the identification of reduced NeuN staining within microlesions that we found to be present in high numbers in human cortical epileptic brain regions (Dachet et al., 2015). Similarly, the upregulation of Cr+PCr correlated with an increase of other neurons and Type 1 Microglia. Interestingly, microglia have also been shown to express high levels of PCr (de Gannes, Merle, Canioni, & Voisin, 1998), which may help explain Cr+PCr as a positive predictor of high spiking activity.

Exactly why lactate is consistently downregulated in these brain regions is not clear. This may be due to unmet energy demands due to frequent IEDs leading to lactate consumption as an alternative energy source. While one would expect surgically excised tissue to become hypoxic and increase lactate levels, our unique study design using multiple paired samplings of both high and low spiking samples from within the same patient should control for this. Recent

work has shown that inhibition of lactate dehydrogenase, the key enzyme that coverts lactate to pyruvate for use in the TCA cycle, can cause hyperpolarization in neurons and suppress epileptiform activity (Sada, Lee, Katsu, Otsuki, & Inoue, 2015). The strong correlational relationship between lactate and the cluster of genes enriched in angiogenesis is further validated by histological evidence of blood vessel proliferation in high spiking samples and may be a compensatory reaction to higher energy demands (Dachet et al., 2015). Selective involvement of angiogenesis factors in high spiking regions also hints at the potential role of anti-angiogenesis therapies as a potential mean to combat epileptogenesis. Indeed, Morin-Brueau and colleagues have recently carried out studies on the interaction between epileptiform activity and angiogenesis in rodent hippocampal cultures (Morin-Brureau et al., 2011). The results of their studies suggest that that targeted inhibitors of one or more downstream pathways associated with VEGF could be used potentially to treat epilepsy (Morin-Brureau et al., 2011; Morin-Brureau, Rigau, & Lerner-Natoli, 2012). More over, there is evidence for disrupted blood brain barrier (BBB) associated with VEGF overexpression in patients with intractable temporal lobe epilepsies (Morin-Brureau et al., 2011; Rigau et al., 2007), potentially allowing for the use of novel therapeutic agents that would have limited penetration through otherwise intact BBBs.

Contrary to what is most often reported in literature where NAA ratios with creatine or choline moieties are typically decreased in epileptic regions (Bernasconi et al., 2002; Breiter et al., 1994; Cendes et al., 1997b; Connelly, 1997; Matthews et al., 1990), NAA was not a significant predictor of high versus low spiking in our regression model. Levels of NAA between high and low spiking tissue samples were also not significantly different based on the results of our two-sample t-test. We suspect localization and partial volume effects to be major causes of this discrepancy. While vast majority of studies in literature specifically studied the

hippocampus or portions of the temporal lobe, we were very precise about using only the superficial layers of the neocortex for our HR-MAS ^{1}H MRS study, given that was where most of the transcriptional changes associated with MAPK/CREB activation were seen. Furthermore, ^{1}H MRS studies of neocortical epilepsy generally study metabolite differences between various regions of the brain where the ROIs typically include mixtures of both gray and white matter. Given the role that NAA is also known to play in myelin lipid synthesis (Chakraborty, Mekala, Yahya, Wu, & Ledeen, 2001; Mehta & Namboodiri, 1995), contributions of white matter NAA to the signal could lead to very different findings compared to NAA signals derived specifically from gray matter.

A key feature of these epileptic brain regions is the presence of microlesions that show dramatic, focal reductions in synaptic connectivity (Dachet et al., 2015). Consistently, the involvement of both choline and GPC in our predictive model suggests heightened cell membrane turnover in high spiking tissue. GPC and free fatty acids (FFA) are key breakdown products of phosphatidylcholine (Podo, 1999), a major membrane constituent. This breakdown process can be initiated under hypoxic conditions with the calcium-dependent activation of phospholipase A2 (PLA2), which is also responsible for the release of arachidonic acid, a potent inflammatory intermediate (Farooqui, Yang, Rosenberger, & Horrocks, 2002). Furthermore, in recurrent seizures, cortical oxygenation level has been show to be inversely related to FFA release (Visioli, Rihn, Rodriguez de Turco, Kreisman, & Bazan, 1993). Choline, also a key component in membrane turnover, is active both as a membrane precursor and as a membrane breakdown product from GPC degradation. Given the comparative lack of free choline despite a relative increase in GPC in high spiking tissue, we suspect a re-distribution of choline into various anabolic pathways, such as regeneration of phosphatidylcholine for new membrane

synthesis or acetylcholine synthesis. In fact, elevated acetylcholine receptor activation is known to increase seizure potential (Priel & Albuquerque, 2002). Pilocarpine, an acetylcholine receptor agonist, is a relatively common agent used to generate seizures in animal models (Cavalheiro et al., 1991; Pitkänen, Schwartzkroin, & Moshé, 2005).

The ability of metabolite profiles to predict accurately whether or not a given tissue sample is high or low spiking is remarkable and is a clear reflection of the distinct metabolic environments associated with persistent epileptiform activity. The metabolites outlined in our predictive model demonstrate that ^{1}H MRS is capable of accurately distinguishing epileptic from non-epileptic regions. With further technical refinement, these metabolites may be adapted for clinical use and become an invaluable tool in our efforts to better understand and treat epilepsy and the underlying processes leading to the disorder.

CHAPTER 4: LONGITUDINAL METABOLITE CHANGES IN A MRI-COMPATIBLE ANIMAL MODEL OF IED AND EPILEPTOGENESIS

4.1 Summary

The clinical nature of epilepsy is such that the vast majority of patients presenting to a clinician will have already suffered at least one seizure episode, and are well on their way toward having an established epileptic condition. This inability to identify patients prior to seizure onset makes the use of a molecularly accurate animal model of epileptiform activity invaluable for the study of IEDs during epileptogenesis. Here, we developed a MRI-compatible EEG monitoring system in a rat animal model of IEDs and seizure development to study longitudinal metabolite changes in the rat cortex using ^{1}H MRS at 7T. The observed metabolite changes in this study are suggestive of energy imbalance in the anterior regions of the rat brain. Involvement of Cr+PCr and GPC+PCh recapitulates similar findings in our *ex vivo* human study presented in Chapter 2. These results provide evidence that ^{1}H MRS can be a sensitive technique for detecting metabolite changes associated with epileptogenesis.

4.2 Introduction

As discussed in Chapter 1, the exact relationship between IEDs and seizures is not well understood. IEDs in the form of interictal spiking activity on electrophysiology are frequently used to assist in the identification of seizure onset regions and the removal of both high spiking and seizure onset regions tends to yield the best treatment outcome (Asano et al., 2003; Bautista et al., 1999; Kanazawa et al., 1996; Lee et al., 2014). They also occur more frequently than seizure episodes, potentially making them a more sensitive marker of neuronal and metabolic dysfunction or of underlying disease progression than seizure frequency. Animal studies have shown that interictal activity may precede the development of seizures with a positive correlation between the frequency of spikes and rate at which epilepsy tend to develop in these animal,

making them a potential biomarker of seizure development (White et al., 2010). Here, we plan to study the temporal and spatial associations between IED frequency and metabolite changes as detected by ^{1}H MRS at 7T in a longitudinal rat model of epileptogenesis with spontaneous and persistent IEDs. This study will also directly assess whether there are metabolite profile differences between animals treated with tetanus toxin and those receiving vehicle injections. This study can also serve as an important *in vivo* validation of our previous *ex vivo* human tissue study (Chapter 3). Consistent metabolite changes common to both studies could indicate biomarkers that may be used to detect both established epilepsy and epileptogenesis.

The identification of metabolite biomarkers *ex vivo* in epilepsy patients (Chapter 3) is an important first step in the development of non-invasive biomarker for epilepsy in humans. However, the question remains whether these metabolite biomarkers may be used to identify metabolite correlates of IEDs or ideally epileptogenesis in vulnerable populations prior to the onset of established epilepsy. Animal models may be an invaluable tool to study these metabolite changes over time and their underlying biochemical changes. The ideal animal model would closely resemble epilepsy in humans with a non-symptomatic prodromal phase followed by chronic and spontaneously generated seizure episodes and recognizable paroxysmal IEDs even in the absence of concomitant seizures. Treatments and methods used to induce epileptogenesis should not result in significant neuronal toxicity or cell death (Barkmeier & Loeb, 2009).

Many models of epilepsy exist and they may be classified into two categories: 1) acute versus chronic models and 2) hippocampal versus neocortical. Acute models such as those using penicillin can induce IED and epilepsy like behavior in a matter of hours, and can be a good choice for studying behaviors associated with epilepsy or mechanisms associated with the spread

of systemic seizures (Rubio, Rubio-Osornio, Retana-Márquez, Verónica Custodio, & Paz, 2010). Unfortunately, it is difficult to determine whether the mechanism underlying these acute changes are similar to the mechanisms underlying chronic changes seen in human epilepsy patients. For this reason, chronic models, with their distinct latent period prior to the development of spontaneous seizures (Pitkänen et al., 2005), are preferred over acute models for studying epileptogenesis. Most of the common chronic models for epilepsy such as kindling or systemic injections of pilocarpine or kainic acid, affect the limbic system in a manner that parallels human temporal lobe epilepsies more than neocortical epilepsies (Sarkisian, 2001), and frequently cause significant neuronal damage to the hippocampus. Tetanus toxin and heavy metals such as zinc and cobalt are the two primary models used for modeling chronic neocortical epilepsies (Barkmeier & Loeb, 2009). Of the two, only tetanus toxin does not cause extensive tissue and neuronal damage when directly applied to the cortex, which is an important for our studies since we are interested in identifying biomarkers that reflect the physiologic basis of epilepsy rather than tissue injury. Tetanus toxin works by transiently inhibiting the release of GABA from inhibitory interneurons with a simultaneous increase in the release of excitatory neurotransmitters (Williamson, Fitzgerald, & Neale, 1992). Injection of the toxin directly into the somatosensory cortex has been observed to primarily result in IEDs (Brener, Amitai, Jefferys, & Gutnick, 1991) with relatively infrequent seizures that develop over the course of days to weeks (Nilsen, Walker, & Cock, 2005) and can persist to upwards of 7 months (Brener et al., 1991). For the purposes of our study, tetanus toxin offers the combination of features most suited for our longitudinal study of IED and epileptogenesis in a chronic setting with minimal neuronal damage.

Further characterizations of the tetanus toxin rodent model by our laboratory revealed

many similarities to human epilepsy (Barkmeier et al., 2012). In this model, IEDs were noted to appear within a few days after treatment and increases in frequency over time with few associated seizures. Similar to human epilepsy (Beaumont et al., 2012), a similar pattern of activated CREB and induction of plasticity genes in layers II/III of the cortex was observed. Blocking of MAPK signaling using a selective MAPK inhibitor attenuated the layer II/III CREB activation and reduced frequency of observed IEDs without affecting seizures (Barkmeier et al., 2012). These findings suggest that this model can accurately recapitulate the molecular and electrophysiological features of epilepsy and may be a useful model for studying IED and its relation to epileptogenesis and may also be a good model system for testing efficacy of novel therapeutics.

For this study, we use ^{1}H MRS at 7T to longitudinally study the changes in metabolites over time in our tetanus toxin rat model. Concurrent electrophysiology studies that provide information on IED frequency and progression over time is measured using an implantable MRI-compatible intracranial EEG recording system developed for this animal model. The main aim of this study is to identify both temporal and spatial changes in potential metabolite biomarkers associated with epilepsy development and how these metabolites may relate to IED activity in these animals. Given the molecular similarities observed in this animal model and in human epilepsy, we hypothesize that we will identify changes in energy balance and synaptic plasticity, similar to what was found in our study of human epilepsy tissue *ex vivo* (Chapter 3).

4.3 Methods

4.3.1 Rodent surgery, tetanus toxin injection, and electrode implantation

All studies were carried out on 4 month old male Sprague-Dawley rats (n = 16) split into 3 groups: tetanus injected treatment group (TET; n = 7) and vehicle injected positive control

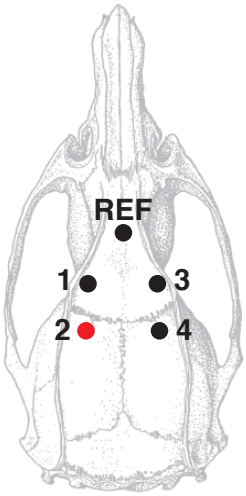

Figure 4.1 Four recording electrodes and one reference electrode were secured directly to the rat skull. Electrode channels are numbered numerically from anterior to posterior and left to right. Electrode placements are indicated by closed circles and were based on distances from the bregma (Paxinos & Watson, 2007). Tetanus toxin was injected into the burr hole drilled for the placement of Channel 2 recording electrode (red closed circle).

group (CTL; n = 5) and normally developing controls with no surgery (NCT; n = 2). Each rat was implanted with 5 MRI-compatible silver recording electrodes: 2 on each hemisphere plus 1 reference electrode over the nasal sinus (Figure 4.1). The selection of electrode material was given extra consideration due to the strong magnetic environment the electrodes would be subjected to. Silver was selected as the primary material of choice due to its malleability, ease of fabrication, biological inertness, is a diamagnetic material, and also has a relatively low susceptibility, a measure of how a particular material would distort its surrounding magnetic field ($\chi_{silver} = -24 \times 10^6$ compared to $\chi_{stainless\ steel} = 3520$ to 6700×10^6 and $\chi_{calcium} = 21.7 \times 10^6$) (Schenck, 1996). Each electrode is constructed from multi-stranded silver wires with PTFE coating (Medwire Corporation, Part #AG7/40T, Mount Vernon, NY) and soldered to a size 1-64 hand-tapped silver screw. The silver recording screw is then chlorided in a saline bath using a pure silver anode with a 1.5 V battery source for 2 minutes (Ives, 2005) to create a Ag/AgCl electrode which, known to have improve recording characteristics compared to Ag electrodes (Geddes & Baker, 1967).

One day prior to surgery, rats were placed on an initial dose of liquid acetaminophen in their drinking water (2 mg/mL of water). General anesthesia was induced using ketamine (80 mg/kg IP) and xyalzine (13 mg/kg IP) combination. Once an adequate plane of anesthesia was confirmed by the absence of a toe pinch reflex, the incision area along the dorsal surface extending from the head to the upper torso of the animal, were shaved and cleaned with betadyne

and ethanol. Ophthalmic ointment and lidocaine gel were placed onto the eyes and ears, respectively, for protection prior to being placed on the stereotaxic frame. Adequate plane of anesthesia was checked approximately every 5 minutes during surgery and an additional ½ dose of ketamine/xyalzine was administered when necessary to maintain anesthesia.

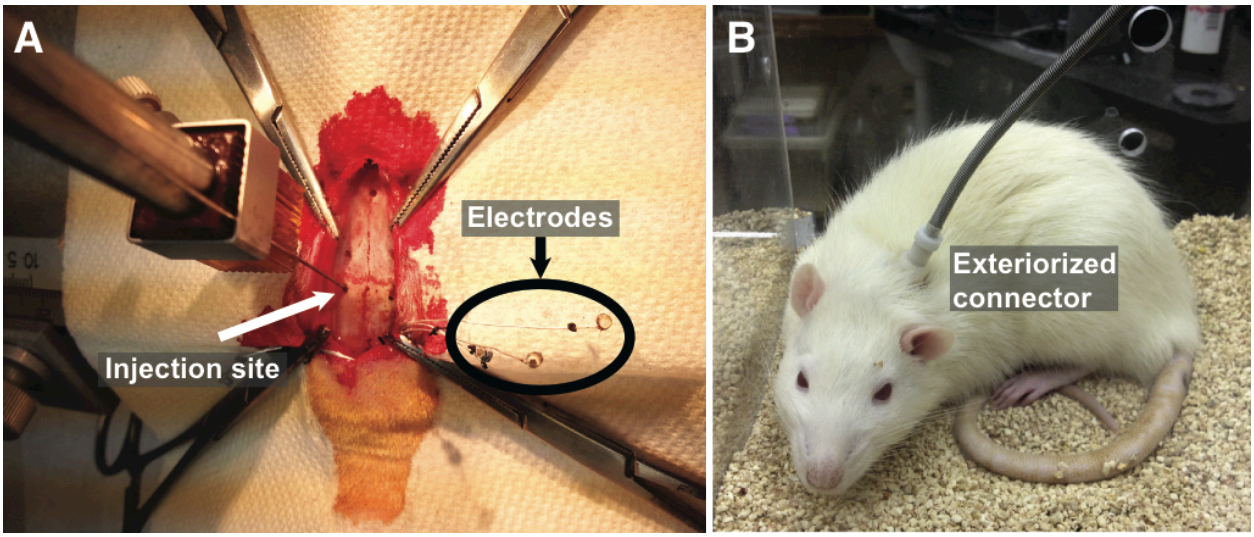

Figure 4.2 Surgical implantation of recording electrodes and exteriorization of the connector. A) Drilled burr holes do not penetrate dura with the exception of the injection site where a Hamilton needle was stereotaxically advanced into the somatosensory cortex, through the dura. Electrodes are then screwed directly into the skull after injection and secured with dental cement. B) EEG connector was exteriorized to the region between the animal's shoulder blades to accommodate placement of the surface head coil during MR sessions.

Once the skull had been adequately exposed, five holes were drilled (Figure 4.2A) through the full thickness of the skull without penetrating the dura. The stereotactic injection is delivered into the left somatosensory cortex (AP -1 mm, L 3.5 mm relative to bregma, depth 1.5 mm) (Paxinos & Watson, 2007). TET animals received tetanus toxin (Sigma, Catalog #T3194; 1 µL at 100 ng/µL in 0.01 M sodium phosphate) into the left somatosensory cortex while CTL animals received vehicle (1 µL 0.01 M sodium phosphate). Injections were made with a blunt tipped Hamilton syringe advanced 1.5 mm into the cortex over the course of 4 minutes and the needle was left in place for 10 minutes prior to retraction from the brain. The bilateral recording electrodes (AP +4 mm, -1 mm , L 3.5 mm relative to bregma) were screwed directly onto the

skull and secured with dental cement. The electrodes were exteriorized to back-mounted connectors (Plastics One Inc., Roanoke, VA) (Figure 4.2B) to accommodate surface coil placement during MR sessions while allowing the animal to maintain mobility during EEG recording sessions.

All incisions were closed and secured with nylon sutures and triple antibiotic ointment (TAO) was applied. The entire surgical procedure typically required 30-45 minutes from anesthesia induction to transferring the animal from the stereotaxic frame to a recovery chamber with a suitable heating source. They were injected with 10 mL of lactated ringer's solution subcutaneously and left undisturbed until they have recovered from the anesthesia, at which point they would be transferred to animal housing facilities. Liquid acetaminophen was provided in their drinking water (2 mg/mL of water) for a period of five days and TAO was applied daily for three days after surgery. Sutures were removed approximately one to two weeks after surgery, when the incisions have healed adequately. EEG recordings were made using Stellate Harmonie video EEG recording system sampling at 200 Hz every other day starting on day 7 after surgery. During recording, animals were placed into a clear-walled recording chamber for 2-3 hours. Recordings were typically done between 9 AM and 1 PM to minimize circadian rhythm effects.

4.3.2 ^{1}H MRI/MRS Assessments

Bi-weekly ^{1}H MRI/MRS scans over 6 weeks were done on a 7 Tesla Bruker ClinScan using a 2-channel phased array receive-only surface coil. For anesthesia induction, the animal was placed in a 1L induction chamber containing 2.0-4.0% isoflurane mixed with medical air connected to an isoflurane-scavenging filter. Induction typically took 5-10 minutes and was considered complete when the animal exhibits loss of righting reflex along with loss of toe pinch

reflex. The animal was then quickly transferred to the MR scanner and maintained on maintenance isoflurane (2% isoflurane mixed with medical air). Adequate body temperature was also maintained for the duration of the scan using warm circulating water (37°C) and the animal's core temperature was monitored between scan sequences, approximately every 10 to 15 minutes using a fiber optic rectal probe. A rapid drop in core temperature (> 1°C) or evidence of excessive motion on MR scans were signs of physiological stress and were causes for immediate removal of the animal from the scanning apparatus.

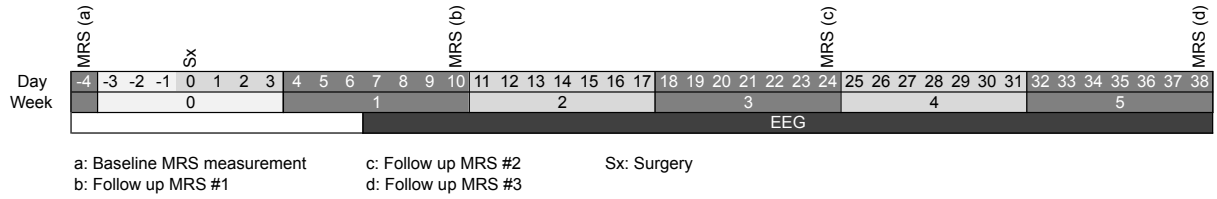

Figure 4.3 Timeline of study. Initial baseline scan (MRS (a)) occurred 4 days prior to surgery. Surgery was performed on day 0. First EEG recording session typically took place on day 7 depending on the animal's recovery progress. First MRS evaluation took place on day 10 (MRS (b)) and repeated every 2 weeks until end of study at day 38.

Initial scout image followed high resolution axial, sagittal, and coronal T_2-weighted images were collected to assist in voxel placement. Major landmarks and voxel positions were observed and recorded to maximize the consistency of measurements between time points. Single voxel spectroscopy of both water suppressed and fully relaxed water unsuppressed signal were collected using PRESS (Point Resolved Spectroscopy) with the following sequence parameters: TE = 14 ms, TR = 3500 ms, 256 averages, spectral bandwidth = 3500 Hz, 2048 points. Each measurement was carried out in a $3.0 \times 3.2 \times 2.0$ mm^3 voxel, placed in the neocortex, adjacent to the location of a recording electrode of interest (Figure 4.6A). ^{1}H MRS measurements were performed every two weeks starting with an initial baseline assessment at four days prior to surgery (Figure 4.3).

4.3.3 ^{1}H MRS quantitation

Quantitation of raw ^{1}H MRS was done using LCModel (Provencher, 1993) with a simulated TE = 14 ms basis set consisting of 17 individual metabolites along with 8 simulated macromolecule resonances. Concentration of metabolites between 0.2 to 4.0 ppm were estimated, normalized to total tissue water obtained from unsuppressed water signal, and expressed in units of $mmol/kg_{wet\ weight}$ (Provencher, 2014). The full list of metabolites used for fitting in this study is provided in Appendix A. As described in Chapter 3, LCModel provides CRLB estimates as indicators of how confident the fitted metabolite spectra matches the original. For the purposes of this study only metabolites and their ratios with CRLB values less than or equal to 10% were retained for further analysis.

4.3.4 IED quantification

Final quantitation of IEDs were carried out in using an automated in-house Matlab (The MathWorks, Inc., Natick, Massachusetts, United States) script that was a modified version of an existing program (Barkmeier et al., 2011) with several key features added: 1) wavelet based de-noising and signal fitting 2) Lowess spline baseline subtraction, and 3) multi-channel spike detection. Conventional frequency filters, such as the Butterworth filter will typically introduce a phase shift in the time dependent signal, which if uncorrected for, can cause a distortion of the final waveform (Figure 4.4). Unfortunately, most programs do not properly compensate for this phase shift, resulting in a distorted waveform such that true spikes may be shifted inappropriately out of phase and go unnoticed by the algorithm or noise may be shifted inappropriately to resemble a spike and be marked as a false-positive spike. Lowess spline baseline subtraction was implemented as a means of removing non-periodic slow moving changes in the baseline of the EEG signal frequently present in the reference montage (i.e. electrode signal minus reference

signal) and was used in the calculation of spike parameters such as peak base width and AUC. The original spike detection program only marked spikes in the channel with the highest amplitude without explicitly recording spike spread into nearby channels. The added feature of multi-channel spike detection allowed us to determine the frequency and manner by which IEDs can spread through the cortex in the form of propagating spikes across electrodes.

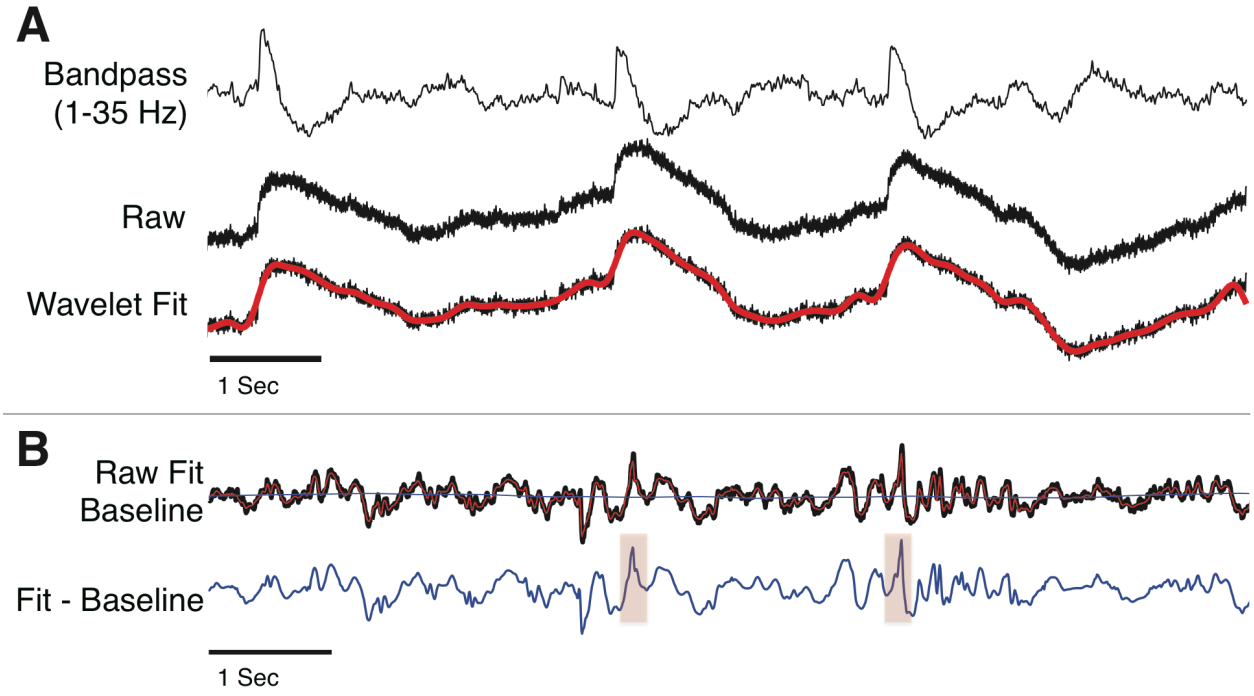

Figure 4.4 Wavelet based de-noising and waveform fitting. A) Conventional frequency filters, such as the Butterworth, can result in phase shifts in the time signal, leading to distortions that can be misinterpreted, as shown by the EEG trace labeled "Bandpass (1-35 Hz)." Wavelet based de-noising does not suffer from this issue and is able to effectively eliminate noise and produce a clean "fit" of the signal (red overlay). B) Subtraction of the estimated baseline obtained (thin grey line running through the signal in the trace labeled "Raw Fit Baseline") from using a Lowess fit eliminated low frequency noise and allowed for uniform characterization of spikes. Shaded rectangles indicate potential spikes that can be marked by the algorithm.

Prior to EEG analysis using the automated spike detection algorithm, periods of excessive motion by the animal, visually identifiable as large amplitude motion artifacts, were marked manually and the spike detection algorithm was programmed to skip those marked sections to speed up the detection process, as spike detection is impossible in the presence of

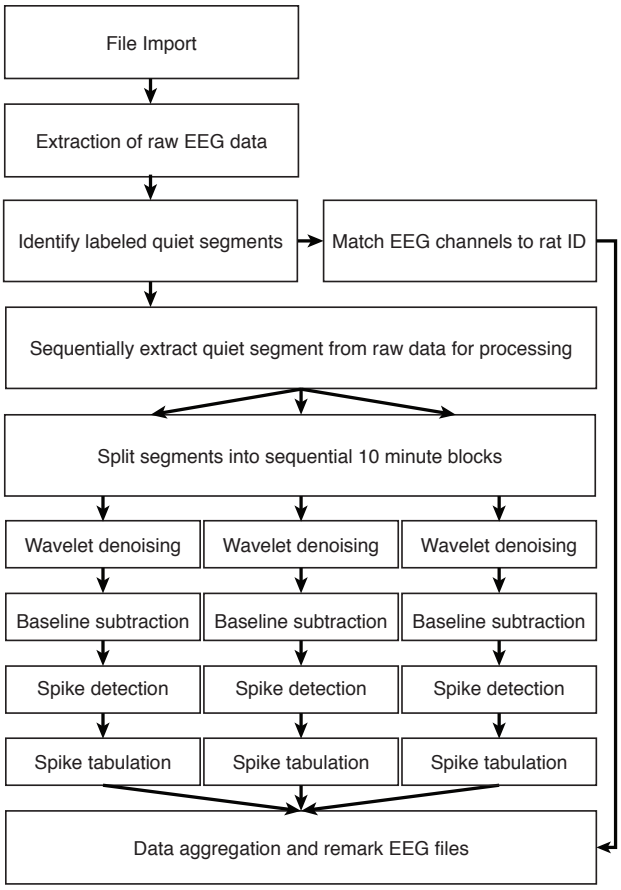

Figure 4.5 Flow chart of EEG data processing and spike detection

those artifacts. Only segments of no motion were analyzed and the total duration of those motion-free segments were determined and used to calculate spike frequency. Flow diagram of the steps involved in the spike detection algorithm is given in Figure 4.5.

The WaveLab (Buckheit & Donoho, 1995) Matlab toolbox was used carry out the wavelet de-noising using Battle-Lemaire wavelets. Baseline fitting and subtraction was done using a Lowess toolbox (Burkey, 2008). Spike detections are carried out in each channel consecutively after wavelet de-noising and baseline subtraction. EEG data on each channel is split into a series of 10 minute blocks and processed in parallel using Matlab's native Parallel Processing toolbox. A high percentage of high amplitude noise in the block relative to the signal's median absolute deviation, or MAD ($\mathrm{MAD} = \mathrm{median}\left(\left|x_i - \mathrm{median}(x_i)\right|\right)$) was indicative of excessive noise, causing the whole block to be rejected. Determination of a positive spike was based on three key criteria evaluated by the algorithm: 1) spike peak height must exceed twice the standard deviation (SD) of the signal relative to the baseline, 2) troughs of the spike must be at least 1 SD below the baseline, and 3) peaks must be between 50 ms to 200 ms in duration. Following spike detection, all identified spikes and their key features such as

location, amplitude, and AUC were tabulated onto a data table in addition to being annotated directly onto a copy of the original EEG file for manual validation and visualization.

4.3.5 Statistical analysis

Several repeated measures mixed GLM regression models were used to analyze both ^{1}H MRS and IED time series data. Several mixed models were used to determine the effects of TIME (Weeks 1 through 5), TREATMENT (CTL and TET), and their interactions (Equations 3.1–3.2) on several electrophysiological parameters including hourly spike count for single spikes, hourly spike count for spreading spikes, amplitude, and AUC. Where appropriate, a log link function was used to analyze the IED time series data, which was represented in spike counts per hour (Poisson distribution) averaged into weekly bins. Otherwise, an identity link function was used for non-count data.

$$\ln(\text{SPIKES}) = \beta_0 + \beta_1 \times \text{TIME} + \beta_2 \times \text{TREATMENT} + \left(b_0 + \sum_i b_i Z_i \right) + \varepsilon$$

$$\ln(\text{SPIKES}) = \beta_0 + \beta_1 \times \text{TIME} + \beta_2 \times \text{TREATMENT} + \beta_3 \times \text{TIME} \times \text{TREATMENT} + \left(b_0 + \sum_i b_i Z_i \right) + \varepsilon$$

(Equations 3.1 – 3.2)

To account for rat aging effects during the study, the time course data for the NCT animals were averaged at each time point and systematically subtracted from both of the TET and CTL groups for each metabolite. A similar set of repeated measures mixed models were used to study the effect of TIME (time points: b, c, d), TREATMENT (CTL and TET), as well as their interactions on the various metabolites (Equations 3.3–3.4). Time point "a" was not included in the model since it was an initial baseline measurement for the animals prior to any surgery or treatment. A complementary verification analysis was also performed using original MRS data not adjusted for aging effects (i.e. average metabolite levels for NCT animals were not

subtracted from TET and CTL groups at each time point) to assess the robustness of the moderation effect that TREATMENT has on the metabolites over time.

$$\text{METABOLITE} = \beta_0 + \beta_1 \times \text{TIME} + \beta_2 \times \text{TREATMENT} + \left(b_0 + \sum_i b_i Z_i \right) + \varepsilon$$

$$\text{METABOLITE} = \beta_0 + \beta_1 \times \text{TIME} + \beta_2 \times \text{TREATMENT} + \beta_3 \times \text{TIME} \times \text{TREATMENT} + \left(b_0 + \sum_i b_i Z_i \right) + \varepsilon$$

(Equations 3.3 – 3.4)

All models were analyzed in R (Team, 2014) using lme4 package (Bates, Mächler, Bolker, & Walker, 2015). Individual animals were included as the random effect to control for within-subject effects. Analyses were stratified both for metabolite and region. The threshold for significance was specified at $p < 0.05$. Unless otherwise stated, all reported significance values were uncorrected for multiple comparisons. In situations where multiple comparison corrections were implemented, a FDR adjusted $p < 0.05$ was considered significant.

4.4 Results

On average, each animal had approximately 45 minutes of motion-free EEG recordings per recording session that could be used for automated spike analysis. Each animal had 3 to 4 EEG recording sessions per week over the entire study duration. The quality of the acquired ^{1}H MRS signals is generally very high with clear separation of major metabolite peaks (Figure 4.6B). LCModel estimated SNR for the dataset was 11.2 ± 3.8 (mean ± s.d.). Similar to our human tissue *ex vivo* study (Chapter 3), only metabolites with mean CRLB of less than or equal to 10% were used for analysis. These metabolites were: Gln, Glu, m-Ins, NAA, Tau, simulated macromolecule at resonance position 0.9 ppm (MM09), GPC+PCh, Cr+PCr, NAA+NAAG, and Glu+Gln.

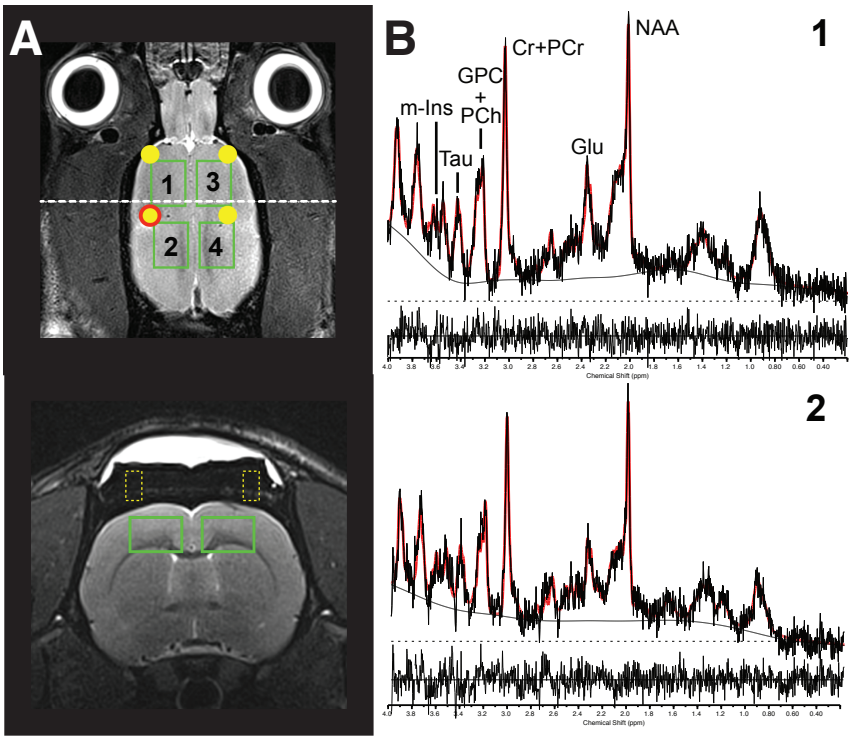

Figure 4.6 Single voxel placement and sample spectra A) Placement of voxels (green rectangle) in relation to recording electrode (yellow closed circles). Location of tetanus or vehicle injection is indicated by open red circle. The location of the axial slice shown in lower panel is indicated by white dashed line in the upper panel. Dashed yellow rectangles indicate location of recording electrode in the skull. B) Representative high quality spectra were obtained from voxel regions 1 and 2 (upper and bottom panels) respectively.

There was a significant decrease in spike rate over time in all of the regions (Figure 4.7A-B), although effect of TREATMENT appears to only have a significant influence on the anterior electrodes, where CTL animals seem to be showing increased spiking activity. The TREATMENT main effect seemed to have little influence in the posterior electrodes. Channel 3 was the only electrode to consistently show a moderating effect by TREATMENT, precipitating a faster rate of decline in spike counts in the CTL group compared to the TET group. Comparing anterior channels (Channels 1, 3) directly to posterior channels (Channels 2, 4) revealed that anterior channels exhibited significantly more spikes and TREATMENT appeared to have a moderating effect on the rate of spike decrease. Other measures of spike properties such as AUC and amplitude also showed a significant decrease over time irrespective of treatment group, with

the exception of Channel 3, where the CTL group showed higher amplitude and AUC and a faster decline in those measures over time compared to the TET group (Figure 4.7C-D).

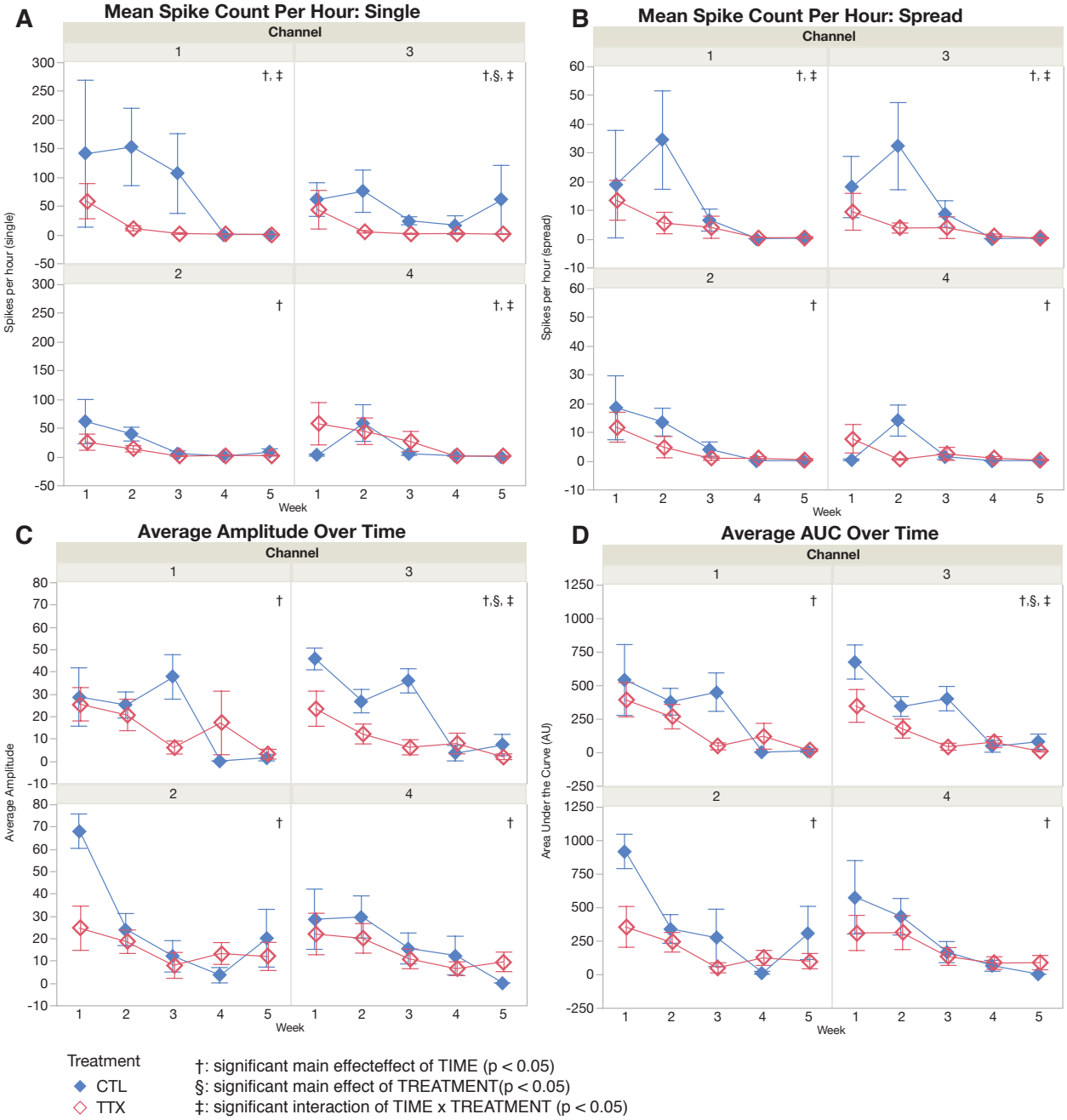

Figure 4.7 No clear difference in spiking over time between tetanus treated and control animals. All electrodes showed significant decreases over time in all 4 measures of interictal spiking: single spike hour count (A), spreading spike hourly count (B), amplitude (C), and AUC (D), with the right anterior electrodes (Channel 3) consistently showing a significant treatment effect in both the number of spikes and the rate of spike count decline.

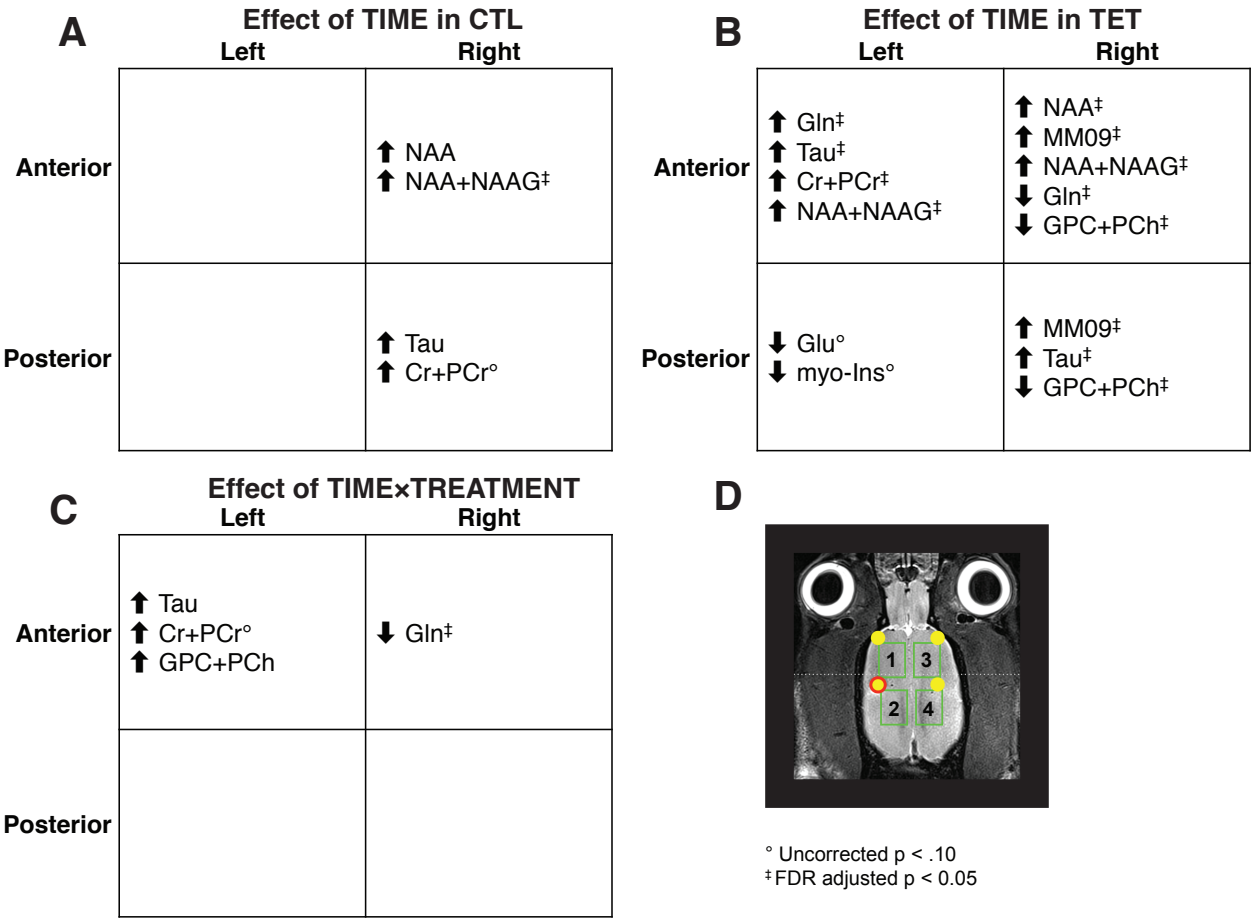

Figure 4.8 Metabolite dynamics over time. A) In general, CTL animals had fewer metabolites that changed significantly over time, with NAA+NAAG being the only metabolite to survive multiple comparison correction. B) TET animals had 7 metabolites that changed significantly over the study period. Most of the metabolite changes were observed in the anterior half of the rat brain. C) Glu, Tau, GPC+PCh were the only metabolites that were significantly moderated by the effect of TREATMENT over the study period, with Gln being the only metabolite to survive multiple comparison correction. The changes in Cr+PCr also appear to be affected by treatment group, although the effect was not statistically significant ($p < 0.07$). D) MRI localization of rat brain with voxel placement for reference has following regional designations: voxel 1 (left anterior), voxel 2 (left posterior), voxel 3 (right anterior), voxel 4 (right posterior). Arrows in panels A-C indicate direction of metabolite difference or rate of change in TET animals relative to CTL animals.

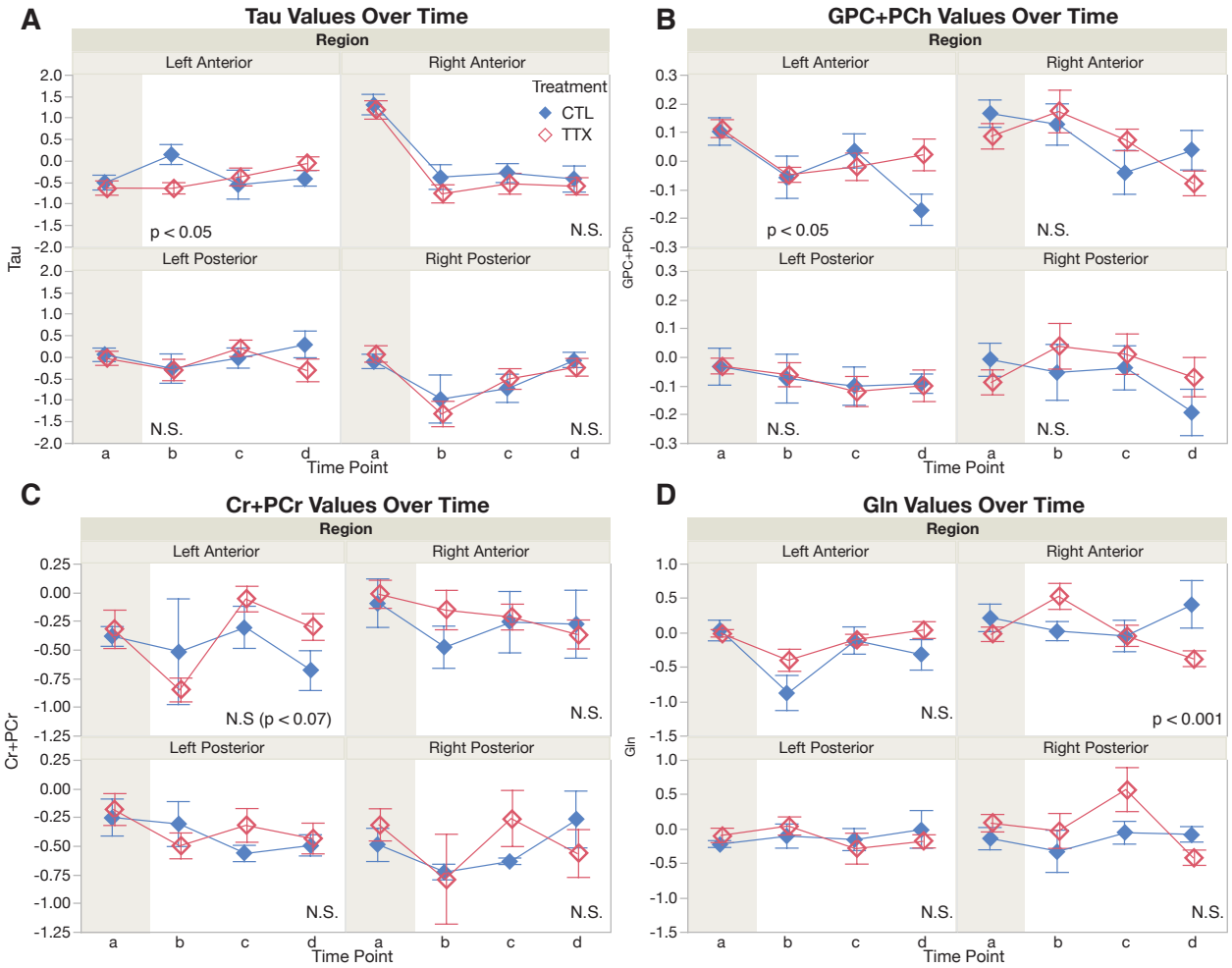

Figure 4.9 Changes in several metabolites over the study period are moderated by treatment group. Several metabolites in the TET group are observed to increase significantly over time while levels in the CTL group remained steady within the left anterior region: Tau (A), GPC (B). Cr+PCr also shows a similar pattern of increase, but the rate of change did not reach statistical significance at the specified cutoff. Gln levels in TET group significantly decreased over time while CTL group also remained unchanged (D). Metabolite concentrations in mmol/$kg_{wet\ weight}$ were normalized to tissue water and expressed as the difference from mean metabolite levels for NCT animals at each corresponding time point. Reported significance values are unadjusted for multiple comparisons. N.S. indicates $p > 0.05$.

Metabolite expression profiles over time were very different between our CTL and TET groups (Figures 4.8-4.9). Comparing the metabolite profiles between the two groups directly, the TET group was much more dynamic than CTL in that 7 different metabolites or their combinations were noted to have significant changes over time in the TET group (Figure 4.8B) while only a single metabolite, NAA+NAAG, was noted to be significantly increased over the

study period in the CTL group (Figure 4.8A). It is interesting to note that the majority of dynamic metabolites were observed in the anterior regions of the brain, where the spike counts were also persistently higher.

Several significant TIME×TREATMENT interactions were also noted for several metabolites in the anterior half of the rat brain (Figure 4.8C). The TET group was more likely to see progressive increases in Tau and GPC+PCh in the left anterior regions of the rat brain, while the CTL group was more likely to remain unchanged. We also observed a similar behavior with respect to Cr+PCr, although the interaction did not reach statistical significance ($p < 0.07$). A significant decline in Gln over time in the TET group compared to an unchanged CTL group was also noted in the right anterior region of the rat brain (Figure 4.9). These findings were replicated in our verification analysis using MRS data unadjusted for aging, which similarly showed a preferential decrease in Gln (right anterior region; $p < 0.001$; FDR adjusted $p < 0.01$) and preferential increases in Tau ($p < 0.01$), GPC+PCh ($p < 0.05$), and Cr+PCr ($p < 0.05$) in the left anterior region of TET animals compared to CTL animals.

4.5 Discussion

The natural extension of our human tissue *ex vivo* study is to determine if similar metabolite changes may be visualized in our rat model longitudinally. Tracking the electrophysiological changes in these animals over the study period becomes extremely important, as spontaneous IEDs generally have no associated physical manifestations that could be easily observed (Gibbs, 1936). The major challenge of this study was to design a set of MR compatible EEG electrodes capable of recording signals for a minimum of five weeks. In many respects, this study was just as much of a test for the design of a durable, MR compatible, long

term intracranial EEG recording method as it was for identifying relevant metabolite biomarkers of epilepsy development.

While the existing non-MR compatible recording setup used by our laboratory has been able to record a progressive increase in IED frequency in tetanus treated animals over the course of several weeks (Barkmeier et al., 2012), this study was unable to replicate those findings. However, the electrophysiology obtained from this study does implicate several major contributing factors that could have led to such different results and point to changes that may be made to improve the procedure in future designs.

First, the progressive attenuation of signal amplitude over time, likely due to oxidation of the electrode tip, with the most severe attenuation seen after the first three weeks of recording, suggests that silver electrodes may not be appropriate for the long term application necessary here. While long term EEG electrodes using silver had been developed for clinical environments and tested successfully over the duration of several days (Ives, 2005), little information was available on how similarly implanted electrodes would perform over the course of several weeks in a biological system. Results from our study indicate that recording sensitivity was severely attenuated after 2 to 3 weeks post-implantation. Other MR compatible materials such as carbon fiber, gold, or platinum-iridium alloys (Jupp, Williams, Tesiram, Vosmansky, & O'Brien, 2006; Mirsattari, Sharpe, & Young, 2004) should be considered for future studies.

Second, the exteriorization of the recording connector to the scapular region, while purposefully done to accommodate the MR surface coil placement above the animal's head, also made the recordings much more sensitive to environmental noise as extra lengths of wires had to run subcutaneously from where the electrodes were secured on the skull to the connector at the scapula. The introduction of extra environmental noise lead to exclusion of a significant portion

of the EEG recording (inter-quartile range: 30% to 86% exclusion) and also increased likelihood performance errors by the spike detection algorithm. A better approach perhaps would be to customize the surface coil architecture to accommodate the design of the EEG connector (Van Audekerkea, Peeters, Verhoye, Sijbers, & Van der Linden, 2000), which ideally would have been secured directly onto the cranium.

Finally, ^{1}H MRS places a great demand on the homogeneity of the magnetic field in order to produce excellent spectral resolution. Introduction of any foreign object or material will cause a distortion in magnetic field, and the degree of distortion will depend heavily on the properties of the material being introduced. Depending on the research question being emphasized and whether or not the end goal is to detect sensitive metabolite biomarkers, an argument could be made to split the animal model into two parallel cohorts. One cohort for performing standard EEG electrophysiology with and without tetanus toxin injections and a separate cohort with no electrodes implanted used specifically for ^{1}H MRS studies, also with and without tetanus toxin injections. Data collected from one cohort may be used to inform the other, and may provide a more complete picture without compromising the quality of ^{1}H MRS or EEG recordings.

Nevertheless, despite the concerns raised here regarding the electrophysiology results, it is still interesting to note that within the first 2-3 three weeks, when the signal attenuation was not as severe, the CTL group still consistently demonstrated higher number of spike along with larger variance as well compared to the TET group (Figure 4.7A-B). While this observation should be interpreted with caution in the absence of additional validation studies, it could be indicative of the surgical procedure itself is producing electrophysiological change in the rat brain and the treatment with or without tetanus toxin acts as a potent modifier to how the rat brain recovers from the insult. More studies that directly compare the surgery procedure with

and without vehicle injection would be needed to truly determine the effect that the procedure itself has on the electrophysiology.

While we were not able to replicate the electrophysiology with our new approach, we may still interpret the ^{1}H MRS metabolite data in context of the known IED behavior associated with this animal model, which is progressive and sustained increase in IED frequency over time (Barkmeier et al., 2012). The dynamic changes in metabolite levels over the course of the study period in the TET group were impressive. A disproportionate number of these metabolite changes were found in the anterior portions of the brain, coinciding with increased spiking activity noted in the anterior electrodes relative to the posterior electrodes. This anterior dominant distribution of both significant metabolite changes and elevated spiking activity points to a potential link between these two phenomena and may reflect downstream changes associated with the upregulation of various plasticity markers noted by Barkmeier and colleagues (Barkmeier et al., 2012) in this animal model.

At 4 months of age at the beginning of the study, these rats are well beyond their early development phases and would generally be considered equivalent to humans at approximately 30 to 40 years of age (Sengupta, 2013). We further attempted to account for aging changes by subtracting metabolite changes observed in a typically developing non-surgical cohort over the same study period from the metabolite values of our treatment groups. It is, therefore, unlikely that these metabolite changes are caused by developmental growth, maturation, or aging effects. For example, taurine, an important modulator of synaptic plasticity (Flint, Liu, & Kriegstein, 1998), is found in high abundance in early brain development and decreases during development to adult age (Tkáč, Rao, Georgieff, & Gruetter, 2003). However, here, we observe a significant increase in taurine over time in the TET group, which may reflect its role as a neuromodulator

and also potentially as a neuroprotectant against glutamate-induced neuronal excitotoxicity (Wu et al., 2005), possibly in response to excessive tissue hyperexcitability associated with epileptogenic activity. The subtraction of NCT metabolite changes over time from the treatment groups only yielded a more extensive list of metabolites that changed significantly over time, particularly in the TET cohort, but the metabolites significantly moderated by treatment group membership (i.e. Gln, Tau, GPC+PCh, Cr+PCr) was quite robust and remained unchanged even without subtraction of NCT group measurements from the measurements of TET and CTL groups.

Also in the anterior regions of the rat brain, several metabolites showed different rates of change over time moderated by the treatment group membership. The only metabolite to survive FDR multiple comparison correction for this moderation effect by treatment group was glutamine in the anterior right region of the rat brain. Glutamine levels tended to decrease over time after an initial rise after surgical manipulation in TET animals while levels in CTL remain relatively unchanged. Glutamine is converted from glutamate in glia by glutamine synthetase, however the conversion between glutamate and glutamine and vice versa as part of the glutamate-glutamine cycle is not necessarily in stoichiometric equivalence and depends heavily on the alternative fates of glutamate (McKenna, 2007). Since we observed a preferential decrease in glutamine over time in the tetanus treated animals compared to the control animals in the absence of a corresponding change in glutamate, the results would seem to indicate a diversion of glutamate into alternative fates, such as the TCA cycle via conversion to α-ketoglutarate for energy production or GABA synthesis (McKenna, 2007). While GABA levels cannot be measured reliably using PRESS on a 7T system, spectral editing techniques that allows for the detection of GABA may provide additional insight.

The increase in GPC+PCh and Cr+PCr lends credence toward the theory of glutamate being diverted for energy generation. Intriguingly, both of these metabolites were also significantly increased in epileptic tissue in our HR-MAS ^{1}H MRS *ex vivo* study, presented in previously in Chapter 2. GPC+PCh is typically a marker of membrane and phospholipid turnover, but it is difficult to determine whether or not the turnover favors the anabolic or catabolic side of membrane breakdown and synthesis pathways. In general, elevated GPC is more indicative of membrane catabolism while elevated PCh is more indicative of membrane synthesis (Stanley, 2002) and the contributions of both to the ^{1}H MRS signal are approximately equal in normal brain tissue (Miller et al., 1996). It is also likely that both mechanisms are at work simultaneously, with the destruction of certain previously normal connections and the creation of new connections elsewhere that serves to reinforce the likelihood of future epileptiform activity. Cr+PCr are key players in high-energy phosphate metabolism. PCr serves as a high-energy phosphate reservoir, and may donate the phosphate group to ADP to generate high ATP be converted to creatine itself (Andres, Ducray, Schlattner, Wallimann, & Widmer, 2008). It is impossible to disentangle the relative contributions of Cr versus PCr to the Cr+PCr signal, but taken together, an elevated Cr+PCr could signal an upregulation of high-energy reserves to accommodate increased energy demand. Taurine, as mentioned previously may serve as an important neuromodulator and relative increase in the tetanus treated animals may indicate its role as a compensatory mechanism to attenuate the hyperexcitable tendencies associated with epileptogenesis.

Despite the ambiguity of the electrophysiology results in this study, the ^{1}H MRS study still provided us with valuable clues on the changing energy demands associated with epilepsy development and IED activity. Most interestingly, several key metabolites related to membrane

plasticity and energy demand observed here were also found in our HR-MAS ^{1}H MRS study of human epileptic tissue and recapitulates many of the same themes of disturbed energy and metabolism balance. This study provides the evidence that non-invasive ^{1}H MRS, when combined with an animal model of epilepsy, can be a powerful tool to not only identify and validate metabolite biomarkers for epilepsy, but also as an opportunity for understanding the underlying biomolecular changes associated with epileptogenesis.

The availability of a well-characterized animal model of epilepsy that can parallel the disorder in humans is extremely helpful for efficient drug testing and informing our mechanistic understand of how epilepsy develops and persists in humans. Because of its flexibility, animal models can also serve as a useful bridge for translating basic molecular findings at the organism level and be used to predict treatment response in humans. While many different models of epilepsy currently exist, they are used to study different aspects of epilepsy (Pitkänen et al., 2005). The neocortical tetanus toxin model in rats produces chronic, sustained IED with relatively few seizures and is ideal for our goal of studying the role of IED in epileptogenesis.

Previous studies in our laboratory have shown that a distinct set of molecular changes promoting plasticity takes place in this animal model (Barkmeier et al., 2012) and these changes parallel what was seen in human epileptic tissues (Beaumont et al., 2012; Rakhade et al., 2007). In Chapter 3, we demonstrated the ability of ^{1}H MRS to identify a unique metabolite expression profile that was highly predictive of epileptic tissue obtained from human subjects. Here, we were able to show partial overlap in the metabolites associated with epileptogenesis in an animal model *in vivo* and those associated with established epilepsy in human neocortical tissue samples *ex vivo*. Specifically, these overlapping metabolites include relative increases in Cr+PCr as well

as GPC or GPC+PCh in regions most affected by epileptiform changes, potentially reflecting a state of increased energy demand as well as enhanced synaptic plasticity.

These metabolite markers have the potential to be developed into a non-invasive biomarker of epilepsy, which would be extremely useful both for research and clinical management. Having a sensitive and reliable non-invasive biomarker would allow for the screening of early signs of epilepsy development in vulnerable individuals (e.g. traumatic brain injuries), assist in the clinical management of existing epilepsy patients, and enable monitoring of medication for therapeutic efficacy. The latter application could open doors for the development a new class of disease modifying medications that have the potential to stop the development of epilepsy prior to seizure onset, unlike most of the ASDs available today, which provide symptomatic management only.

CHAPTER 5: DISCUSSION AND FUTURE DIRECTIONS

5.1 Discussion

Technological advances in the last hundred years have ushered in the era of modern medicine, finally allowing individuals with epilepsy to be perceived as having a true neurological condition with observable electrophysiological underpinnings. Despite such remarkable progress, epilepsy has stubbornly remained a disorder that can only be managed symptomatically. Surgical resection of focal seizure onset regions is the only treatment option that resembles a cure for the condition, and even so, long-term seizure freedom cannot be guaranteed.

One of the biggest challenges currently facing epilepsy is the symptomatic nature by which the disorder is diagnosed and managed. By the time they are diagnosed, epilepsy patients usually have already suffered at least several episodes of seizure. This is akin to only treating patients with potential myocardial infarctions after they have experienced an infarction. Given the self-reinforcing nature of seizure activity in the brain, the truly ideal time for treatment would be prior to the appearance of the first seizure episode. The development of a reliable yet non-invasive biomarker for epileptogenesis could dramatically change the way epilepsy is detected and managed.

Such a biomarker would come with at least two very obvious benefits. First, this tool would pave the way for the development of a new class of disease modifying pharmaceuticals that can target the underlying etiologies. Even after such a drug has been developed, having these non-invasive biomarkers would dramatically increase the efficiency and decrease the cost of the necessary clinical trials required to bring the product to market (Engel et al., 2013). Such a biomarker tool could help identify those most likely to develop epilepsy to participate in these clinical trails and also act as surrogate markers of efficacy, providing early information on drug

efficacy without having to use the delayed measure of seizure frequency as an indicator. Second, a biomarker would enable the screening of vulnerable populations for early signs of epileptogenesis. Those who are found have early signs of epileptogenesis are also the ones who would benefit the most from the disease modifying drugs, which may be able to halt the epileptogenic process before the patient even develops seizures.

Previous studies in our laboratory have consistently observed robust but localized MAPK/CREB activations in regions of the brain most affected by epileptiform activity in the form of IEDs (Barkmeier et al., 2012; Beaumont et al., 2012). The downstream effects of MAPK/CREB dependent transcriptional activation are numerous and typically favor cell growth and proliferation. The downstream protein, macromolecule, and metabolic consequences associated with MAPK/CREB activation may be used as biomarkers for epilepsy. We proposed here, that ^{1}H MRS might be a sufficiently sensitive technique for detecting these changes.

Besides accuracy and sensitivity, other features that are desirable in a biomarker tool for epilepsy include: 1) applicable and useful for both research and clinical care, 2) non-invasive for repeated follow up measurements and, 3) good spatial resolution for identification of the seizure focus. One of the major advantages of ^{1}H MRS is the ease by which the technique may be adapted for *in vitro*, *ex vivo*, *in vivo*, and clinical use. Hypotheses generated in one experimental modality may be tested in a parallel approach in a different modality. *In vivo* research and clinical ^{1}H MRS are also non-invasive. For the clinical side specifically, the technique uses much of the same equipment and hardware as conventional MRI scans and may be incorporated as an additional sequence for a patient who is already scheduled to receive a MRI. While the spatial resolution of ^{1}H MRS is not necessarily high compared to anatomical imaging, it is currently capable of achieving nominal resolutions of around 1 cm^3 (Chu et al., 2000; Maudsley

et al., 2006). This spatial resolution is adequate for our proposed application and is on par with the spatial resolution offered by subdural ECoG, typically at 1 cm^2, and is also superior to the resolution of scalp EEG, estimated to be around 10 cm^2 (Tao et al., 2005).

One potential weakness of ^{1}H MRS is its relative lack of sensitivity compared to more invasive counterparts such as microdialysis, high-performance liquid chromatography (HPLC), or even mass spectrometry, as it requires concentrations of at least 0.5 to 1 $mmol/kg_{wet\ weight}$ or greater (Govindaraju et al., 2000) for reliable detection. This is a significant change in concentration for a well buffered organ, where concentration changes associated with physiologic functions are on the scale of nM to μM. Nevertheless, and as reviewed in Chapter 1, many ^{1}H MRS studies in the past few decades have examined metabolite changes associated with epilepsy, particularly in the temporal lobe epilepsies, with relatively consistent outcomes. The results of our own studies here also demonstrate that ^{1}H MRS has sufficient sensitivity to detect metabolite changes associated with epilepsy. These are good indications that epilepsy produces metabolite changes that are of a sufficient magnitude to be detected by ^{1}H MRS.

5.2 Identification of epileptic metabolite profile using HR-MAS ^{1}H MRS

Using HR-MAS ^{1}H MRS on surgically resected human epileptic tissue was a natural place to start the search for epileptic biomarkers, as it maximizes the likelihood that a useful metabolite marker could be detected. The HR-MAS system, at 11.7T, is exquisitely sensitive to small metabolite changes with well-resolved peaks, flat baseline, and ability to detect numerous metabolites that cannot easily be detected or resolved *in vivo*. Its ability to analyze intact tissue is also more advantageous than traditional chemical extraction procedures (e.g. perchloric acid extraction), which can perturb the relative composition of compounds within the tissue. Also, the study of epileptic tissue in patients with more established and intractable epilepsies, while not

ideal for studying epileptogenesis itself, it is useful for identifying metabolites that are key players in epilepsy and provide clues for the biochemical changes underlying the disorder. Dynamic changes in those metabolites could also be important modulators of epileptogenesis as well.

The most remarkable finding from this study is the identification of a unique metabolite profile that is highly predictive of high and low spiking tissue samples. The optimized accuracy of this predictive metabolite profile was 83% and these predictions can be made in a relatively systematic and non-biased manner. While direct comparisons cannot be made given the uniqueness of this study, for perspective, the ability of ^{1}H MRSI to correctly lateralize the side of the affected temporal lobe in temporal lobe epilepsy is reported to be between 62 - 86% (Capizzano et al., 2001; Cendes et al., 1997b). These prediction accuracies appear comparable, but it can be argued that accurate classification of neocortical tissue samples both within and across different patients, as done here, is more challenging and more informative than simple left or right lateralization of the affected temporal lobes specifically in patients with temporal lobe epilepsies.

Transcriptional microarray and histology data, all gathered as part of SBEP (Loeb, 2010), provided this study the opportunity to further characterize these metabolite changes and their associated metabolite changes. Correlational clustering studies done between genes that were differentially expressed in high spiking samples and key metabolites revealed two major clusters centered on the down-regulation of lactate and the up-regulation of Cr+PCr in high spiking regions. Together, the two clusters provided hints of energy and metabolic disequilibrium in the high spiking cortex. The differentially expressed genes associated with the lactate cluster were also significantly enriched in genes participating in GPCR signaling and angiogenesis. The

upregulation of genes associated with angiogenesis, and also validated by histology, was yet another piece of evidence that pointed to a state of persistent energy imbalance in the tissue. These findings suggest that energetic demand of the epileptic cortex outstrips production, resulting in the activation of various compensatory mechanisms and utilization of alternative energy sources. The enrichment of GPCR related genes, while not necessarily surprising given the dramatic impact of recurrent electrical discharges on the epileptic neocortex, remain an interesting topic for further study and may implicate potential new pharmaceutical candidates for the treatment of epilepsy.

While this study revealed some interesting findings on the metabolite profile of human epileptic tissue, there are several limitations that should be considered. This study was performed on a relatively small number of patients, thus limiting the number of unique samples we had available for analysis. As a result, the predictive model was generated from and operated on the same set of samples. While statistical approaches like leave-one-out cross-validation and bootstrapping can be extremely helpful in characterizing how robust the predictive model is in these situations, there is no substitute for true validation in a completely new dataset. Therefore, one of the key next steps for this project would be the collection of a new dataset for validation purposes. The *ex vivo* nature of this study, where we are studying tissues outside of their natural environment (i.e. within a living organism), is also a major limitation. This study is extremely useful as a first step to demonstrate that ^{1}H MRS can detect metabolite differences unique to epilepsy, but to truly translate these findings to human epilepsy for research or clinical purposes would require further investigations in both animal models and human subjects *in vivo*.

Clearly, much more work would need to be done to apply the findings of this study toward non-invasive clinical use. Nevertheless, the predictive metabolite profile identified here

is a clear demonstration that ^{1}H MRS is capable of discerning changes in focal metabolic environments associated with persistent epileptiform activity. Using this metabolite profile, our prediction model was able to make systematic and unbiased classification of tissue with good accuracy. Transcriptional microarray and histology data collected in parallel also provided useful insight into the events underlying the observed metabolic changes.

5.3 Identification of key metabolites changes in an animal model of IED

Applying ^{1}H MRS to a longitudinal animal model of IED and epileptogenesis addressed two very important questions from a biological perspective. First, it served as an important follow-up to the HR-MAS ^{1}H MRS *ex vivo* human tissue study by directly examining metabolite changes associated with epileptogenesis and compared that with the profile found in our *ex vivo* human tissue study for similarities and differences. Second, given the ambiguity over the role of IED in epileptogenesis, this was an opportunity to study how changes in IED load over time may lead to seizure generation and how that transition process may be characterized by changes in metabolite levels. ^{1}H MRS measurements can help disentangle the relationship between IED and seizure development by addressing the following questions: a) are there any metabolites that are strongly related to IED frequency and if so, b) are those metabolite changes consistent with changes seen in established epilepsy. Presence of one or more common metabolites between those associated with IED and those associated with epilepsy provide further proof that these two electrophysiological phenomena are linked. The causal relationship between IEDs and seizures may be partially inferred based on the temporal play out of these two phenomena (e.g. IEDs preceding seizure activity or vice versa). A more complete determination of causal effects would require directly manipulating of IED frequency itself and observing its impact on seizure occurrence. Attempts at those types of causal experiments have been made by both

pharmacologic manipulations (Barkmeier et al., 2012) as well as by simple observations of the relationship between changes in IED frequency and rate of seizure onset based on natural variations in the experiment (White et al., 2010). Both studies have concluded that IEDs play an important role in the generation of seizure activity.

While shortcomings in the experimental design, as discussed in depth in Chapter 3, may have limited our interpretation of the longitudinal electrophysiology data collected from our *in vivo* rat study and prevented this studying from providing satisfactory results to address the second question, posed above, of how IEDs affect seizure development, the ^{1}H MRS data remained a valuable source of information and can be used to address the first question of whether established epilepsy share common metabolite features with epileptogenesis. A reasonable case can also be made for the interpretation of ^{1}H MRS data in the context of historical electrophysiology information our laboratory collected previously on this animal model.

The first interesting observation to emerge from this study was the difference in metabolite dynamics over time between CTL and TET groups, concentrated in the anterior portions of the rat brain, which also happened to coincide with the greatest number of IED observed in our experimental EEGs. Many more metabolites in TET showed significant concentration changes over the study period, even after correcting for multiple comparisons (7 metabolites in TET versus 1 metabolite in CTL). This phenomenon could be a reflection of the dramatic plasticity and remodeling taking place in epileptogenic regions of the brain.

Several metabolites also showed significantly different rates of change over time depending on the treatment the animal received. As mentioned in Chapter 3, glutamine was the only metabolite to survive multiple comparison correction and its preferential decrease in tetanus

treated animals without a concurrent increase in glutamate levels suggested the possibility that glutamate was being diverted to alternative fates, such as energy production. Despite not being statistically significant after multiple comparison correction, increases in taurine, a neuromodulator of plasticity, and GPC+PCh, an indicator of increased membrane turnover, point to significant tissue remodeling within the cortex, which would presumably be an energetically demanding process given the high cost of *de novo* membrane synthesis (Harris & Attwell, 2012). This theory of increased energy demand was also corroborated by the preferential increase in Cr+PCr levels, another key player in high-energy phosphate metabolism, although the change was not statistically significant ($p < 0.07$).

Similar to the results of our *ex vivo* human tissue study, the metabolite changes over time observed in this study, also reflected a state of energy and metabolism disequilibrium in epileptic tissues. Changes seen in GPC+PCh and Cr+PCr, despite neither being statistically significant after multiple comparisons correction in this study, very much parallels their involvement as important predictors of epileptic in our *ex vivo* human study. While this overlap in metabolites should be interpreted with caution as neither were statistically significant in a technical sense, it is still a cause for optimism, considering differences in experimental design between the two studies, with one being performed on the superficial layers of surgically excised human neocortex and the other being performed on the full thickness cortex of an intact rat model. While further studies are needed to validate these results, this study provides additional evidence that ^{1}H MRS may be a viable tool for identifying non-invasive biomarkers of epilepsy.

Beyond the obvious lack of high quality and reliable long term EEG recording from these animals, this study has several other limitations worthy of consideration. Given the high level of metabolite dynamics observed in the TET animal over the course of study, future studies could

benefit from having more frequent MRS sessions than the every other week schedule we used for this study to better capture the behavior of these dynamics. For this tetanus toxin animal model in particular, our observation of control animals producing more interictal spikes than tetanus treated animals was surprising and raises the important question of what the ideal control group (e.g. vehicle injection versus sham surgery with no injection) should be and just what the impact of the surgery itself has on the course of epilepsy development in these animal models. Epilepsy itself is a disorder with a heterogeneous set of symptoms and semiologies. A truly useful biomarker of epilepsy would have the ability to detect metabolite changes in several different forms of the disorder. Therefore, the study of other well-characterized animal models of epilepsy could also be extremely informative.

5.4 Future directions

While many potential future studies have been suggested through the various chapters and will not be repeated here, a few more general thoughts are included here for additional consideration. It should be mentioned that a pilot study determining the usefulness of ^{1}H MRS in human epilepsy patients, discussed below, is currently underway.

5.4.1 Application of ^{1}H MRS to human epileptic patients in vivo

Despite the importance of tissue and animal studies, a critical test for the viability of this approach is to conduct them in humans. Applying ^{1}H MRS to human epileptic patients *in vivo* is an important step to determine whether or not this we have capability to detect these changes in a clinical setting. As we are interested in studying how metabolites specifically in the cortex change in response to disease onset and progression, high spatial resolution and whole brain coverage are especially necessary and also difficult to obtain using conventional approaches as there are no regions of interest that can be defined *a priori*. Continued development of the EPSI

sequence (Posse et al., 1994), capable of full brain coverage and effective spatial resolution of approximately 1 cm^3, by Maudsley and colleagues in recent years has made this study a possibility (Maudsley et al., 2006; Maudsley et al., 2009b).

Two studies thus far have used ^1H EPSI in epilepsy patients (Maudsley et al., 2010; Mueller et al., 2010) and have also shown widespread decreases in NAA level changes, similar to what has been described in the literature. However, to the best of our knowledge, no studies to date have tried to isolate the gray matter specific metabolite level changes in epilepsy patients *in vivo* and attempted to correlate these changes to quantitative electrophysiology recorded from ECoG obtained from the patients during the surgical workup to precisely identify the location of their seizure focus. The aim of this *in vivo* human study would be to show how metabolite levels as detected by ^1H EPSI would differ between regions of high versus low IED rates in patients with intractable epilepsy.

We are currently conducting a prospective study on 24 adult patients between the ages of 18 and 65 with the diagnosis of intractable epilepsy who are undergoing evaluation for epilepsy surgery at the Comprehensive Epilepsy Program at Wayne State University/Detroit Medical Center. Inclusion and exclusion criteria are provided in Supplementary Table 5.1.

Briefly, all patients will receive the ^1H EPSI scan several weeks prior to their scheduled surgery date. The scans are performed on a 3 Tesla Siemens Verio whole-body MR scanner with a 12 channel ^1H volume head coil. The scanning protocol consists of acquiring an initial set of scout images, automatic and manual shimming, collecting the 3D EPSI data, followed by a set of T_1-weighted anatomic MRI images. The entire scanning process takes approximately 50 minutes.

The initial 3-plane scout image acquisition will be first obtained to ensure proper alignment, patient cooperation, and image quality. The scout images will be used to prescribe the *in vivo* ^{1}H EPSI, with the slices oriented -15° above the AC-PC line. Shimming, for improving B_0 field homogeneity for maximal spectral resolution, will be done automatically with additional manual optimization. The specifics of the ^{1}H EPSI sequence are described elsewhere (Ebel & Maudsley, 2003; Ebel, Soher, & Maudsley, 2001; Maudsley et al., 2009a).

Acquired spectroscopic data will be analyzed using the MIDAS software (Maudsley et al., 2006), designed specifically for processing ^{1}H EPSI data. To take full advantage of high resolution whole brain ^{1}H MRS, we will co-register spectroscopic data with electrophysiology data from intracranial electrodes using a combination of pre-implantation anatomical MRI, post implantation CT, and intraoperative photographs. IED rates, as determined from three distinct 10 minute segments of awake intracranial EEG recordings, along with covariates such as age, gender, and years of disorder, will be used to predict levels of NAA, Cr+PCr, and GPC+PCh in a repeated measures type linear regression model. If IED dependent changes in metabolite levels are seen, a logistic regression model similar to the one used in the *ex vivo* human tissue study can be implement to predict whether a particular voxel or group of voxels could be epileptic in nature.

A preliminary analysis of our ^{1}H EPSI in two subjects who underwent temporal lobectomies without long term ECoG recordings have been performed. In the absence of actual electrophysiology, placement intracranial electrodes were simulated in this preliminary analysis to cover portions of the superior and middle temporal lobe in both patients, bilaterally. These simulated electrode locations are used to guide voxel extraction from the spectroscopic data for analysis. In all, 121 unique voxels between 2 patients, with 55 voxels in the left temporal lobe

and 66 voxels in the right temporal lobe were analyzed using repeated measures GLM, where we tested for side to side differences in either NAA, Cr+PCr, or GPC+PCh (ipsilateral or contralateral to affected temporal lobe). We failed to detect ipsilateral versus contralateral differences in GPC+PCh and Cr+PCr in these two subjects, but a slight increase in NAA levels (uncorrected $p < 0.05$) was observed in the ipsilateral cortex compared to the contralateral cortex. Representative sample spectra from both the cortex of the ipsilateral and contralateral temporal lobes are shown in Figure 5.1.

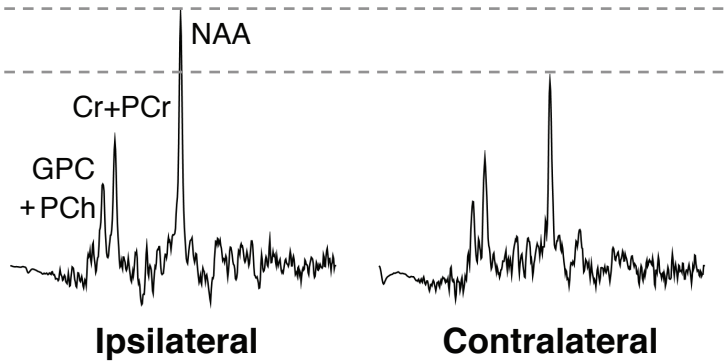

Figure 5.1 Representative spectra from bilateral temporal lobe neocortex in a representative patient. Ipsilateral refers to the side of known seizure activity based on scalp EEG measures and contralateral refers to a matching location on the opposite side. NAA levels appear elevated in the ipsilateral side compared to the contralateral side.

While these metabolite findings need to be replicated and confirmed with the full study sample, this preliminary analysis serves as a demonstration of feasibility. Based on the quality of the data obtained from these two subjects, ^{1}H EPSI appears to be capable of collecting spectra of adequate quality in the neocortex for the analysis of NAA, Cr+PCr, and GPC+PCh in our epilepsy patient population while its relatively high spatial resolution would facilitate successful co-registrations to subdural ECoG data.

5.4.2 Exploring energetics with ^{31}P and ^{13}C spectroscopy

The results of our ^{1}H MRS studies implicate, in multiple lines of evidence, that epileptic tissues consistently exhibit signs of energy derangement, where the demand for energy appear to

exceed that of supply and alternative energy sources are being recruited, based on inferences made from other metabolites such as the relative decreases in lac and Gln. Because of the overlap in resonances between Cr and PCr to form the combined Cr+PCr peak, it is impossible to disambiguate the relative contributions Cr compared to PCr and therefore difficult to say if the observed elevation in Cr+PCr is due to increases in Cr or PCr alone or due to simultaneous increases in both, where each of those scenarios could lead to a different interpretation of the results. A similar issue applies to GPC+PCh, particularly *in vivo*, where GPC and PCh resonances overlap but individually they are associated with different sides of the membrane turnover equation (i.e. synthesis versus breakdown).

To improve our understanding of what is happening, especially *in vivo*, with Cr, PCr, GPC, and PCh, ^{31}P MRS could be implemented as a supplementary technique, where those individual metabolites, especially Cr and PCr can be easily discerned. GPC and PCh would be incorporated into the peaks for phosphodiesters (PDE) and phosphomonoesters (PME), respectively. Fortunately, interpretation of PDE and PME levels remains very similar to that of GPC and PCh, where PDE are typically considered membrane breakdown components while PME are considered membrane synthesis precursors (Stanley, 2002).

Our results of decreased Lac and Gln on ^{1}H MRS led us to theorize that Lac and Glu may have been diverted as alternative sources of energy. While we do not have a direct way of testing that hypothesis using ^{1}H MRS, ^{13}C MRS studies may be a useful in this setting. ^{13}C MRS is a well characterized and non-invasive way to measure metabolite synthesis rates and metabolic flux (Boumezbeur et al., 2010; Shen & Rothman, 2002), although it is not a widely adopted technique due to the need for hyper-polarization or enrichment of ^{13}C isotopes. Nevertheless, if

feasible, a ^{13}C study could help elucidate the fates of both Lac and Glu and how they may relate to the TCA cycle.

5.5 The future of MRS in epilepsy

MRS as a technique can be a very versatile for identifying changes in a variety of compounds, across a variety of experimental environments. However, it can be made much more powerful with the integration of various other experimental modalities, such as electrophysiology, genomics, pharmacological manipulations, optogenetic manipulations, dissection of animal models, and a variety of other molecular studies, as evidenced by the studies presented in this dissertation. Much work still needs to be done to better identify and validate biomarkers that can reflect the underlying mechanistic changes taking place in epilepsy, but ^{1}H MRS shows great promise.

The results of this project indicate that ^{1}H MRS does have the ability to detect metabolite differences between epileptic and non-epileptic regions and that our finds are suggestive of an overlap in metabolite profile between established epilepsy cases and epileptogenesis in an animal model. These studies are crucial first steps for demonstrating the potential of this technique for non-invasive epilepsy biomarker identification. When applied appropriately, this is a technique that has the potential to dramatically change how clinicians diagnose and manage epilepsy and inform the direction of future ASD research efforts.

APPENDIX A: LIST OF METABOLITES FITTED IN THIS PROJECT

Complete list of fitted metabolites for HR-MAS ^{1}H MRS (CPMG) at 11.7T

1. Acetate
2. Alanine
3. Aspartate
4. Betaine
5. Carnitine
6. Choline
7. Citrate
8. Creatine plus phosphocreatine
9. GABA
10. Glutathione
11. Glycerophosphorylcholine
12. Glutamine
13. Glutamate
14. Glycine
15. *myo*-Inositol
16. Lactate
17. N-acetylaspartate
18. N-acetylaspartyl glutamic acid
19. Phosphorylcholine
20. Phosphorylethanolamine
21. Pyruvate
22. *scyllo*-Inositol
23. Succinate
24. Taurine
25. Simulated macromolecule at 1.67 ppm
26. Simulated macromolecule at 1.75 ppm
27. Simulated macromolecule at 1.40 ppm

Complete list of fitted metabolites for ^{1}H SVS MRS (PRESS) at 7T

1. Alanine
2. Aspartate
3. Cr+PCr
4. GPC+PCh
5. GABA
6. Glucose
7. Glutamine
8. Glutamate
9. Glutathione
10. *myo*-Inositol
11. Lactate
12. N-acetylaspartate
13. N-acetylaspartyl glutamic acid
14. *scyllo*-Inositol
15. Taurine
16. Simulated macromolecule at 1.3 ppm
17. Simulated macromolecule at 0.9 ppm
18. Simulated macromolecule at 2.0 ppm
19. Simulated macromolecule at 1.2 ppm
20. Simulated macromolecule at 1.4 ppm
21. Simulated macromolecule at 1.7 ppm

APPENDIX B: SUPPLEMENTARY TABLE

Inclusion criteria	Exclusion criteria
1 Age 18 or older	1 Presence of metal implants; may be hazardous to patient health or cause significant signal distortion
2 Patients with history of intractable epilepsy being evaluated through the Comprehensive Epilepsy Program and Wayne State University/Detroit Medical Center	2 Brain malformations that may confound identification of key anatomical landmarks
3 Are planning on undergoing extraoperative subdural intracranial EEG recordings as part of their presurgical evaluation	3 Patient discomfort, anxiety, or inability to remain still during duration of scan
4 Are willing to undergo an additional hour of MR scanning for research purposes	

Supplementary Table 5.1 Inclusion and exclusion criteria for patient recruitment in human epilepsy study using whole brain ^{1}H EPSI.

REFERENCES

2014 NINDS Benchmarks for Epilepsy Research. (2014). Retrieved from http://www.ninds.nih.gov/research/epilepsyweb/2014benchmarks.htm

Aarts, J. H., Binnie, C. D., Smit, A. M., & Wilkins, A. J. (1984). Selective cognitive impairment during focal and generalized epileptiform EEG activity. *Brain, 107 (Pt 1)*, 293-308.

Andres, R. H., Ducray, A. D., Schlattner, U., Wallimann, T., & Widmer, H. R. (2008). Functions and effects of creatine in the central nervous system. *Brain Research Bulletin, 76*(4), 329-343. doi:10.1016/j.brainresbull.2008.02.035

Andrew, E. R., Bradbury, A., & Eades, R. G. (1959). Removal of Dipolar Broadening of Nuclear Magnetic Resonance Spectra of Solids by Specimen Rotation. *Nature, 183*(4678), 1802-1803. doi:DOI 10.1038/1831802a0

Asano, E., Muzik, O., Shah, A., Juhasz, C., Chugani, D. C., Sood, S., . . . Chugani, H. T. (2003). Quantitative interictal subdural EEG analyses in children with neocortical epilepsy. *Epilepsia, 44*(3), 425-434.

Barkmeier, D. T., & Loeb, J. A. (2009). An animal model to study the clinical significance of interictal spiking. *Clinical EEG and Neuroscience, 40*(4), 234-238.

Barkmeier, D. T., Senador, D., Leclercq, K., Pai, D., Hua, J., Boutros, N. N., . . . Loeb, J. A. (2012). Electrical, molecular and behavioral effects of interictal spiking in the rat. *Neurobiology of Disease*, 1-10. doi:10.1016/j.nbd.2012.03.026

Barkmeier, D. T., Shah, A. K., Flanagan, D., Atkinson, M. D., Agarwal, R., Fuerst, D. R., . . . Loeb, J. A. (2011). High inter-reviewer variability of spike detection on intracranial EEG addressed by an automated multi-channel algorithm. *Clinical Neurophysiology, 123*(6), 1088-1095. doi:10.1016/j.clinph.2011.09.023

Bates, D., Mächler, M., Bolker, B., & Walker, S. (2015). Fitting Linear Mixed-Effects Models Using lme4. *Journal of statistical software, 67*(1), 48. doi:10.18637/jss.v067.i01

Bautista, R. E., Cobbs, M. A., Spencer, D. D., & Spencer, S. S. (1999). Prediction of surgical outcome by interictal epileptiform abnormalities during intracranial EEG monitoring in patients with extrahippocampal seizures. *Epilepsia, 40*(7), 880-890.

Beaumont, T. L., Yao, B., Shah, A., Kapatos, G., & Loeb, J. A. (2012). Layer-Specific CREB Target Gene Induction in Human Neocortical Epilepsy. *Journal of Neuroscience, 32*(41), 14389-14401. doi:10.1523/JNEUROSCI.3408-12.2012

Beckonert, O., Coen, M., Keun, H. C., Wang, Y., Ebbels, T. M., Holmes, E., . . . Nicholson, J. K. (2010). High-resolution magic-angle-spinning NMR spectroscopy for metabolic profiling of intact tissues. *Nat Protoc, 5*(6), 1019-1032. doi:10.1038/nprot.2010.45

Benjamini, Y., & Hochberg, Y. (1995). Controlling the false discovery rate: a practical and powerful approach to multiple testing. *Journal of the Royal Statistical Society. Series B, Statistical methodology*, 289-300.

Bernasconi, A., Tasch, E., Cendes, F., Li, L. M., & Arnold, D. L. (2002). Proton magnetic resonance spectroscopic imaging suggests progressive neuronal damage in human temporal lobe epilepsy. In T. Sutula & A. Pitkänen (Eds.), *Progress in Brain Research* (Vol. 135, pp. 297-304): Elsevier.

Boumezbeur, F., Petersen, K. F., Cline, G. W., Mason, G. F., Behar, K. L., Shulman, G. I., & Rothman, D. L. (2010). The contribution of blood lactate to brain energy metabolism in humans measured by dynamic 13C nuclear magnetic resonance spectroscopy. *Journal of Neuroscience, 30*(42), 13983-13991. doi:10.1523/JNEUROSCI.2040-10.2010

Breiter, S. N., Arroyo, S., Mathews, V. P., Lesser, R. P., Bryan, R. N., & Barker, P. B. (1994). Proton MR spectroscopy in patients with seizure disorders. *AJNR. American Journal of Neuroradiology, 15*(2), 373-384.

Brener, K., Amitai, Y., Jefferys, J. G., & Gutnick, M. J. (1991). Chronic epileptic foci in neocortex: in vivo and in vitro effects of tetanus toxin. *The European Journal of Neuroscience, 3*(1), 47-54.

Bromfield, E. B., Cavazos, J. E., & Sirven, J. I. (2006). *An Introduction to Epilepsy*: American Epilepsy Society.

Buckheit, J. B., & Donoho, D. L. (1995). Wavelab and reproducible research *Wavelets and statistics* (pp. 55-81): Springer.

Burkey, J. (2008). LOWESS, Locally Weighted Scatterplot Smoothing for linear and non-linear data (enhanced): Matlab Central File Exchange. Retrieved from http://www.mathworks.com/matlabcentral/fileexchange/22470-lowess--locally-weighted-scatterplot-smoothing-for-linear-and-non-linear-data--enhanced-/content/lowess.m

Capizzano, A. A., Vermathen, P., Laxer, K. D., Ende, G. R., Norman, D., Rowley, H., . . . Weiner, M. W. (2001). Temporal lobe epilepsy: qualitative reading of 1H MR spectroscopic images for presurgical evaluation. *Radiology, 218*(1), 144-151. doi:10.1148/radiology.218.1.r01ja48144

Cavalheiro, E. A., Leite, J. P., Bortolotto, Z. A., Turski, W. A., Ikonomidou, C., & Turski, L. (1991). Long-term effects of pilocarpine in rats: structural damage of the brain triggers kindling and spontaneous recurrent seizures. *Epilepsia, 32*(6), 778-782.

Cavus, I., Kasoff, W. S., Cassaday, M. P., Jacob, R., Gueorguieva, R., Sherwin, R. S., . . . Abi-Saab, W. M. (2005). Extracellular metabolites in the cortex and hippocampus of epileptic patients. *Annals of Neurology, 57*(2), 226-235. doi:10.1002/ana.20380

Cendes, F. (2012). Epilepsy in 2011: Insights into epilepsy treatments and biomarkers. *Nature reviews. Neurology, 8*(2), 70-71. doi:10.1038/nrneurol.2011.223

Cendes, F., Andermann, F., Dubeau, F., Matthews, P. M., & Arnold, D. L. (1997a). Normalization of neuronal metabolic dysfunction after surgery for temporal lobe epilepsy. Evidence from proton MR spectroscopic imaging. *Neurology, 49*(6), 1525-1533.

Cendes, F., Caramanos, Z., Andermann, F., Dubeau, F., & Arnold, D. L. (1997b). Proton magnetic resonance spectroscopic imaging and magnetic resonance imaging volumetry in the lateralization of temporal lobe epilepsy: a series of 100 patients. *Annals of Neurology, 42*(5), 737-746. doi:10.1002/ana.410420510

Cendes, F., Stanley, J. A., Dubeau, F. O., Andermann, F., & Arnold, D. L. (1997c). Proton magnetic resonance spectroscopic imaging for discrimination of absence and complex partial seizures. *Annals of Neurology, 41*(1), 74-81. doi:10.1002/ana.410410113

Chakraborty, G., Mekala, P., Yahya, D., Wu, G., & Ledeen, R. W. (2001). Intraneuronal N‐acetylaspartate supplies acetyl groups for myelin lipid synthesis: evidence for myelin‐associated aspartoacylase. *Journal of Neurochemistry, 78*(4), 736-745.

Cheng, L. L., Lean, C. L., Bogdanova, A., Wright, S. C., Ackerman, J. L., Brady, T. J., & Garrido, L. (1996). Enhanced resolution of proton NMR spectra of malignant lymph nodes using magic‐angle spinning. *Magnetic Resonance in Medicine, 36*(5), 653-658.

Cheng, L. L., Ma, M. J., Becerra, L., Ptak, T., Tracey, I., Lackner, A., & González, R. G. (1997). Quantitative neuropathology by high resolution magic angle spinning proton magnetic resonance spectroscopy. *Proceedings of the National Academy of Sciences of the United States of America, 94*(12), 6408-6413.

Chu, W. J., Hetherington, H. P., Kuzniecky, R. I., Simor, T., Mason, G. F., & Elgavish, G. A. (1998). Lateralization of human temporal lobe epilepsy by 31P NMR spectroscopic imaging at 4.1 T. *Neurology, 51*(2), 472-479.

Chu, W. J., Kuzniecky, R. I., Hugg, J. W., Abou-Khalil, B., Gilliam, F., Faught, E., & Hetherington, H. P. (2000). Statistically driven identification of focal metabolic abnormalities in temporal lobe epilepsy with corrections for tissue heterogeneity using 1H spectroscopic imaging. *Magnetic Resonance in Medicine, 43*(3), 359-367.

Connelly, A. (1997). Proton magnetic resonance spectroscopy (MRS) in epilepsy. *Epilepsia, 38*, 33-38.

Connelly, A., Van Paesschen, W., Porter, D. A., Johnson, C. L., Duncan, J. S., & Gadian, D. G. (1998). Proton magnetic resonance spectroscopy in MRI-negative temporal lobe epilepsy. *Neurology, 51*(1), 61-66.

Dachet, F., Bagla, S., Keren-Aviram, G., Morton, A., Balan, K., Saadat, L., . . . Loeb, J. A. (2015). Predicting novel histopathological microlesions in human epileptic brain through transcriptional clustering. *Brain, 138*(2), 356-370. doi:10.1093/brain/awu350

De Certaines, J. D., Bovée, W. M. M., & Podo, F. (1992). *Magnetic resonance spectroscopy in biology and medicine: Functional and pathological tissue characterization*. Oxford: Pergamon Press.

de Gannes, F. M., Merle, M., Canioni, P., & Voisin, P. J. (1998). Metabolic and cellular characterization of immortalized human microglial cells under heat stress. *Neurochemistry International, 33*(1), 61-73.

De Graaf, R. A. (2007). *In vivo NMR spectroscopy : principles and techniques*. Chichester, West Sussex, England; Hoboken, NJ: John Wiley & Sons.

Dziuban, C. D., & Shirkey, E. C. (1974). When is a correlation matrix appropriate for factor analysis? Some decision rules. *Psychological bulletin, 81*(6), 358-361. doi:10.1037/h0036316

Ebel, A., & Maudsley, A. A. (2003). Improved spectral quality for 3D MR spectroscopic imaging using a high spatial resolution acquisition strategy. *Magnetic Resonance Imaging, 21*(2), 113-120.

Ebel, A., Soher, B. J., & Maudsley, A. A. (2001). Assessment of 3D proton MR echo-planar spectroscopic imaging using automated spectral analysis. *Magnetic Resonance in Medicine, 46*(6), 1072-1078.

Engel, J. (1993a). *Surgical treatment of the epilepsies* (2 ed.). New York: Raven press.

Engel, J. (1993b). *Update on surgical treatment of the epilepsies. Summary of the Second International Palm Desert Conference on the Surgical Treatment of the Epilepsies (1992).* Paper presented at the Neurology. http://eutils.ncbi.nlm.nih.gov/entrez/eutils/elink.fcgi?dbfrom=pubmed&id=8102482&retmode=ref&cmd=prlinks

Engel, J., Jerome, & Ojemann, G. A. (1993). The Next Step. In J. Engel (Ed.), (2 ed., pp. 319-329). New York: Raven press.

Engel, J., Pitkänen, A., Loeb, J. A., Dudek, F. E., Bertram, E. H., Cole, A. J., . . . Vezzani, A. (2013). Epilepsy biomarkers. *Epilepsia, 54 Suppl 4*, 61-69. doi:10.1111/epi.12299

Farooqui, A. A., Yang, H.-C., Rosenberger, T. A., & Horrocks, L. A. (2002). Phospholipase A2 and Its Role in Brain Tissue. *Journal of Neurochemistry, 69*(3), 889-901. doi:10.1046/j.1471-4159.1997.69030889.x

Fisher, R. S., van Emde Boas, W., Blume, W., Elger, C., Genton, P., Lee, P., & Engel, J., Jr. (2005). Epileptic seizures and epilepsy: definitions proposed by the International League Against Epilepsy (ILAE) and the International Bureau for Epilepsy (IBE). *Epilepsia, 46*(4), 470-472. doi:10.1111/j.0013-9580.2005.66104.x

Flint, A. C., Liu, X., & Kriegstein, A. R. (1998). Nonsynaptic glycine receptor activation during early neocortical development. *Neuron, 20*(1), 43-53.

Garcia, P. A., Laxer, K. D., van der Grond, J., Hugg, J. W., Matson, G. B., & Weiner, M. W. (1995). Proton magnetic resonance spectroscopic imaging in patients with frontal lobe epilepsy. *Annals of Neurology, 37*(2), 279-281. doi:10.1002/ana.410370222

Geddes, L. A., & Baker, L. E. (1967). Chlorided silver electrodes. *Medical research engineering, 6*(3), 33-34.

Ghoddoussi, F., Galloway, M. P., Jambekar, A., Bame, M., Needleman, R., & Brusilow, W. S. A. (2010). Methionine sulfoximine, an inhibitor of glutamine synthetase, lowers brain glutamine and glutamate in a mouse model of ALS. *Journal of the Neurological Sciences, 290*(1-2), 41-47. doi:10.1016/j.jns.2009.11.013

Gibbs, F. A. (1936). The electro-encephalogram in diagnosis and in localization of epileptic seizures. *Archives of neurology and psychiatry (Chicago), 36*(6), 1225. doi:10.1001/archneurpsyc.1936.02260120072005

Gotman, J. (1991). Relationships between interictal spiking and seizures: human and experimental evidence. *The Canadian journal of neurological sciences. Le journal canadien des sciences neurologiques, 18*(4 Suppl), 573-576.

Govindaraju, V., Young, K., & Maudsley, A. A. (2000). Proton NMR chemical shifts and coupling constants for brain metabolites. *NMR in Biomedicine, 13*(3), 129-153.

Hammen, T., Schwarz, M., Doelken, M., Kerling, F., Engelhorn, T., Stadlbauer, A., . . . Stefan, H. (2007). 1H-MR Spectroscopy Indicates Severity Markers in Temporal Lobe Epilepsy: Correlations between Metabolic Alterations, Seizures, and Epileptic Discharges in EEG. *Epilepsia, 48*(2), 263-269. doi:10.1111/j.1528-1167.2006.00856.x

Harris, J. J., & Attwell, D. (2012). The energetics of CNS white matter. *Journal of Neuroscience, 32*(1), 356-371. doi:10.1523/JNEUROSCI.3430-11.2012

Hetherington, H. P., Kim, J. H., Pan, J. W., & Spencer, D. D. (2004). 1H and 31P spectroscopic imaging of epilepsy: spectroscopic and histologic correlations. *Epilepsia, 45 Suppl 4*(s4), 17-23. doi:10.1111/j.0013-9580.2004.04004.x

Hetherington, H. P., Kuzniecky, R. I., Vives, K., Devinsky, O., Pacia, S., Luciano, D., . . . Pan, J. W. (2007). A subcortical network of dysfunction in TLE measured by magnetic resonance spectroscopy. *Neurology, 69*(24), 2256-2265. doi:10.1212/01.wnl.0000286945.21270.6d

Hetherington, H. P., Mason, G. F., Pan, J. W., Ponder, S. L., Vaughan, J. T., Twieg, D. B., & Pohost, G. M. (1994). Evaluation of cerebral gray and white matter metabolite differences by spectroscopic imaging at 4.1T. *Magnetic Resonance in Medicine, 32*(5), 565-571.

Hetherington, H. P., Pan, J. W., Mason, G. F., Adams, D., Vaughn, M. J., Twieg, D. B., & Pohost, G. M. (1996). Quantitative 1H spectroscopic imaging of human brain at 4.1 T using image segmentation. *Magnetic Resonance in Medicine, 36*(1), 21-29.

Hirtz, D., Thurman, D. J., Gwinn-Hardy, K., Mohamed, M., Chaudhuri, A. R., & Zalutsky, R. (2007). How common are the "common" neurologic disorders? *Neurology, 68*(5), 326-337. doi:10.1212/01.wnl.0000252807.38124.a3

Højsgaard, S., Halekoh, U., & Yan, J. (2005). The R Package geepack for Generalized Estimating Equations. *Journal of statistical software, 15*, 1-11.

Hugg, J. W., Kuzniecky, R. I., Gilliam, F. G., Morawetz, R. B., Fraught, R. E., & Hetherington, H. P. (1996). Normalization of contralateral metabolic function following temporal lobectomy demonstrated by 1H magnetic resonance spectroscopic imaging. *Annals of Neurology, 40*(2), 236-239. doi:10.1002/ana.410400215

Ives, J. R. (2005). New chronic EEG electrode for critical/intensive care unit monitoring. *Journal of clinical neurophysiology, 22*(2), 119.

Jupp, B., Williams, J. P., Tesiram, Y. A., Vosmansky, M., & O'Brien, T. J. (2006). MRI compatible electrodes for the induction of amygdala kindling in rats. *Journal of Neuroscience Methods, 155*(1), 72-76. doi:10.1016/j.jneumeth.2005.12.024

Kamburov, A., Stelzl, U., Lehrach, H., & Herwig, R. (2013). The ConsensusPathDB interaction database: 2013 update. *Nucleic Acids Research, 41*(Database issue), D793-800. doi:10.1093/nar/gks1055

Kanazawa, O., Blume, W. T., & Girvin, J. P. (1996). Significance of spikes at temporal lobe electrocorticography. *Epilepsia, 37*(1), 50-55.

Keeler, J. (2005). *Understanding NMR spectroscopy*. Chichester, England; Hoboken, NJ: Wiley.

Klunk, W. E., Xu, C. J., Panchalingam, K., McClure, R. J., & Pettegrew, J. W. (1994). Analysis of magnetic resonance spectra by mole percent: comparison to absolute units. *Neurobiology of Aging, 15*(1), 133-140.

Kreis, R., Ernst, T., & Ross, B. D. (1993). Absolute Quantitation of Water and Metabolites in the Human Brain .2. Metabolite Concentrations. *Journal of Magnetic Resonance Series B, 102*(1), 9-19.

Kuzniecky, R., Elgavish, G. A., Hetherington, H. P., Evanochko, W. T., & Pohost, G. M. (1992). In vivo 31P nuclear magnetic resonance spectroscopy of human temporal lobe epilepsy. *Neurology, 42*(8), 1586-1590.

Kuzniecky, R., Palmer, C., Hugg, J., Martin, R., Sawrie, S., Morawetz, R., . . . Knowlton, R. (2001). Magnetic resonance spectroscopic imaging in temporal lobe epilepsy: neuronal dysfunction or cell loss? *Archives of Neurology, 58*(12), 2048-2053.

Kwan, P., & Brodie, M. J. (2000). Early identification of refractory epilepsy. *New England Journal of Medicine, 342*(5), 314-319. doi:10.1056/NEJM200002033420503

Lee, C., Kim, J. S., Jeong, W., & Chung, C. K. (2014). Usefulness of interictal spike source localization in temporal lobe epilepsy: electrocorticographic study. *Epilepsy Res, 108*(3), 448-458. doi:10.1016/j.eplepsyres.2013.12.008

Liang, K.-Y., & Zeger, S. L. (1986). Longitudinal data analysis using generalized linear models. *Biometrika, 73*(1), 13-22.

Lipovich, L., Dachet, F., Cai, J., Bagla, S., Balan, K., Jia, H., & Loeb, J. A. (2012). Activity-dependent human brain coding/noncoding gene regulatory networks. *Genetics, 192*(3), 1133-1148. doi:10.1534/genetics.112.145128

Loeb, J. A. (2010). A human systems biology approach to discover new drug targets in epilepsy. *Epilepsia, 51 Suppl 3*, 171-177. doi:10.1111/j.1528-1167.2010.02635.x

Loeb, J. A. (2011). Identifying targets for preventing epilepsy using systems biology. *Neuroscience Letters, 497*(3), 205-212. doi:10.1016/j.neulet.2011.02.041

Lüders, H. O., Engel, J., Jerome, & Munari, C. (1993). General Principles. In J. Engel (Ed.), (2 ed., pp. 137-153). New York: Raven press.

Magiorkinis, E., Diamantis, A., Sidiropoulou, K., & Panteliadis, C. (2014). Highights in the history of epilepsy: the last 200 years. *Epilepsy Research and Treatment, 2014*, 582039. doi:10.1155/2014/582039

Magiorkinis, E., Sidiropoulou, K., & Diamantis, A. (2010). Hallmarks in the history of epilepsy: epilepsy in antiquity. *Epilepsy & Behavior, 17*(1), 103-108. doi:10.1016/j.yebeh.2009.10.023

Matthews, P. M., Andermann, F., & Arnold, D. L. (1990). A proton magnetic resonance spectroscopy study of focal epilepsy in humans. *Neurology, 40*(6), 985-989.

Maudsley, A. A., Darkazanli, A., Alger, J. R., Hall, L. O., Schuff, N., Studholme, C., . . . Zhu, X. (2006). Comprehensive processing, display and analysis forin vivo MR spectroscopic imaging. *NMR in Biomedicine, 19*(4), 492-503. doi:10.1002/nbm.1025

Maudsley, A. A., Domenig, C., Govind, V., Darkazanli, A., Studholme, C., Arheart, K., & Bloomer, C. (2009a). Mapping of brain metabolite distributions by volumetric proton MR spectroscopic imaging (MRSI). *Magnetic Resonance in Medicine, 61*(3), 548-559. doi:10.1002/mrm.21875

Maudsley, A. A., Domenig, C., Ramsay, R. E., & Bowen, B. C. (2010). Application of volumetric MR spectroscopic imaging for localization of neocortical epilepsy. *Epilepsy Research, 88*(2-3), 127-138. doi:10.1016/j.eplepsyres.2009.10.009

Maudsley, A. A., Domenig, C., & Sheriff, S. (2009b). Reproducibility of serial whole-brain MR Spectroscopic Imaging. *NMR in Biomedicine*, n/a-n/a. doi:10.1002/nbm.1445

McKenna, M. C. (2007). The glutamate-glutamine cycle is not stoichiometric: fates of glutamate in brain. *Journal of Neuroscience Research, 85*(15), 3347-3358. doi:10.1002/jnr.21444

Mehta, V., & Namboodiri, M. A. (1995). N-acetylaspartate as an acetyl source in the nervous system. *Brain Res Mol Brain Res, 31*(1-2), 151-157.

Miller, B. L., Chang, L., Booth, R., Ernst, T., Cornford, M., Nikas, D., . . . Jenden, D. J. (1996). In vivo 1H MRS choline: correlation with in vitro chemistry/histology. *Life Sciences, 58*(22), 1929-1935.

Mirsattari, S. M., Sharpe, M. D., & Young, G. B. (2004). Treatment of refractory status epilepticus with inhalational anesthetic agents isoflurane and desflurane. *Archives of Neurology, 61*(8), 1254-1259. doi:10.1001/archneur.61.8.1254

Moffett, J. R., Ross, B., Arun, P., Madhavarao, C. N., & Namboodiri, A. M. A. (2007). N-Acetylaspartate in the CNS: from neurodiagnostics to neurobiology. *Progress in Neurobiology, 81*(2), 89-131. doi:10.1016/j.pneurobio.2006.12.003

Morin-Brureau, M., Lebrun, A., Rousset, M. C., Fagni, L., Bockaert, J., de Bock, F., & Lerner-Natoli, M. (2011). Epileptiform activity induces vascular remodeling and zonula occludens 1 downregulation in organotypic hippocampal cultures: role of VEGF signaling pathways. *Journal of Neuroscience, 31*(29), 10677-10688. doi:10.1523/JNEUROSCI.5692-10.2011

Morin-Brureau, M., Rigau, V., & Lerner-Natoli, M. (2012). Why and how to target angiogenesis in focal epilepsies. *Epilepsia, 53 Suppl 6*, 64-68. doi:10.1111/j.1528-1167.2012.03705.x

Moshé, S. L., Perucca, E., Ryvlin, P., & Tomson, T. (2014). Epilepsy: new advances. *Lancet*. doi:10.1016/S0140-6736(14)60456-6

Mountford, C. E., MacKinnon, W. B., Delikatny, E. J., & Russell, P. (1992). High Resolution Proton MRS in Cancer Pathology. In J. D. de Certaines, W. M. M. J. Bovee, & F. Podo (Eds.), *Magnetic Resonance Spectroscopy in Biology and Medicine: Functional and Pathological Tissue Characterization*. Oxford: Pergamon Press.

Mueller, S. G., Ebel, A., Barakos, J., Scanlon, C., Cheong, I., Finlay, D., . . . Laxer, K. D. (2010). Widespread extrahippocampal NAA/(Cr+Cho) abnormalities in TLE with and without mesial temporal sclerosis. *Journal of Neurology, 258*(4), 603-612. doi:10.1007/s00415-010-5799-6

Nilsen, K. E., Walker, M. C., & Cock, H. R. (2005). Characterization of the Tetanus Toxin Model of Refractory Focal Neocortical Epilepsy in the Rat. *Epilepsia, 46*(2), 179-187. doi:10.1111/j.0013-9580.2005.26004.x

Noachtar, S., & Borggraefe, I. (2009). Epilepsy surgery: a critical review. *Epilepsy & Behavior, 15*(1), 66-72. doi:10.1016/j.yebeh.2009.02.028

Nobel Media AB. (2014a). The Nobel Prize in Physics 1944. Retrieved from http://www.nobelprize.org/nobel_prizes/physics/laureates/1944/

Nobel Media AB. (2014b). The Nobel Prize in Physics 1952. Retrieved from http://www.nobelprize.org/nobel_prizes/physics/laureates/1952/

Pan, J. W., Bebin, E. M., Chu, W. J., & Hetherington, H. P. (1999). Ketosis and epilepsy: 31P spectroscopic imaging at 4.1 T. *Epilepsia, 40*(6), 703-707.

Pan, J. W., Spencer, D. D., Kuzniecky, R., Duckrow, R. B., Hetherington, H., & Spencer, S. S. (2012). Metabolic networks in epilepsy by MR spectroscopic imaging. *Acta Neurologica Scandinavica*, n/a-n/a. doi:10.1111/j.1600-0404.2012.01665.x

Pan, J. W., Williamson, A., Cavus, I., Hetherington, H. P., Zaveri, H., Petroff, O. A. C., & Spencer, D. D. (2008). Neurometabolism in human epilepsy. *Epilepsia, 49*(s3), 31-41. doi:10.1111/j.1528-1167.2008.01508.x

Park, S. A., Kim, G. S., Lee, S. K., Lim, S. R., Heo, K., Park, S. C., . . . Lee, B. I. (2002). Interictal epileptiform discharges relate to 1H-MRS-detected metabolic abnormalities in mesial temporal lobe epilepsy. *Epilepsia, 43*(11), 1385-1389.

Paxinos, G., & Watson, C. (2007). *The Rat Brain in Stereotaxic Coordinates* (6 ed.): Academic Press.

Peeling, J., & Sutherland, G. (1993). 1H magnetic resonance spectroscopy of extracts of human epileptic neocortex and hippocampus. *Neurology, 43*(3 Pt 1), 589-594.

Petroff, O. A., Hyder, F., Mattson, R. H., & Rothman, D. L. (1999). Topiramate increases brain GABA, homocarnosine, and pyrrolidinone in patients with epilepsy. *Neurology, 52*(3), 473-478.

Petroff, O. A., Pleban, L. A., & Spencer, D. D. (1995). Symbiosis between in vivo and in vitro NMR spectroscopy: the creatine, N-acetylaspartate, glutamate, and GABA content of the epileptic human brain. *Magnetic Resonance Imaging, 13*(8), 1197-1211.

Petroff, O. A., Prichard, J. W., Behar, K. L., Alger, J. R., & Shulman, R. G. (1984). In vivo phosphorus nuclear magnetic resonance spectroscopy in status epilepticus. *Annals of Neurology, 16*(2), 169-177. doi:10.1002/ana.410160203

Petroff, O. A., Rothman, D. L., Behar, K. L., Collins, T. L., & Mattson, R. H. (1996). Human brain GABA levels rise rapidly after initiation of vigabatrin therapy. *Neurology, 47*(6), 1567-1571.

Petroff, O. A., Rothman, D. L., Behar, K. L., Lamoureux, D., & Mattson, R. H. (1996). The effect of gabapentin on brain gamma-aminobutyric acid in patients with epilepsy. *Annals of Neurology, 39*(1), 95-99. doi:10.1002/ana.410390114

Petroff, O. A., Rothman, D. L., Behar, K. L., & Mattson, R. H. (1996a). Human brain GABA levels rise after initiation of vigabatrin therapy but fail to rise further with increasing dose. *Neurology, 46*(5), 1459-1463.

Petroff, O. A., Rothman, D. L., Behar, K. L., & Mattson, R. H. (1996b). Low brain GABA level is associated with poor seizure control. *Annals of Neurology, 40*(6), 908-911. doi:10.1002/ana.410400613

Petroff, O. A. C., Errante, L. D., Rothman, D. L., Kim, J. H., & Spencer, D. D. (2002). Neuronal and glial metabolite content of the epileptogenic human hippocampus. *Annals of Neurology, 52*(5), 635-642. doi:10.1002/ana.10360

Pillai, J., & Sperling, M. R. (2006). Interictal EEG and the diagnosis of epilepsy. *Epilepsia, 47 Suppl 1*, 14-22. doi:10.1111/j.1528-1167.2006.00654.x

Pitkänen, A., Schwartzkroin, P. A., & Moshé, S. L. (2005). *Models of seizures and epilepsy*. Oxford: Elsevier Academic.

Podo, F. (1999). Tumour phospholipid metabolism. *NMR in Biomedicine, 12*(7), 413-439.

Posse, S., DeCarli, C., & Le Bihan, D. (1994). Three-dimensional echo-planar MR spectroscopic imaging at short echo times in the human brain. *Radiology, 192*(3), 733-738.

Pressler, R. M., Robinson, R. O., Wilson, G. A., & Binnie, C. D. (2005). Treatment of interictal epileptiform discharges can improve behavior in children with behavioral problems and epilepsy. *Journal of Pediatrics, 146*(1), 112-117. doi:10.1016/j.jpeds.2004.08.084

Priel, M. R., & Albuquerque, E. X. (2002). Short-Term Effects of Pilocarpine on Rat Hippocampal Neurons in Culture. *Epilepsia, 43*, 40-46. doi:10.1046/j.1528-1157.43.s.5.18.x

Provencher, S. W. (1993). Estimation of metabolite concentrations from localized in vivo proton NMR spectra. *Magnetic Resonance in Medicine, 30*(6), 672-679.

Provencher, S. W. (2014). *LCModel and LCMgui User's Manual* Retrieved from lcmodel.ca

Rakhade, S. N., Shah, A. K., Agarwal, R., Yao, B., Asano, E., & Loeb, J. A. (2007). Activity-dependent Gene Expression Correlates with Interictal Spiking in Human Neocortical Epilepsy. *Epilepsia, 48*(s5), 86-95. doi:10.1111/j.1528-1167.2007.01294.x

Rakhade, S. N., Yao, B., Ahmed, S., Asano, E., Beaumont, T. L., Shah, A. K., . . . Loeb, J. A. (2005). A common pattern of persistent gene activation in human neocortical epileptic foci. *Annals of Neurology, 58*(5), 736-747. doi:10.1002/ana.20633

Rigau, V., Morin, M., Rousset, M. C., de Bock, F., Lebrun, A., Coubes, P., . . . Lerner-Natoli, M. (2007). Angiogenesis is associated with blood-brain barrier permeability in temporal lobe epilepsy. *Brain, 130*, 1942-1956.

Robin, X., Turck, N., Hainard, A., Tiberti, N., Lisacek, F., Sanchez, J.-C., & Müller, M. (2011). pROC: an open-source package for R and S+ to analyze and compare ROC curves. *BMC Bioinformatics, 12*, 77. doi:10.1186/1471-2105-12-77

Rubio, C., Rubio-Osornio, M., Retana-Márquez, S., Verónica Custodio, M. L., & Paz, C. (2010). In vivo experimental models of epilepsy. *Central nervous system agents in medicinal chemistry, 10*(4), 298-309.

Sada, N., Lee, S., Katsu, T., Otsuki, T., & Inoue, T. (2015). Targeting LDH enzymes with a stiripentol analog to treat epilepsy. *Science*.

Sanchez Fernandez, I., Loddenkemper, T., Galanopoulou, A. S., & Moshe, S. L. (2015). Should epileptiform discharges be treated? *Epilepsia, 56*(10), 1492-1504. doi:10.1111/epi.13108

Sander, J. W. (2003). The epidemiology of epilepsy revisited. *Current Opinion in Neurology, 16*(2), 165-170. doi:10.1097/01.wco.0000063766.15877.8e

Sarkisian, M. R. (2001). Overview of the Current Animal Models for Human Seizure and Epileptic Disorders. *Epilepsy & Behavior, 2*(3), 201-216. doi:10.1006/ebeh.2001.0193

Schenck, J. F. (1996). The role of magnetic susceptibility in magnetic resonance imaging: MRI magnetic compatibility of the first and second kinds. *Medical Physics, 23*(6), 815-850.

Schwab, R. S. (1939). A method of measuring consciousness in petit mal epilepsy. *The journal of nervous and mental disease, 89*, 690.

Sengupta, P. (2013). The Laboratory Rat: Relating Its Age With Human's. *International Journal of Preventive Medicine, 4*(6), 624-630.

Serles, W., Li, L. M., Antel, S. B., Cendes, F., Gotman, J., Olivier, A., . . . Arnold, D. L. (2001). Time Course of Postoperative Recovery of N-Acetyl-Aspartate in Temporal Lobe Epilepsy. *Epilepsia, 42*(2), 190-197. doi:10.1046/j.1528-1157.2001.01300.x

Serles, W., Li, L. M., Caramanos, Z., Arnold, D. L., & Gotman, J. (1999). Relation of Interictal Spike Frequency to 1H‐MRSI‐Measured NAA/Cr. *Epilepsia, 40*(12), 1821-1827.

Shen, J., & Rothman, D. L. (2002). Magnetic resonance spectroscopic approaches to studying neuronal: glial interactions. *Biological Psychiatry, 52*(7), 694-700.

Simister, R. J., Woermann, F. G., McLean, M. A., Bartlett, P. A., Barker, G. J., & Duncan, J. S. (2002). A Short-echo-time Proton Magnetic Resonance Spectroscopic Imaging Study of Temporal Lobe Epilepsy. *Epilepsia, 43*(9), 1021-1031. doi:10.1046/j.1528-1157.2002.50701.x

Spencer, S., & Huh, L. (2008). Outcomes of epilepsy surgery in adults and children. *Lancet Neurol, 7*(6), 525-537. doi:10.1016/S1474-4422(08)70109-1

Srivastava, N. K., Pradhan, S., Mittal, B., Kumar, R., Pandey, C. M., & Gowda, G. A. (2008). Novel corrective equations for complete estimation of human tissue lipids after their partial destruction by perchloric acid pre-treatment: high-resolution (1)H-NMR-based study. *NMR in Biomedicine, 21*(2), 89-100. doi:10.1002/nbm.1159

Stanley, J. A. (2002). In vivo magnetic resonance spectroscopy and its application to neuropsychiatric disorders. *Canadian journal of psychiatry. Revue canadienne de psychiatrie, 47*(4), 315-326.

Stanley, J. A., Cendes, F., Dubeau, F., Andermann, F., & Arnold, D. L. (1998). Proton magnetic resonance spectroscopic imaging in patients with extratemporal epilepsy. *Epilepsia, 39*(3), 267-273.

Tao, J. X., Ray, A., Hawes-Ebersole, S., & Ebersole, J. S. (2005). Intracranial EEG substrates of scalp EEG interictal spikes. *Epilepsia, 46*(5), 669-676. doi:10.1111/j.1528-1167.2005.11404.x

Team, R. C. (2014). *R: A Language and Environment for Statistical Computing*. Retrieved from Vienna, Austria: http://www.R-project.org/

Temkin, N. R. (2009). Preventing and treating posttraumatic seizures: The human experience. *Epilepsia, 50*, 10-13. doi:10.1111/j.1528-1167.2008.02005.x

Tkáč, I., Rao, R., Georgieff, M. K., & Gruetter, R. (2003). Developmental and regional changes in the neurochemical profile of the rat brain determined by in vivo 1H NMR spectroscopy. *Magnetic Resonance in Medicine, 50*(1), 24-32. doi:10.1002/mrm.10497

Van Audekerkea, J., Peeters, R., Verhoye, M., Sijbers, J., & Van der Linden, A. (2000). Special designed RF-antenna with integrated non-invasive carbon electrodes for simultaneous magnetic resonance imaging and electroencephalography acquisition at 7T. *Magnetic Resonance Imaging, 18*(7), 887-891.

Visioli, F., Rihn, L. L., Rodriguez de Turco, E. B., Kreisman, N. R., & Bazan, N. G. (1993). Free fatty acid and diacylglycerol accumulation in the rat brain during recurrent seizures is related to cortical oxygenation. *Journal of Neurochemistry, 61*(5), 1835-1842.

White, A., Williams, P. A., Hellier, J. L., Clark, S., Edward Dudek, F., & Staley, K. J. (2010). EEG spike activity precedes epilepsy after kainate-induced status epilepticus. *Epilepsia, 51*(3), 371-383. doi:10.1111/j.1528-1167.2009.02339.x

Williamson, L. C., Fitzgerald, S. C., & Neale, E. A. (1992). Differential effects of tetanus toxin on inhibitory and excitatory neurotransmitter release from mammalian spinal cord cells in culture. *Journal of Neurochemistry, 59*(6), 2148-2157.

Wu, H., Jin, Y., Wei, J., Jin, H., Sha, D., & Wu, J.-Y. (2005). Mode of action of taurine as a neuroprotector. *Brain Research, 1038*(2), 123-131. doi:10.1016/j.brainres.2005.01.058

Wyllie, E. (2001). *The treatment of epilepsy: principles and practice*. Philadelphia, PA: Lippincott Williams & Wilkins.

Young, R. S., Chen, B., Petroff, O. A., Gore, J. C., Cowan, B. E., Novotny, E. J., Jr., . . . Zuckerman, K. (1989). The effect of diazepam on neonatal seizure: in vivo 31P and 1H NMR study. *Pediatric Research, 25*(1), 27-31. doi:10.1203/00006450-198901000-00006

ABSTRACT

IDENTIFICATION OF METABOLITE BIOMARKERS IN EPILESPY USING ^{1}H MRS

by

HELEN C. WU

August 2016

Advisors: Dr. Jeffrey Loeb, Dr. Jeffrey Stanley

Major: Translational Neuroscience

Degree: Doctor of Philosophy

Epilepsy is a serious neurological disorder that affects 1% percent of the global population. Despite its status as one of the oldest neurological disorders known to man, its mechanisms remain poorly understood. Available medications are not curative but provide symptomatic management and do not work for well for more than 30 percent of patients. Because it is nearly impossible to predict on an individual level who will eventually develop epilepsy, it is also a disorder that can only be diagnosed after the patient has experienced established seizure activity, eliminating any possibility of stopping the disorder in its prodromal phase, before the patients are symptomatic. Availability of a reliable and non-invasive biomarker tool that can predict and identify the development of epilepsy would dramatically change how the disorder is detected, monitored, managed, and treated. In this project, we tested the potential of ^{1}H MRS to provide metabolite biomarkers of epilepsy and epileptogenesis, both in human neocortical tissue obtained from intractable epilepsy patients who underwent resective surgery and also in a longitudinal rat model of epileptogenesis, using interictal epileptiform discharges as a surrogate indicator of disease progression. Using ^{1}H MRS, we found unique metabolite differences that are highly predictive of epileptic and non-epileptic neocortex in humans that also partially overlaps with findings from our rat model. These findings provide

evidence that ^{1}H MRS is capable of identifying metabolite changes specific to epilepsy and may lead to reliable and non-invasive biomarkers of epilepsy and epileptogenesis in the future.

AUTOBIOGRAPHICAL STATEMENT

How is it that a few pools of ions across some semi-permeable membranes could generate the electrical activities allowing us to see, breathe, think, laugh—when those same ions and membranes can give us disorders like epilepsy?

In his own words, my father once said that he was born to be an engineer. He perceived the world in a series of question. How is this made? How does it work? How can I use this to make my own work better? From as far back as I could remember, he had always tried to foster and encourage a similar mindset in me—ask questions, solve problems. A graduate of the University of Michigan with a degree in Biomedical Engineering, and currently a student in the MD/PhD program at Wayne State University, I am constantly mindful of the intersections between science, medicine, knowledge, and applications.

I have been blessed with the opportunity to work on this project under the supervision of Drs. Jeffrey Loeb and Jeffrey Stanley. This project has been an incredibly enriching experience, in terms of my intellectual, academic, technical, and social development. This project has been very unique in the sense that we attempted to apply technology to a real medical disorder in a way that can have significant clinical impact, while continuing to learn more about fundamental aspects of the disorder. Epilepsy is an incredibly interesting disorder to study, not only for its complexities, but also for the tantalizing clues it provides for how our own brain functions.

Ideally, I would like to continue my future research work within neuroscience, perhaps even in epilepsy. I am especially interested in learning more about the molecular, physiologic, and electrophysiological factors underpinning behavior and cognitive function and how that information may be in turn used to inform clinical understanding and management of neurologic and psychiatric conditions.